



Theses and Dissertations

2007-03-16

Solute Chemistry and Isotopic Investigation of the Groundwater Flow Paths in Honey Lake Basin, Lassen County, California and Washoe County, Nevada

Rachel M. Henderson
Brigham Young University - Provo

Follow this and additional works at: <https://scholarsarchive.byu.edu/etd>



Part of the [Geology Commons](#)

BYU ScholarsArchive Citation

Henderson, Rachel M., "Solute Chemistry and Isotopic Investigation of the Groundwater Flow Paths in Honey Lake Basin, Lassen County, California and Washoe County, Nevada" (2007). *Theses and Dissertations*. 1307.

<https://scholarsarchive.byu.edu/etd/1307>

This Thesis is brought to you for free and open access by BYU ScholarsArchive. It has been accepted for inclusion in Theses and Dissertations by an authorized administrator of BYU ScholarsArchive. For more information, please contact scholarsarchive@byu.edu, ellen_amatangelo@byu.edu.

SOLUTE CHEMISTRY AND ISOTOPIC INVESTIGATION OF THE
GROUNDWATER FLOW PATHS IN HONEY LAKE BASIN, LASSEN COUNTY,
CALIFORNIA AND WASHOE COUNTY, NEVADA

By

Rachel M. Henderson

A thesis submitted to the faculty of
Brigham Young University
in partial fulfillment of the requirements for the degree of
Master's of Science

Department of Geological Sciences

Brigham Young University

April 2007

BRIGHAM YOUNG UNIVERSITY

GRADUATE COMMITTEE APPROVAL

Of the thesis submitted by

Rachel M. Henderson

This thesis has been read by each member of the following graduate committee and by majority has been found to be satisfactory.

Date

Alan L. Mayo

Date

Stephen T. Nelson

Date

Barry R. Bickmore

BRIGHAM YOUNG UNIVERSITY

As chair of the candidate's graduate committee, I have read the thesis of Rachel M. Henderson in its final form and have found that (1) its format, citations, and bibliographical style are consistent and acceptable and fulfill university and department style requirements; (2) its illustrative materials including figures, tables, and charts are in place; and (3) the final manuscript is satisfactory to the graduate committee and is ready for submission to the university library.

Date

Alan L. Mayo
Chair, Graduate Committee

Accepted for the Department

Michael J. Dorias
Graduate Coordinator

Accepted for the Department

Thomas W. Sederberg
Dean, College of Physical and Mathematical
Sciences

ABSTRACT

SOLUTE CHEMISTRY AND ISOTOPIC INVESTIGATION OF THE GROUNDWATER FLOW PATHS IN HONEY LAKE BASIN, LASSEN COUNTY, CALIFORNIA AND WASHOE COUNTY, NEVADA

Rachel M. Henderson

Department of Geological Sciences

Master's of Science

Honey Lake Basin is a large, hydrologically closed valley with two playa lakes that are separated by a low elevation sill. The Basin has a complex hydrogeologic setting, with numerous groundwater flow paths that interact with surface waters and three basic aquifers; shallow, deep, and geothermal. Thirteen flow paths; eleven cold and two thermal, are identified and the geochemical evolution of those paths are characterized by integrating solute chemistry and isotopic data. The chemical flow paths include recharge in either granitoid or volcanic terrains in the Sierra Nevada Range and the Modoc Plateau, respectively. The groundwater then flows through alluvial fan and stream sedimentary environments and eventually flows through lacustrine and playa sediments in the closed basin. This investigating characterizes geochemical evolution of groundwater flow from both mafic and granitic terrains to lacustrine sediments with evaporite minerals, in a closed basin environment.

Temperature data reveal that thermal waters circulate to 1.6-3.0 km and 2.8-3.8 km along two major fault zones. Shallow groundwaters above 17°C are determined to

have a component of thermal water and mixing ratios are presented. $\delta^{18}\text{O}$ and δD data show that deep groundwater was recharged by cooler, more humid precipitation from the last ice age, whereas shallow groundwaters reflect current meteoric conditions and show extensive evaporation trends. The two thermal flow paths show exchange with silicate minerals at high temperatures ($>100^\circ\text{C}$). $\delta^{13}\text{C}$ data show interaction with carbonate minerals in basin fill lacustrine sediments. ^3H concentrations and ^{14}C ages show that deep groundwaters throughout the Basin and shallower groundwaters in the center of the basin are not greatly affected by post-1952 recharge. Mean ^{14}C ages range from modern to 23,500 years old.

NETPATH was used to model geochemical evolution along the flow paths. Groundwater on the west side of the basin (granitic terrain) is typically low TDS (~ 150 mg/L) calcium-bicarbonate water and evolves into higher TDS (~ 300 mg/L) sodium-bicarbonate groundwater as it interacts with granitic rocks and then lacustrine sediments. Groundwater on the east side of the basin (mafic terrain) is typically low TDS (~ 200 mg/L) sodium-bicarbonate water and evolves into high TDS (~ 300 mg/L) sodium-bicarbonate water groundwater as it interacts with mafic rocks and then lacustrine sediments. Dissolution of silicate minerals and calcite, and ion exchange with clays is responsible for major chemistry changes. As both of these types of groundwaters come into contact with lacustrine sediments with evaporite minerals on the playas, dissolution of halite and gypsum dominate and the groundwater becomes extremely high in TDS (~ 1100 mg/L on the Honey Lake Playa and $\sim 43,000$ mg/L on the Fish Spring Playa) and strongly sodium-chloride in character.

TABLE OF CONTENTS

INTRODUCTION	1
METHODS	4
GEOLOGIC SETTING	8
HYDROLOGIC SETTING	11
ANALYSIS.....	13
Flow Path Solute Chemistry	13
Temperature and Groundwater Circulation Depth	15
Isotopes	18
Oxygen-18 and Deuterium.....	18
Tritium	21
Carbon-13	21
Carbon-14	23
NETPATH	24
FLOW PATH DESCRIPTIONS	33
Fault Controlled Flow Paths	33
Susan River Flow Path.....	34
Shaffer Mountain Flow Path.....	35
Long Valley Creek Flow Path.....	37
Sierra Nevada Flow Path	38
West Skedaddle/Amedee Flow Path.....	39
East Skedaddle/Amedee Flow Path	40
Neversweat Flow Path	41
Astor/Sand Pass Flow Path.....	42
Virginia Mountains Flow Path.....	43
Cottonwood Flow Path	44
Fort Sage Mountains Flow Path.....	45
CONCLUSION.....	47
REFERENCES	49
APPENDIX A	91

LIST OF FIGURES

Figure 1.	Geologic map.	55
Figure 2.	Sample location map.	56
Figure 3.	Cross section.	57
Figure 4.	Groundwater level map.	58
Figure 5.	Isohyetal map.	59
Figure 6.	Stiff diagrams and locations.	60
Figure 7.	Piper diagrams.	61
Figure 8.	Temperature histogram.	63
Figure 9.	Temperature contour map.	64
Figure 10.	Silica contour map.	65
Figure 11.	Thermal groundwater Piper diagram.	66
Figure 12.	Temperature and depth scatter plot.	67
Figure 13.	$\delta^{18}\text{O}$ and δD scatter plot interpretation guide.	67
Figure 14.	$\delta^{18}\text{O}$ and δD scatter plot for western flow paths.	68
Figure 15.	$\delta^{18}\text{O}$ and δD scatter plot for eastern flow paths.	69
Figure 16.	$\delta^{18}\text{O}$ and δD scatter plot for central and fault zone flow paths.	70
Figure 17.	$\delta^{18}\text{O}$ and δD contour maps.	71
Figure 18.	^3H concentration map.	72
Figure 19.	^3H and depth scatter plot.	73
Figure 20.	$\delta^{13}\text{C}$ contour map.	74
Figure 21.	$\delta^{13}\text{C}$ and depth scatter plot.	75
Figure 22.	Mean ^{14}C age map.	76

Figure 23.	^{14}C and depth scatter plot.	77
Figure 24	Mean ^{14}C ages vs. ^3H scatter plot.	77
Figure 25.	NETPATH models for eastern flow paths.	78
Figure 26	NETPATH models for western flow paths.	79
Figure 27	NETPATH models for fault zone and mixing flow paths.	80
Figure 28	Summary chart of flow path geochemical evolutions.	81
Figure 29	Post Lahontan episodic flooding diagram.	82

LIST OF TABLES

Table 1.	Stream flow data.	83
Table 2.	Median solute chemistry data.	84
Table 3.	GEO THERM temperature data.	85
Table 4.	GEO THERM results.	86
Table 5.	Published maximum temperature values.	87
Table 6.	Mixing ratios.	87
Table 7.	Mean ¹⁴ C age data.	88
Table 8.	NETPATH constraints and phases.	89
Table 9.	NETPATH model results.	90

INTRODUCTION

The northwest-trending Honey Lake Basin is located approximately 57 km north of Reno, Nevada on the California-Nevada border (Figure 1). This large closed basin, about 72.5 km northwest-southeast and 24 km north-south, is situated at the junction of three geologic provinces; the Basin and Range (normal faults) to the east, the Sierra Nevada Batholith (granitic terrain) to the south and west, and the Modoc Plateau (volcanic terrain) to the north (Varian, 1997). Two playas occupy the valley; to the west a large playa containing Honey Lake is the terminus of Susan River and Long Valley Creek. To the east the smaller Fish Springs Playa is usually dry and is supported by the perennial Cottonwood Creek and other ephemeral streams. These two playas are separated by a low elevation surface water divide located close to the California-Nevada border. Along with this complex geologic setting, Honey Lake Basin has an equally complex hydrogeologic setting with numerous groundwater flow paths.

Investigating the Honey Lake Basin groundwater flow paths will provide a better understanding of the geochemical evolution of groundwater flow from both mafic and granitic terrains to lacustrine sediments with evaporite minerals, in a closed basin environment. The data will also provide insight into the salinity relationship between groundwater beneath the two playas. This is accomplished by analyzing solute chemistry to determine interactions with local igneous and sediment deposits, temperature to determine circulation depths, stable isotopes of oxygen and hydrogen to determine recharge sources and other environmental conditions, Tritium and carbon-14 to determine the extent of modern recharge and groundwater residence time, and carbon-13 to

determine the extent of interaction with carbonate minerals and possibly organic material. All of these individual analyses must be used to completely characterize the geochemical evolution of a groundwater flow path.

In an effort to understand the hydrogeology of Honey Lake Basin, two thesis studies, by Webber (1996) at Brigham Young University and Varian (1997) at the University of Nevada, Reno, have been conducted. Webber (1996) concentrated on the solute chemistry of the shallow groundwater systems in the basin, whereas Varian (1997) concentrated on the use of isotopes ($\delta^{18}\text{O}$, δD , ^3H , and ^{14}C) to evaluate the hydrologic processes in the basin. Webber (1996) concluded that the solute load of the groundwater increases as it flows toward the basin floor, but that the magnitude of the increase depends on the availability and abundance of CO_2 and deposits of calcite, dolomite, fluorite, gypsum, halite and clay minerals along flow paths; all of which appear to be more abundant on the Fish Springs Playa side of the basin. Varian (1997) concluded that modern Sierra Nevada runoff is present in the groundwater on the Honey Lake Playa side of the basin in limited amounts and that recharge in this area likely occurred several thousand years ago. Conversely, on the Fish Springs Playa side of the basin, modern recharge occurs, but is limited due to minimal precipitation. Also, isotopic data indicates that the groundwater in the northern part of the basin is recharged from further north in the Willow Creek drainage, and that the deep groundwater system in the basin was recharged during a cooler, wetter climate than today, possibly some 17,000 years ago.

Although both of these studies were thorough and useful, neither provided a complete solute chemistry and isotopic analysis of the various Honey Lake Basin flow paths, and lacked any analysis of temperature, carbon-13, and the solute chemistry of

thermal groundwaters. A combination of their methods and further interpretation must be used to gain a complete understanding of the various Honey Lake Basin groundwater flow paths and their geochemical evolutions.

The purpose of this investigation is to integrate these studies and supplement their data to evaluate the groundwater flow path geochemical evolutions in a closed basin with granitic and mafic terrains. Specifically, geothermal analysis, $\delta^{13}\text{C}$ data and ^{14}C data help to define groundwater movement along flow paths. To achieve this purpose, existing data was verified to check validity and internal consistency. It was then combined and samples were collected to fill in data gaps. Solute chemistry and isotopic data were then used to characterize groundwater flow paths, and the factors responsible for the different geochemical evolutions were evaluated.

The results of this investigation provide understanding of groundwater flow paths and geochemical evolutions in areas of similar geology (granitic to lacustrine terrain and/or mafic to lacustrine terrain) and in closed basins throughout the world.

METHODS

Existing solute and isotopic data (220 wells, 61 springs, 29 streams, and 2 snow samples) were obtained from published and unpublished sources. Data from 178 samples from Webber (1996), 189 samples from Varian (1997), 115 samples from Rose et. al. (1997), 36 samples taken by BYU class field trips, 3 samples from Reed (1978), and 1 sample from Laird et. al. (1986) were all included in the database. This data was supplemented with analysis of 36 wells, 12 springs, and 9 surface waters collected as part of this investigation. The data includes samples from 312 different locations in the Honey Lake Basin area (Figure 2). Several of these locations were sampled by different investigators at different times, and the data from these different sample events for the same location were combined.

Field Methods (this investigation)

Temperature and conductivity were measured in the field using an YSI 30/10 conductivity meter, and pH was measured using a VWR Scientific pH meter. Before sampling, wells were pumped or allowed to free-flow until the temperature stabilized. Sample locations, reported in UTM coordinates, were taken using a Trimble GeoExplorer3.

Thirty seven samples were collected for solute chemistry analysis in 1.0 L polyethylene bottles. Fifty five samples were collected for $\delta^{18}\text{O}$ and δD analysis in 50mL amber vials with polyseal caps. Thirty eight samples were collected in 1 L high-density brown polyethylene bottles for ^3H analysis. Five samples were collected for ^{13}C and ^{14}C analysis in acid washed high-density polyethylene containers. These samples were

immediately treated with 30 g of BaCl₂ and 100 g of NaOH per 5 gallons of sample, to precipitate dissolved carbonate species as BaCO₃ (Clark and Fritz, 1997).

Laboratory Analytical Methods (this investigation)

Samples were analyzed for major cation and anion concentrations: Na⁺, Ca⁺, K⁺, Mg⁺, SiO₂, HCO₃⁻, F⁻, SO₄²⁻, Br⁻ and Cl⁻, and for the isotopes δ¹⁸O, δD, ³H, δ¹³C, and ¹⁴C.

All solute chemistry analysis was performed at Brigham Young University. Samples were filtered and split for cation and anion analysis. Cation splits were acidified with 5-6 drops of nitric acid per ~50 mL of sample. Cation concentrations were measured with a PerkinElmer 5100C Atomic Absorption Spectrometer. Anion concentrations were determined using an ICS-90 ion chromatograph. Bicarbonate (HCO₃⁻) was measured on a Mettler Toledo DL50 Graphix automatic titrator. Cation and anion measurements were evaluated for accuracy by determining charge balance error based on mil-equivalents per liter. The acceptable charge balance error was within ±5%.

Stable isotope ratios for δ¹⁸O and δD were determined by BYU using a Finnigan MAT Delta^{plus} mass spectrometer equipped with the GasbenchII and HDevice. Methods similar to Epstein and Mayeda (1953) and Gehre et. al. (1996) were used. Reproducibility was evaluated using an internal laboratory standards. Data were reduced by the method established by Nelson (2000) and Nelson and Dettman (2001), according to which δ¹⁸O and δD values were normalized to the VSMOW/SLAP scale. The reproducibility of the internal laboratory standard is <±1.0‰ (n= 102) for δD_{vsmow} and 0.12‰ (n= 30) for δ¹⁸O_{vsmow}. All values are reported in permil (‰) by delta notation.

All tritium (^3H) samples were measured at BYU. Sample preparation included distilling, enriching and vacuum distilling in a method similar to the University of Waterloo Environmental Isotope Laboratory (1998), before a liquid scintillation cocktail was added. This method decreases the lower limit of detection (LLD) from ~ 5 TU to < 0.2 TU. Samples were run on a PerkinElmer Quantulus liquid scintillation counter for 12, 120 minute cycles. Final results were calculated as described by Neary (1997). Concentrations are reported in tritium units (TU; 1 TU = 3.2 pCi/L).

Samples that had been treated in the field to precipitate dissolved carbonate species as BaCO_3 were monitored and treated with BaCl_2 and NaOH until a $\text{pH} > 11$ was achieved (Clark and Fritz, 1997). The samples were then decanted into a 1 L high-density polyethylene container where they were stored until they were decanted further and transferred to amber glass bottles with polyseal caps. These carbonates slurries were vacuum dried prior to reacting with phosphoric acid. CO_2 gas resulting from this reaction was isolated, split, and then analyzed for $\delta^{13}\text{C}$ using a Finnigan MAT Delta^{plus} mass spectrometer (McCrea, 1950)

A portion of the CO_2 gas splits for four of the ^{14}C samples were analyzed by AMS (Accelerated Mass Spectrometry) methods at the University of Georgia, Center for Applied Isotope Studies for ^{14}C . One of the ^{14}C samples was analyzed at Brigham Young University by a method similar to Polach and Stipp (1967). Precipitated barium carbonate was converted into benzene, and once the benzene was synthesized, 0.5 mL of spectrograde benzene containing POP and POPOP flours were added prior to counting in a PerkinElmer 1414 Guardian scintillation counter. Samples were counted in 6, 100 minute cycles. Percent modern carbon (pmc) were calculated following the method of

Stuvier and Polach (1977). Carbon-14 ages were calculated by the methods described by Fontes and Garnier (1979), Fontes (1983), and Pearson and Henshaw (1970).

Data Analysis

Appendix A contains all solute and isotopic data. Selected subsets are included as tables in the text.

Major ion chemistry was plotted as Stiff diagrams, contour maps, and Piper diagrams. Stable isotopic data was analyzed relative to the local meteoric water line (LWML) of Varian (1997) and was used to evaluate potential thermal rock-water interactions. Carbon-14 ages were determined and compared with ^3H data. Carbon-13 data were analyzed to determine the sources for carbon in Honey Lake groundwaters. Conceptual models of potential groundwater flow paths for various regions of the basin were then developed. Geochemical evolutions along the conceptual models were quantitatively analyzed using the computer programs GEOTHERM and NETPATH (Plummer et. al., 1994 and Truesdell, 1976).

GEOLOGIC SETTING

Honey Lake Basin is a fault bounded valley filled with unconsolidated and semi-consolidated material derived from lacustrine, terrestrial, fluvial, and volcanic sediments (Figure 3). Deep (1500 to 1700 m thick) semi-consolidated Pliocene lacustrine deposits consist of thick layers of volcanic tuff and ash along with clay, silt, and minor amounts of sand (Mayo and Slosson, 1992; Handman et. al., 1990; and California Department of Water Resources, 2003). These deposits have low permeability and interfinger with volcanic rocks on the north- northeast side of the basin (Figure 3). Shallower (maximum of 300 m thick) Pleistocene Lake Lahontan deposits consist of mostly low permeability fine grained clay and silt on the east side of the basin and coarse, more permeable deltaic deposits to the west (Handman et. al., 1990). Deltaic deposits consisting of sand and gravel formed when the Susan River and Long Valley Creek flowed into the Pleistocene Lake Lahontan and are located to the northwest and southeast of Honey Lake. Poorly sorted, highly permeable alluvial fan deposits, consisting of clasts derived from granodiorite and volcanic rocks, flank the basin in most areas and interfinger with lacustrine deposits (Handman et. al., 1990 and California Department of Water Resources, 2003). These valley fill sediments can be up to 1800 meters thick (California Department of Water Resources, 1963 and Varian, 1997). Shoreline and geothermal tufa deposits are also present.

The basin is bounded on all sides by mountain ranges (Figure 1). The Honey Lake Playa area in the west is bounded by the northern Sierra Nevada Mountains to the south and west, and by the Modoc Plateau (the Shaffer, Skedaddle, and Amedee Mountains) to the north. The Fish Springs Playa area in the east is bounded by the

Amedee Mountains to the north, the Terraced Hills to the northeast, and the Virginia and Fort Sage Mountains to the southeast and south. The Sierra Nevada and Fort Sage Mountains are comprised of relatively impermeable Cretaceous granodiorite overlain by Tertiary volcanic rocks (Handman et. al., 1990 and Grose et. al., 1991; Figure 3). The remaining mountains are comprised of porous, highly transmissive, Tertiary basalt flows and andesite volcanic rocks overlying rhyolitic tuffs and a granodiorite basement (McDonald, 1966; Grose, 1984; Handman et. al., 1990; and Tylor, 1992). Rhyolitic ash-flow tuffs and volcanic-flow breccias are present in the pass that separates the Fort Sage and Virginia Mountains (Handman et. al., 1990).

Basin and Range extension has displaced the granitic bedrock (Figure 3) below the basin to depths of about 1,500 – 2,100 meters below the land surface (Bonham, 1969; Reed, 1978; Grose, 1984; Grose et. al., 1991; and Varian, 1997). According to Fuis et. al. (1987), granitic bedrock with a seismic-refraction velocity similar to Sierra Nevada bedrock, also underlies the Modoc Plateau. On the east side of the basin, granitic bedrock lies about 300 meters beneath lacustrine deposits and basalts on the valley floor (Mayo and Slosson, 1992).

Several fault zones exist in Honey Lake Basin. The major fault zones include the Antelope Mountain, Litchfield, and Amedee fault zones to the north, and the Honey Lake and Warm Springs fault zones to the south (Figure 1). These are northwest-trending right lateral faults and north-trending normal faults (Bonham, 1967 and Varian, 1997). A small horst, Bald Mountain, separates the smaller Susanville structural basin from the large Honey Lake structural basin (Schimschal, 1991).

Hydrothermal tufa deposits are associated with faults in the basin (Reed, 1978). These tufa deposits formed as hydrothermal groundwater escaped along the faults into Pleistocene Lake Lahontan and precipitated calcium carbonate. These faults continue to sustain hot springs throughout the basin as thermal water at depth leaks out along the faults (Schimschal, 1991).

HYDROLOGIC SETTING

Water-bearing material in the Honey Lake Basin occurs in the fractured volcanic rocks, alluvial fans, and unconsolidated to semi-consolidated lake deposits. Possible sources for recharge include: direct precipitation, spring discharges, runoff from rivers and streams, seepage of irrigation water, and groundwater inflow from outside areas (Handman et. al., 1990; Varian, 1997; and California Department of Water Resources, 2003). Three groundwater systems exist in Honey Lake Basin; shallow (<180 m), deep (>180 m), and geothermal (Varian, 1997).

The basin has a total drainage area of 5700 km² and due to the semi-arid climate much of the potential recharge water is lost to evapotranspiration (Rockwell, 1993). Recharge not lost to evapotranspiration infiltrates through unconsolidated sediments, faults, and fractures. Later, it either discharges as springs or continues to flow down gradient toward the basin playas. Most springs occur in the surrounding mountains, although several fault related thermal springs discharge along the edge of the basin floor. On the basin floor, groundwater ascends and discharges onto the playas or is lost through evapotranspiration. Discharge is controlled by a transition from high to low hydraulic conductivity material; unconsolidated valley fill to semi-consolidated, clay-rich material (Taylor et. al., 1992).

The Honey Lake and Fish Springs Playas are hydrologically distinct. A low elevation surface water divide currently separates the playas and prevents hydrologic communication, or mixing, between the two sides of the basin (Webber, 1996; Figure 4). The Honey Lake play commonly is covered with water due to relatively high precipitation (~36 in/yr) in the west and inflow from the Susan River and Long Valley

Creek (Figure 5). Conversely, the Fish Spring Playa and the surrounding streams typically have low flow (Table 1) and are often dry due to low precipitation (~16 in/yr; Figure 5) in the east caused by the Sierra Nevada rain shadow (Webber, 1996 and Varian, 1997). Shallow groundwater in the Fish Spring Playa has higher maximum Total Dissolved Solids (TDS; 50,295 mg/L) content than shallow groundwater associated with the Honey Lake Playa (1790 mg/L; Figure 6).

ANALYSIS

Flow Path Solute Chemistry

Eleven groundwater flow paths in Honey Lake Basin are designated based on groundwater potential (Figure 4), and assuming that shallow, non-thermal, groundwater flow mimics surface topography – flows perpendicular to elevation and potentiometric contours. Two thermal flow paths are based on fault locations and groundwater temperature data. These flow paths are (Figure 6):

Non-thermal

1. Susan River (SR)
2. Sierra Nevada (SN)
3. Long Valley Creek (LV)
4. Fort Sage Mountains (FSM)
5. Cottonwood (CW)
6. Virginia Mountains (VM)
7. Neversweat (NV)
8. Astor/Sand Pass (ASP)
9. East Skedaddle/Amedee (ESA)
10. West Skedaddle/Amedee (WSA)
11. Shaffer Mountain (SHAF)

Thermal

12. Honey Lake/Warm Springs Fault Zone (HLW), and
13. Antelope Mountain/Litchfield Fault Zone (AML)

Near the down gradient end of four physical flow paths; Susan River, Shaffer Mountain, Long Valley Creek, and West Skedaddle/Amedee, it appears as if some thermal fault water upwells and mixes with the overlying cold water systems, consequently effecting both groundwater temperature and chemistry. Also, the ends of the Susan River and Shaffer Mountain flow paths mix before finally terminating in Honey Lake.

The 13 groundwater flow paths have been organized into seven chemical evolutionary paths; five cold and two thermal (Table 2). The chemistries in Table 2 are the mean compositions of spring and well samples located at critical locations along the flow path. Along each groundwater chemical path, low TDS recharge (i.e. highland) waters evolve to elevated TDS water in the basin floor (Figure 6). The seven chemical paths are described below and illustrated in the following Piper diagrams (Figure 7).

1. Susan River, Shaffer Mountain, and Long Valley (SR/SHAF/LV): The low TDS (~ 150 mg/L) calcium-bicarbonate groundwater at the head of the SR/SHAF/LV chemical flow path evolves into high TDS (~ 530 mg/L) sodium-bicarbonate groundwater with considerable sulfate concentrations, on the basin floor (Figure 7a).
2. Sierra Nevada (SN): As the low TDS (~ 130 mg/L) groundwater from the highlands of this chemical flow path travels to the basin floor, it increases slightly in TDS (~ 190 mg/L) but remains calcium-bicarbonate in character (Figure 7d).
3. West Skedaddle/Amedee (WSA): The low TDS (~ 190 mg/L) groundwater at the head of the WSA chemical flow path is sodium-bicarbonate and as it flows down gradient, it increases in TDS (~ 620 mg/L) and becomes sodium-chloride dominated (Figure 7d).
4. Fort Sage Mountains, Virginia Mountains, and Cottonwood (FSM/VM/CW): The low TDS (~ 170 mg/L) FSM/VM/CW beginning groundwater is typically calcium-bicarbonate in character and evolves into extremely high TDS (~ 10,000 mg/L), sodium-chloride groundwater on the basin floor (Figure 7b).

5. East Skedaddle/Amedee, Astor/Sand Pass, and Neversweat (ESA/ASP/NV):
The ESA/ASP/NV chemical flow path highland groundwater is low TDS (~ 200 mg/L) sodium-bicarbonate that, like the FSM/VM/CW flow path, evolves into extremely high TDS (~ 32,350 mg/L), sodium-chloride groundwater (Figure 7c).
6. Honey Lake/Warm Springs Fault Zone (HLW): The HLW thermal groundwaters (41°C mean temperature) are low TDS (~ 290 mg/L), primarily sodium-bicarbonate groundwater with considerable sulfate concentrations (Figure 7d).
7. Antelope Mountain/Litchfield Fault Zone (AML): The much hotter AML thermal waters (83°C mean temperature) are higher TDS (~ 820 mg/L), sodium-sulfate groundwater with much chloride (Figure 7d).

Geochemical evolution models for these seven chemical flow paths are discussed below.

Temperature and Groundwater Circulation Depth

Groundwater temperatures in the Honey Lake Basin range from 5°C to 102.8°C (Table 2 in Appendix A). Although most groundwater are 20-30°C, thermal waters can be as warm as 60-102°C (Figure 8). A contour map of groundwater temperatures (Figure 9) shows that the hottest groundwaters are associated with fault zones, especially at fault intersections.

The hottest of the fault related thermal groundwaters; > 50°C in the Antelope Mountain/Litchfield Fault Zone (AML) and > 30°C in the Honey Lake/Warm Springs Fault Zone (HLW), were analyzed using GEOTHERM to determine maximum in-situ

aquifer temperature conditions (Table 3). GEOTHERM is based on temperature equilibrium of mineral-water reactions (Fournier and Rowe, 1966; Fournier and Truesdell, 1973; Fournier and Rowe, 1977; and Fournier, 1979). Maximum temperatures were calculated using the assumptions described by (Fournier et. al., 1974). The silica-conductive, silica-adiabatic, and Na-K-Ca (1/3) geothermometers were determined to be good geothermometers (Mayo, written communication, 2005) for the thermal waters in Honey Lake Basin as described in Table 4. The silica geothermometers were used when ever possible because the amount of dissolved silica increases substantially with temperature (Figure 10), and Fournier and Rowe (1966) reported that the silica method consistently yields maximum temperatures within 2°C of the measured temperatures at depth.

According to the selected geothermometers, the AML groundwaters have a maximum temperature of 117-140°C (Table 4). These estimates agree with, or are slightly lower than, previously published geothermometer estimates (Table 5). They also agree well with published field measurements of 121°C for the maximum down-hole well temperature in the vicinity of the Wendel and Amedee Hot Springs (Skiba, 1985).

According to the selected geothermometers, the HLW groundwaters have a maximum temperature of 65-112°C (Table 4). There is no published data on the thermal waters in the HLW path to use for comparison. The cooler of the HLW groundwaters, samples RE1 and W21, have slightly different chemistries than the other samples in this flow path (Figure 11) and are located at the very western end of the fault zone. This may indicate different sources, different circulation patterns and mixing, or both (Hardt et. al., 1975). These samples may need to be considered as a separate thermal flow path. If they

are separate, then the estimated maximum temperature for that path would be 102-112°C, and 65°C for the HLW. For now, however, they will be included in the HLW flow path based on their relatively “low” temperatures.

Nathenson and Guffanti (1988) averaged the geothermal gradient for the western United States as 34°C/km. Using this gradient and the GEOTHERM estimated maximum temperatures, it was calculated that the waters along the HLW flow path circulate to a depth of about 1.6-3.0 kilometers and the waters along the AML flow path circulate to a depth of 2.8-3.8 kilometers (Table 4). This is slightly less than the 4-6 kilometers reported by Blackwell et. al. (2000) for most extensional systems in the U.S.

According to the Western Regional Climate Center (2007), the mean annual air temperature in Honey Lake Basin is about 10°C. However, many of the groundwaters in the basin are much hotter than 10°C. Statistical analysis was conducted on the 248 temperature data sets using SAS (SAS Institute, 2004) procedures to evaluate the temperature at which mixing of cold and thermal waters becomes significant (Eggett, personal communication 2007). Based on cumulative percents from the SAS analysis, groundwaters cooler than 17°C have little to no thermal component, and groundwaters warmer than 17°C have an increasingly significant component of thermal water. Of the 248 samples, 113 of those (46%) have a temperature greater than 17°C (Table 2 in Appendix A). Approximate mixing ratios for the groundwater (> 17°C) in Honey Lake Basin based on mixing with thermal waters from HLW (87°C average maximum temperature) and AML (123°C average maximum temperature) flow paths are presented in Table 6. These mixing ratios can be applied to shallow, warm groundwaters found in the western portion of the basin in the Susan River, Sierra Nevada, Long Valley Creek,

Fort Sage Mountains, Shaffer Mountain, and West Skedaddle/Amedee flow paths.

Temperatures above 17°C for deep groundwaters do not indicate thermal mixing, but do indicate heating by the natural geothermal gradient (Figure 12).

Several flow paths on the east side of the basin, Astor/Sand Pass, East Skedaddle/Amedee and Neversweat (Table 2 in Appendix A), also appear to be influenced by thermal waters, as evidenced by warm, shallow waters and the presence of geothermally deposited tufa. However, no thermal groundwaters (> 30°C) have been sampled on the east side of the basin, and thus maximum temperatures, circulation depths, and mixing ratios could not be calculated. The calculated mixing ratios can be applied to these flow paths, but are less reliable since the fault zones present on the east side of the basin may allow groundwater to circulate to different depths, and thus have a different effect when mixed with the cold groundwaters.

Isotopes

Oxygen-18 and Deuterium

Stable isotopes of oxygen and hydrogen are useful in defining groundwater environmental conditions. Isotope abundances (δ) are reported as positive or negative deviations of heavy to light isotope ratios, compared to Standard Mean Ocean Water (SMOW) (Domenico and Schwartz, 1998).

Craig (1961) determined a linear correlation in the relationship between $\delta^{18}\text{O}$ and δD abundances in natural meteoric waters from all over the world. This correlation, known as the meteoric water line (MWL), is defined as:

$$\delta D = 8\delta^{18}O + 10 \quad (1)$$

$\delta^{18}O$ and δD values along the MWL are controlled by the temperature of condensation, altitude, and distance from the ocean of the precipitation event (Faure and Mensing, 2005). Values that deviate from the MWL experienced fractionation due to, evaporation and hydrothermal exchange, following precipitation. A full discussion of oxygen and hydrogen fractionation is given by Clark and Fritz (1997).

Varian (1997) defined a local meteoric water line (LMWL) for the basin as:

$$\delta D = 7.1\delta^{18}O - 8.4 \quad (2)$$

This LMWL was derived by fitting a regression line, with a correlation coefficient of 0.98, to $\delta^{18}O$ and δD values from local precipitation. The LMWL varies quite a bit from the MWL in both the slope (7.1) and the deuterium excess factor (-8.4), and is controlled by local climate factors, including the origin of vapor mass, secondary evaporation during rainfall and seasonality of precipitation (Clark and Fritz, 1997).

When $\delta^{18}O$ vs. δD values are plotted, recharge waters from direct infiltration of precipitation lie along the LMWL because they are unaltered (have the same isotopic composition as the precipitation) and reflect the latitude at which precipitation occurred. Groundwaters that have undergone evaporation, or that were recharged from waters which experienced evaporation, are enriched in heavier isotopes and therefore deviate to the right of the LMWL (Figure 13). Groundwaters that have experienced ^{18}O exchange with silicate minerals due to high temperatures ($> 100^{\circ}C$), usually in basinal flow or geothermal systems, are enriched in ^{18}O (Domenico and Schwartz, 1998).

Two hundred and seven samples from surface waters, springs, and wells with $\delta^{18}\text{O}$ and δD data are plotted in Figure 14 through 16 by the physical flow paths. The majority of these waters plot close to the local meteoric water line, indicating a meteoric origin of winter precipitation that fell in a cool, high latitude, high altitude, inland region. This is consistent both with what one would expect from current precipitation in the highlands of the Honey Lake Basin area and from cooler, more humid precipitation from the last ice age (up to 17,000 years ago), which is likely the source of deep ($> 180\text{m}$) groundwater in the basin (Varian, 1997).

Those waters that do not plot close to the local meteoric water line, typically plot to the right and thus have experienced evaporation to some extent. Again, this is expected of groundwater in the arid Honey Lake Basin. The flow paths farthest from the main areas of recharge – Astor/Sand Pass, East Skedaddle/Amedee, Fort Sage Mountains, Long Valley, and West Skedaddle/Amedee, show a more pronounced evaporation trend than those located close to the areas that receive much precipitation (Figure 5, 14d, 15a, 15d, 16a and 16b).

The Antelope Mountain/Litchfield Fault Zone flow path isotopes are enriched in $\delta^{18}\text{O}$ and therefore show that the groundwater has experienced exchange with rock minerals at high temperatures ($> 100^\circ\text{C}$) in this deeply circulating geothermal system (Figure 16d). The West Skedaddle/Amedee and Susan River flow path shows a similar trend due to mixing with thermal waters from the Antelope Mountain/Litchfield Fault Zone flow path (Figure 14). Conversely, the cooler Honey Lake/Warm Springs Fault Zone flow path plots directly along the local meteoric water no exchange with rock minerals (Figure 16c).

Contour maps of $\delta^{18}\text{O}$ and δD values in Honey Lake Basin (Figure 17) show that the groundwaters at the ends of the flow paths, or on the basin floor, are much more enriched in both $\delta^{18}\text{O}$ and δD than those at the beginning of the flow paths, or in the highlands, reflecting the effects of evaporation.

Tritium

All ^3H data reported in previous studies were normalized to 2005, the year samples were collected for this investigation, using a half life of 12.32 years (Table 6 in Appendix A). A map of the ^3H values (Figure 18) shows that the highlands have the highest concentrations of ^3H , and are thus composed of modern water. Generally, the concentration of ^3H in each flow path decreases down gradient toward the basin floor and eventually become non-detectable at the end of the flow path (Figure 19). Thus, groundwaters at the start of the flow paths are modern waters, but groundwaters in the center of the basin are not greatly affected by post-1952 recharge.

Carbon-13

The $\delta^{13}\text{C}$ values for 68 groundwater samples in Honey Lake Basin range from -20.7 to +0.4 ‰. According to Clark and Fritz (1997), a $\delta^{13}\text{C}$ value of -23‰ is typical for soil gas in areas with C3 plants, and values of +8 to 9‰ are common for fractionation between soil gas and bicarbonate. Based on these assumptions, $\delta^{13}\text{C}$ values of ~ -15 to -14‰ are expected for groundwaters in the Sierra Nevadas, and have been documented in other highlands in the north-western United States which lack carbonate minerals (Tarbet, 2005). Honey Lake Basin groundwater generally becomes more enriched in $\delta^{13}\text{C}$ as it

flows down gradient from the highlands toward the center of the basin (Figure 20), indicating increased interaction with carbonate minerals ($\sim 0\%$).

Carbonate mineral sources in the basin are found in lacustrine sediments, shoreline and geothermal tufa deposits, and likely in the soil zone. Large HCO_3^- concentrations ($> 300 \text{ mg/L}$) and enriched $\delta^{13}\text{C}$ values (significantly $> -15\%$) indicate a carbonate mineral source (Table 7 in Appendix A; Mayo, personal communication, 2007). Honey Lake Basin samples which fit this description are, for the most part, located on the basin floor at the end of the flow paths (Figure 20), and thus are not associated with shoreline and geothermal tufas. These samples have enriched $\delta^{13}\text{C}$ values due to interaction with carbonates which precipitated directly from Lake Lahontan, similar to those found in sediments deposited by Lake Bonneville (Oviatt et. al., 1994). During the Pleistocene, the mean annual air temperature of Honey Lake Basin would have been $\sim 5^\circ\text{C}$ and atmospheric CO_2 would have had a $\delta^{13}\text{C}$ value of $\sim -7\%$ (Nelson, personal communication, 2007). Under these conditions, calcite that precipitated in Lake Lahontan would have a $\delta^{13}\text{C}$ value of $\sim 5\%$ (Beaudoin and Therrien, 2007, and Deines, 1974). Groundwater flowing down gradient from the surrounding highlands becomes increasingly enriched in $\delta^{13}\text{C}$ toward the center of the basin as it interacts with this calcite.

According to Benson et. al. (1996), tufa deposited by Lake Lahontan has $\delta^{13}\text{C}$ values that range from 0.44 to 5.68‰ for shoreline tufa, and $\sim 4.76\%$ for geothermal tufa. Groundwater interaction with these tufa and other lacustrine carbonates deposited by Lake Lahontan would effectively enrich $\delta^{13}\text{C}$. The Astor Pass B2041 sample (Table 7

in Appendix A) has much HCO_3^- , is enriched in $\delta^{13}\text{C}$, and is located at the head of the flow path, indicating interaction with shoreline tufa.

The three samples in Honey Lake Basin (W96, B682, and H4099; Table 7 in Appendix A) with $\delta^{13}\text{C}$ values that are more depleted than the -15‰ value expected for groundwaters in the Sierra Nevadas are likely the result of the effects of organic matter in aerobic conditions. These three samples are located at the beginning of their respective flow paths.

Carbon-13 values become less variable with depth and range between -13 and -10‰ (Figure 21), suggesting that the effects of interactions with carbonates and organic matter on $\delta^{13}\text{C}$ balance each other at depth.

The possible role of organic matter in $\delta^{13}\text{C}$ changes in Honey Lake Basin requires further investigation and $\delta^{13}\text{C}_{\text{CH}_4}$ measurement.

Carbon-14

Forty four samples from Honey Lake Basin, with ^{14}C activities ranging from 2.8 pmc to 112.8 pmc, were included in this thesis (Table 8 in Appendix A). Carbon-14 ages were calculated by the methods described by Fontes and Garnier (1979) and Fontes (1983) for samples with $\delta^{13}\text{C}$ values between -8 and -12‰, and the method described by Pearson and Henshaw (1970) for samples with $\delta^{13}\text{C}$ values of -14‰ and larger (Table 9 in Appendix A). Mean ^{14}C ages range from modern to 23,500 years old (Figure 22). The oldest groundwaters are found along fault zones and at the ends of flow paths on the basin floor. Generally, ^{14}C activities decrease, and thus mean groundwater ages increase, with depth (Figure 24). Deep (>180 m) groundwaters have small ^{14}C activities (< 40 pmc) and are much older than the shallow groundwaters. Deep wells with high pmc

activities have large perforation intervals that span shallow and deep aquifers, and therefore do not reflect accurate measurements for the well bottom. Shallow groundwaters (>100 m) have a variety of ^{14}C activities (13 to 113 pmc) that, according to Rose et. al. (1997), represent the mixing of young groundwater with old waters that ascend to discharge zones. ^3H vs. mean ^{14}C ages (Figure 24) show limited mixing between young and old groundwaters in Honey Lake Basin.

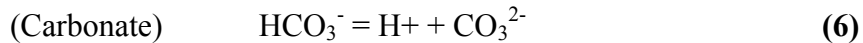
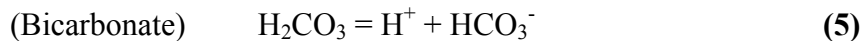
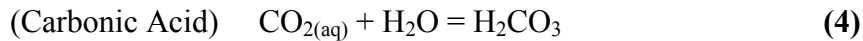
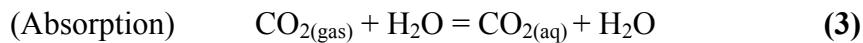
NETPATH

NETPATH (Plummer et. al., 1994), a mass balance computer modeling code, was used to determine a model for the geochemical evolution of the groundwater along each of the seven chemical flow paths. Mean solute chemistry values for the end members of each physical flow path, as explained earlier, were organized according to similarities in solute chemistry (Table 2). The low TDS groundwater at the beginning of each flow path was defined as the “initial” water. The high TDS groundwater on the valley floor, at the end of the flow paths, was designated as the “final” water. For the three chemical flow paths with more than one physical flow path member, the physical flow that was most representative of overall chemical changes was modeled to show the possible groundwater evolution for those paths (marked with a † in Table 2). Two of the chemical flow paths; SR/SHAF/LV and WSA are believed to mix with neighboring thermal waters and were modeled as mixing problems. An additional model was run to account for mixing of the Susan River and Shaffer Mountain flow paths on the basin floor near Honey Lake.

In order to use NETPATH to model flow path geochemical evolutions, the possible chemical reactions that the groundwater would undergo had to first be identified. This was done by evaluating the solute chemistry of the water samples and the mineralogy of the basin using geologic maps. The following chemical reaction regimes (Domenico and Schwartz, 1998 and Klein, 2002) are possible reactions that the groundwater could undergo, as it flowed through the igneous and lake sediment deposits of Honey Lake Basin. These reactions were used to determine the constraints and phases used for modeling.

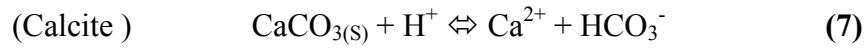
Soil Zone

When the precipitation that falls in Honey Lake Basin infiltrates the unsaturated zone, or soil zone, it absorbs CO₂ gas generated by soil zone activities such as root and microbial respiration (Domenico and Schwartz, 1998). This absorption of CO₂ gas in an open environment forms carbonic acid which disassociates in the groundwater into bicarbonate and carbonate.



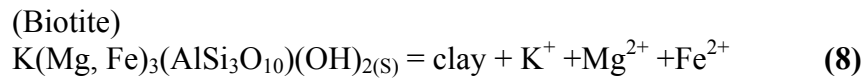
Slightly acidic, carbonate undersaturated groundwater easily dissolves carbonate minerals, such as calcite, present in small quantities in the mountain

soils (Webber, 1996). Dissolution of calcite will increase Ca^{2+} and HCO_3^- concentrations in the groundwater. Calcite may be precipitated if groundwater becomes supersaturated with respect to calcite.

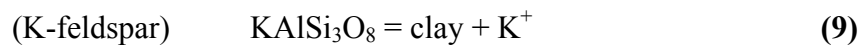


Igneous Deposits

When groundwater comes in contact with the igneous rocks in the mountains of Honey Lake Basin, several reactions may occur. Incongruent dissolution takes place with biotite, which produces clay and ions of K^+ , Mg^{2+} , and Fe^{2+} . Biotite is more common in the Cretaceous granodiorites than in the Tertiary volcanics.

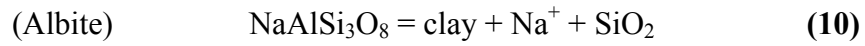


Incongruent dissolution of K-feldspar also produces clay and increases the concentration of K^+ .

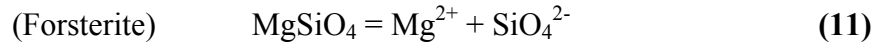


The same process happens when water comes in contact with plagioclase feldspars. Incongruent dissolution of albite, a Na-rich aluminosilicate, causes Na^+ and SiO_2 concentrations increase. Ca-rich aluminosilicates, such as anorthite, are

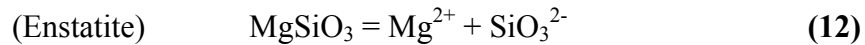
likely present in the basin, but as discussed by Webber (1996), are not believed to be major contributors to solute chemistry and were therefore not included in NETPATH.



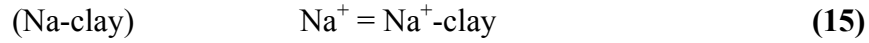
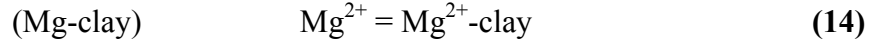
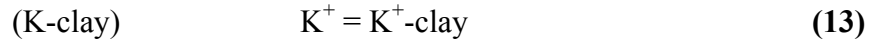
Olivine is common in the mafic volcanics in the northern and eastern mountains of Honey Lake Basin (Grose, 1984). Olivine readily reacts with groundwater, due to its instability at low temperatures, thus increasing concentrations of Mg^{2+} , and SiO_4^{2-} . Forsterite, the magnesium rich end-member of the olivine group, was used in NETPATH.



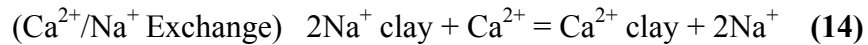
Much Mg^{2+} and SiO_3^{2-} are added to the groundwater system from pyroxenes such as enstatite that are present in the local mafic volcanics (Grose, 1984).



The above silicates; biotite, K-feldspar, albite, forsterite, and enstatite, cannot be precipitated, but the products of their incongruent dissolution can (K^+ , Mg^{2+} , and Na^+) be precipitated out and incorporated into clays.



Ion exchange may occur when water comes in contact with these clays. These clays may be found in alluvial fans, near shore deposits, and in basin fill sediments (Handman et. al., 1990). The most common type of ion exchange happens with Na-clays and is between Ca^{2+} and Na^+ ions. Ion exchange will increase the concentration of Na^+ while at the same time decreasing the concentration of Ca^{2+} . Ion exchange is not an easily reversible chemical reaction, but it is possible when there are extremely large concentrations of Na^+ .



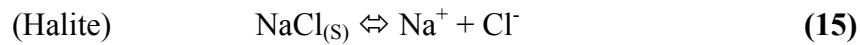
Lacustrine Deposits

Lacustrine sediments found on the basin floor contain much carbonate minerals. These minerals commonly occur as cements or as tufa. Studies done on lacustrine carbonate deposits in Pyramid Lake, NV, western Utah, and Death Valley, CA suggest that the composition is dominantly calcite (5) with little dolomite present (Benson, 1993 and 2004; Anderson et. al, 2005; Nelson et. al, 2005; Miner et. al, 2006). It was determined that Lake Lahontan deposits in Honey Lake Basin are similar in composition. Dolomite, therefore, was not

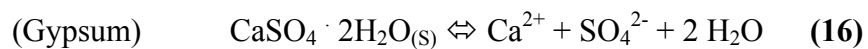
included in the NETPATH models as it was not considered a major contributor to solute chemistry compared with calcite. Dissolution of calcite would add increase both Ca^{2+} and HCO_3^- concentrations in groundwater.

Clay minerals, and therefore ion exchange, (14) are also common in lacustrine deposits in the basin.

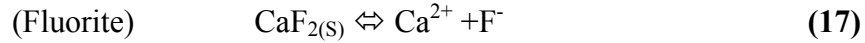
Halite, an abundant precipitate on the basin margins and increasingly more abundant toward the middle of the basin, easily dissolves upon contact with halite undersaturated water and just as easily precipitates in halite supersaturated water. Concentrations of Na^+ and Cl^- in the water increase when halite disassociates, and vice versa. Calcium and magnesium sulfates and chlorides are common, but minor, impurities in halite and disassociate in, or precipitate from, water as easily as halite. Although they occur on the basin playas, they do not contribute significantly to the solute chemistry and were not included in the NETPATH models. Halite may also be present in the soil zone in small quantities.



Gypsum, a common precipitate with calcite, disassociates in gypsum undersaturated water and thus increases Ca^{2+} and SO_4^{2-} concentrations (Klein, 2002). Gypsum may also be present in the soil zone in small quantities.



Fluorite is a common hydrothermal deposit and is also associated with calcite and gypsum deposits (Klein, 2002). When fluorite reacts with undersaturated water, it disassociates and the concentrations of Ca^{2+} and F^- in the water increase.



Sylvite easily precipitates from, or disassociates in, groundwater depending on the saturation conditions. High concentrations of K^+ from the dissolution of biotite and K-feldspar, and high concentrations of Cl^- from the dissolution of halite may result in the precipitation of sylvite on the playas (Klein, 2002).



The occurrence of these minerals, along with those of calcite, clay minerals, halite, gypsum, fluorite, and sylvite increase in deep (>180 m) water and playa deposits (Webber, 1996).

The constraints used in all of the NETPATH models included the major ions involved in the possible flow path reactions: C, Ca^{2+} , Mg^{2+} , Na^+ , K^+ , Cl^- , SO_4^{2-} , F^- , and Si, and $\delta^{13}\text{C}$ isotope values. The major phases that could produce these ions include CO_2 gas, calcite, gypsum, halite, fluorite, biotite, sylvite, $\text{Ca}^{2+}/\text{Na}^+$ Exchange, albite, K-

feldspar, forsterite, enstatite, quartz, Na-clay, and Mg-clay. Not all of the phases were included in each flow path model – only those deemed applicable to each path were included in the individual models (Table 8).

The published solute chemistry data for Mt. Lassen, CA snow (Laird et. al., 1986) and initial waters for the seven chemical flow paths were used to model geochemical changes at the very beginning of the flow paths. Geochemical changes from initial to final waters were then modeled. Each NETPATH run produced one or more feasible models which describe the water's evolution from precipitation to the initial water and then to the final water (Table 9 and Figures 25 through 27). For the flow paths with more than one model, the author assumes that a combination of the models is the best representation of the processes occurring in Honey Lake Basin. Carbon-13 was used to determine the credibility of the models produced by NETPATH using Rayleigh calculations and a CO₂ gas value of -20‰. A comparison of observed and computed values shows that there is excellent agreement (Table 9), and that the reported NETPATH models are reasonable.

The models from NETPATH indicate that the precipitation in the high elevations easily evolves into the flow path initial waters because it is undersaturated with respect to all minerals. Upon infiltration, the precipitation generally dissolves CO₂ gas and minor amounts of calcite, gypsum, halite, and fluorite from the soil zone, and undergoes some ion exchange. Feldspars are also dissolved from the igneous rocks, and enstatite and/or forsterite are dissolved along the more mafic flow paths. The Susan River and Sierra Nevada flow paths do not undergo ion exchange, but lose K⁺, as the product of

incongruent dissolution, to the production of clays. Additionally, and Mg^{2+} was removed and incorporated in to clays along the Antelope Mountain/Litchfield flow path.

As the still undersaturated and unmixed initial waters flow down gradient to the basin floor and evolve into the final waters, they generally dissolve CO_2 gas, calcite, gypsum, halite, feldspars, biotite, and fluorite and undergo ion exchange. Exceptions include the release of CO_2 gas and precipitation of gypsum along the Sierra Nevada flow path, and no ion exchange along the West Skedaddle/Amedee flow path. Enstatite and forsterite are dissolved along the more mafic flow paths while quartz is dissolved in the more felsic areas. Few solutes are removed from solution expect for Na^+ which is incorporated into clays as a product for an incongruent dissolution of feldspar.

For the Susan River and Shaffer Mountain mixing model, NETPATH determined that an approximately 40/60, Susan River/Shaffer Mountain ratio was need and that this mixture would dissolve CO_2 gas, albite, calcite, and fluorite, undergo ion exchange, and precipitate halite, gypsum, sylvite, and Na-clay.

For the two chemical flow paths, Susan River and West Skedaddle/Amedee, which were modeled using a mix of initial waters and thermal waters, NETPATH determined that 5-28% of the final water was from the thermal component. With these mixtures, the initial waters dissolved CO_2 gas, calcite, halite, gypsum, fluorite, K-feldspar, biotite, enstatite, forsterite, and quartz, and experienced ion exchange. Both mixing flow paths lost Na^+ to the formation of clays.

FLOW PATH DESCRIPTIONS

Fault Controlled Flow Paths

There are two main fault controlled groundwater flow paths in Honey Lake Basin: the Honey Lake/Warm Springs Fault Zone and the Antelope Mountain/Litchfield Fault Zone. They are located along the edges of the basin floor in the west-southwest and in the north, respectively, where several deep cutting normal faults are exist. These faults are the western extension of the Basin and Range Province.

The Honey Lake/Warm Springs Fault Zone flow path has Na^+ - HCO_3^- to Ca^{2+} - HCO_3^- groundwaters that range in temperature from 35-52°C and circulate approximately 1.6-3.0 km down along the faults. Oxygen-18 and δD isotopes show that these groundwaters do not deviate from the local meteoric water line and were thus recharged from precipitation that fell under similar climatic conditions as the present. Very little ^3H (0.4 TU) was detected along this flow path and therefore, post-1952 precipitation is not thought to play a significant role in recharge. Carbon-14 ages could not be calculated. Carbon-13 values (mean of -13‰) show moderate interaction with carbonates. NETPATH results indicate the thermal waters of this flow path evolved from precipitation. Upon infiltration, the recharge waters dissolved CO_2 gas from the soil zone, dissolve calcite, fluorite, gypsum, and halite from lacustrine deposits, experienced ion exchange with clays, and dissolved K-feldspar, biotite, and quartz from the granitoid basement. None of which was done in large amounts, and thus these groundwaters have relatively low conductivity (TDS ~ 290 mg/L).

The Antelope Mountain/Litchfield Fault Zone flow path groundwaters are Na⁺-SO₄²⁻ in composition, range in temperature from 63-103°C, and circulate to approximately 2.8-3.8 km along the faults. Very little (0.2 TU) to no ³H was detected in these thermal groundwaters. Carbon-14 isotopes indicate that the mean groundwater age along the Antelope Mountain Fault Zone is 13,000-14,500 years. This suggest that the flow path contains very little, if any, modern recharge. Carbon-13 values (mean of -12‰) show moderate interaction with carbonates. Oxygen-18 and δD isotopes show that the Antelope Mountain/Litchfield Fault Zone groundwaters were recharged by cool, high latitude and altitude precipitation, but also experienced much rock-water interaction due to extremely high groundwater temperatures. NETPATH results indicate the thermal waters of this flow path easily evolve from precipitation and that high temperatures allowed the groundwater to dissolve CO₂, halite and gypsum and some calcite from lacustrine deposits, quartz, albite, and biotite from the igneous rocks, undergo ion exchange, and produce Mg-clays.

Susan River Flow Path

The Susan River flow path begins as precipitation in the northernmost Sierra Nevada Mountains and eventually terminates at the Susan River delta, where it flows into Honey Lake. As the groundwater flows along this path, it interacts with the Sierra Nevada granodiorites, some volcanics from the Modoc Plateau, and basin fill lacustrine sediments. It also mixes with thermal waters from the north-western portion of the Honey Lake Fault Zone, at a ratio of approximately 30/70 thermal to cold water. Consequently, the groundwater at the beginning of the flow path is fairly clean but as it

flows toward Honey lake, it slightly increases in Ca^{2+} , Mg^{2+} , and K^+ concentrations and increases much in Na^+ , HCO_3^- , Cl^- , SO_4^{2-} , and SiO_2 concentrations. These increases are a result of the dissolution of CO_2 from the soil zone, small amounts of biotite, K-feldspar, enstatite, and forsterite and much quartz from granodiorites and volcanics, calcite, gypsum, and halite from lacustrine sediments, ion exchange with clays, and the production of much Na-clay.

Groundwaters at the head of this flow path have detectable ^3H measurements and thus have a component of post-1952 recharge. However, these measurements decrease toward the basin floor where ^3H eventually becomes non-detectable. This trend is also reflected in the calculated mean ^{14}C ages. Most of the groundwaters have modern ages, except those near the terminus of the path (21,500-23,500 years) and those located near the faults (2500 years near the Honey Lake Fault Zone, and 13,000-14,500 years near the Antelope Mountain/Litchfield Fault Zone).

Carbon-13 values increase toward the end of this flow path, reflecting an increasing interaction with carbonates as the groundwater interacts with more lacustrine sediments.

Oxygen-18 and δD isotopes for groundwaters along this flow path plot close to the local meteoric water line and exhibit little evaporation, with some rock-water interactions as a result of mixing with thermal waters.

Shaffer Mountain Flow Path

The Shaffer Mountain flow path begins as precipitation on Shaffer Mountain and the surrounding highlands of the Modoc Plateau. It then infiltrates the ground, where it comes in contact with Tertiary Volcanics and lacustrine sediments as it flows down

gradient. Along its way, it mixes with some of the high temperature thermal waters from the Antelope Mountain/Litchfield Fault Zone at an approximately 30/70 thermal to cold water ratio. It eventually terminates at the Susan River delta where it mixes with the end of the Susan River flow path before discharging into Honey Lake.

Like the Susan River flow path, the Shaffer Mountain flow path slightly increases in Ca^{2+} , Mg^{2+} , and K^+ concentrations and increases much in Na^+ , HCO_3^- , Cl^- , SO_4^{2-} , and SiO_2 concentrations as the groundwater flows to the basin floor. These increases are a result of the dissolution of CO_2 from the soil zone, small amounts of biotite, K-feldspar, enstatite, and forsterite and much quartz from granodiorites and volcanics, calcite, gypsum, and halite from lacustrine sediments, ion exchange with clays, and the production of much Na-clay. This flow path then mixes with the Susan River flow path close to Honey Lake at an approximately 40/60, Susan River/Shaffer Mountain ratio. The mixture then dissolves CO_2 gas, albite, calcite, and fluorite, undergoes ion exchange, and precipitates halite, gypsum, sylvite, and Na-clay.

Unlike the Susan River flow path, none of the samples in the Shaffer Mountain flow path that were analyzed for ^3H contained an appreciable amount (maximum of 0.6 TU). Indicating that post-1952 recharge does not play a large role in this flow path. Mean ^{14}C ages, however, indicate that the groundwaters at the head and toward the end of the flow path are relatively modern. This supports Varian's (1997) conclusion that groundwater in the northwestern part of the basin are recharged from waters further to the north, and not locally.

Carbon-13 values increase toward the end of this flow path, reflecting an increasing interaction with carbonates as the groundwater interacts with more lacustrine sediments.

Oxygen-18 and δD isotopes plot close to the local meteoric water line, but also show some rock-water interactions as a result of mixing with thermal waters.

Long Valley Creek Flow Path

The Long Valley Creek flow paths begins as precipitation in both the eastern Sierra Nevada Mountains and the western Fort Sage Mountains and terminates down gradient in Honey Lake. As it travels, it interacts with granodiorites, Tertiary volcanics, and much lacustrine sediment. It also mixes with thermal groundwaters from the Honey Lake/Warm Springs Fault Zone at an approximately 30/70 thermal to cold water mixing ratio.

This flow path's geochemical evolution is similar to that of the Susan River flow path in that the groundwater slightly increases in Ca^{2+} , Mg^{2+} , and K^+ concentrations and increases much in Na^+ , SO_4^{2-} , HCO_3^- , Cl^- , and SiO_2 concentrations along the flow path. These increases are a result of the dissolution of CO_2 from the soil zone, small amounts of biotite, K-feldspar, enstatite, and forsterite and much quartz from granodiorites and volcanics, calcite, gypsum, and halite from lacustrine sediments, ion exchange with clays, and the production of much Na-clay.

Many waters in the Long Valley flow path are believed to have a component of post-1952 recharge, as reflected by 3H measurements which are generally large in the highlands at the beginning of the flow path and decrease toward the basin floor where 3H was not detected. Mean ^{14}C ages also show that most of the groundwater along this path

consists of modern water, with noted exceptions in the area of the Sierra Army Depot, along the Warm Springs Fault Zone. These groundwaters were found to range between 1000-12,000 years old, with ^{14}C ages increasing with depth (Varian, 1997).

Carbon-13 values tend to increase toward the end of this flow path, reflecting an increasing interaction with carbonates as the groundwater interacts with more lacustrine sediments.

Several of the $\delta^{18}\text{O}$ and δD isotopes plot close to the local meteoric water line, but the majority exhibit a consistent evaporative trend that becomes more pronounced toward the end of the flow path.

Sierra Nevada Flow Path

The Sierra Nevada flow path begins as precipitation in the highlands of the Sierra Nevada Mountains and flows down into the basin toward Honey Lake. This flow path is fairly wide, but relatively short, compared with the other twelve flow paths. It consequently interacts with much granodiorite and a limited amount of lacustrine sediments as it flows down gradient.

According to the NETPATH results, the groundwater dissolves small amounts of CO_2 from the soil zone, biotite, K-feldspar, and quartz from the igneous bedrock, and calcite, halite, fluorite, and gypsum from lacustrine sediments, and undergoes some ion exchange with clays. The groundwater also loses some Na^+ , from incongruent dissolution of albite, to clays. This results in a rather small net increase of Ca^{2+} , Mg^{2+} , K^+ , Na^+ , HCO_3^- , SO_4^{2-} , Cl^- , F^- , and SiO_2 .

Tritium measurements are generally large in the highlands at the beginning of the flow path, reflecting post-1952 recharge, and decrease toward the basin floor where ^3H becomes non-detectable. No ^{14}C ages were calculated for this flow path.

Groundwater $\delta^{13}\text{C}$ values along this path remain relatively depleted because of limited interaction with lacustrine sediments.

Like the Susan River flow path, $\delta^{18}\text{O}$ and δD isotopes for groundwaters along this flow path plot close to the local meteoric water line.

West Skedaddle/Amedee Flow Path

The West Skedaddle/Amedee flow path begins as precipitation in the Modoc Plateau and flows down gradient, and west, toward Honey Lake where it terminates. As it travels, it interacts with Tertiary volcanics and lacustrine sediments, and mixes with the high temperature thermal waters of the Antelope Mountain/Litchfield Fault Zone at an approximately 5/95 thermal to cold water ratio. Consequently, the groundwater along this flow path increases in Ca^{2+} , Mg^{2+} , K^+ , Na^+ , HCO_3^- , SO_4^{2-} , Cl^- , F^- , and SiO_2 concentrations much more so than the groundwaters along Sierra Nevada flow path. These increases are due to dissolution of CO_2 from the soil zone, K-feldspar, enstatite, forsterite and quartz from the igneous bedrock, and calcite, halite, gypsum, and fluorite from lacustrine sediments, and the production of Na-clay.

Like the Shaffer Mountain flow path, none of the samples analyzed contained much (maximum 0.3 TU), if any ^3H , again, indicating that post-1952 recharge does not play a large role in this flow path. Mean ^{14}C ages show that the groundwaters in this flow path are considerably older than those on the opposite side of the basin. They range in

age from 9000-13,500 years old and are closely associated with the deeply circulating, old, thermal waters of the Antelope Mountain/Litchfield Fault Zone flow path.

Carbon-13 values along this flow path appear to be constant (~ 10‰) throughout the flow path. Groundwater at the beginning of this flow path is likely more depleted at but no samples have been collected from that area.

Several of the $\delta^{18}\text{O}$ and δD isotopes for groundwaters along this flow path plot close to the local meteoric water line, however, the influence of mixing with the Antelope Mountain/Litchfield Fault Zone thermal waters can be seen in the shift to the right in the rock-water interaction direction. Some of these waters also appear to experience evaporation.

East Skedaddle/Amedee Flow Path

The East Skedaddle/Amedee flow path begins as precipitation in the Modoc Plateau and flows down gradient, and east, toward Fish Springs Playa where it terminates. It is separated from the West Skedaddle/Amedee flow path by a low elevation surface water divide. As the groundwater travels along this flow path, it interacts with Tertiary volcanics and lacustrine sediments and thus experiences moderate increases in Ca^{2+} , Mg^{2+} , K^+ , HCO_3^- , SO_4^{2-} , and F^- , extremely large increases in Cl^- and Na^+ , and a decrease of SiO_2 . According to NEPATH, this is a result of the dissolution of much CO_2 from the soil zone, K-feldspar, quartz, enstatite, and forsterite from the volcanics, and calcite, gypsum, halite, and some fluorite from lacustrine sediments, much ion exchange, and the production of much Na-clay.

Some ^3H (maximum of 1 TU) was found in several water samples in this flow path, indicating a small component of post-1952 recharge to the flow path. Mean ^{14}C

ages show that the groundwater toward the middle of the flow path shows some modern ages, but that closer to Fish Springs Playa, the groundwater becomes much older (7500-10,000 years old).

Carbon-13 values increase along the flow path, reflecting an increased interaction with carbonates as the groundwater flows through lacustrine sediments.

Several of the $\delta^{18}\text{O}$ and δD isotopes plot close to the local meteoric water line, but the majority exhibit a consistent evaporative trend, which is present in both the samples in the highlands and on basin floor.

Neversweat Flow Path

The Neversweat flow path begins as precipitation in the north-eastern Virginia Mountains where upon infiltration, interacts with Tertiary volcanics and lacustrine sediments as it flows down gradient and terminates in the Fish Springs Playa. Along this path, the groundwater experiences a moderate increases in Ca^{2+} , Mg^{2+} , K^{+} , HCO_3^{-} , SO_4^{2-} , and F^{-} , extremely large increases in Cl^{-} and Na^{+} , and decrease in SiO_2 . According to NEPATH, this is a result of the dissolution of much CO_2 from the soil zone, K-feldspar, quartz, enstatite, and forsterite from the volcanics, and calcite, gypsum, halite, and some fluorite from lacustrine sediments, much ion exchange, and the production of much Na-clay.

Tritium analysis along the Neversweat flow path show that ^3H , and therefore post-1953 recharge, is present in the highlands in some groundwaters, but is absent in others. Mean ^{14}C ages indicate the groundwaters at the start and middle of this flow path are modern. Samples taken at the end of this flow path were not analyzed for ^{14}C and therefore, no ages could be calculated.

The limited amount of $\delta^{13}\text{C}$ data available shows values that indicate some interaction with carbonates along this flow path.

Extremely few locations were available for sample collection along this flow path, but those that were show $\delta^{18}\text{O}$ and δD isotope values that bound the local meteoric water line.

Astor/Sand Pass Flow Path

The Astor/Sand Pass flow path begins as precipitation in the Terraced Hills, north of the Virginia Mountains, and flows down gradient into the basin where it eventually terminates in Fish Springs Playa. Along this path, it interacts with Tertiary volcanics and lacustrine sediments, and thus experiences the same changes in solute chemistry as the Neversweat flow path; a moderate increases in Ca^{2+} , Mg^{2+} , K^+ , HCO_3^- , SO_4^{2-} , and F^- , extremely large increases in Cl^- and Na^+ , and a decrease in SiO_2 . According to NEPATH, these changes are a result of the dissolution of much CO_2 from the soil zone, K-feldspar, quartz, enstatite, and forsterite from the volcanics, and calcite, gypsum, halite, and some fluorite from lacustrine sediments, much ion exchange, and the production of much Na-clay.

Little ^3H data is available for the groundwaters in this flow path, but in it as found in the one sample that was analyzed. This sample was located more toward the middle of the flow path, indicating that post-1952 recharge could be fairly important to this flow path. No ^{14}C ages were available for age calculations.

Carbon-13 values along this flow path are low ($\sim -5.5\text{‰}$), indicating much interaction with carbonates or organic matter.

Like the Neversweat flow path, extremely few locations were available for sample collection along this flow path but those that were, show $\delta^{18}\text{O}$ and δD isotope values that bound the local meteoric water line and follow an evaporative trend.

Virginia Mountains Flow Path

The Virginia Mountains Flow Path begins as precipitation in the Virginia Mountains where upon infiltration, the groundwater interacts with Tertiary volcanics and lacustrine sediments as it flows down gradient and eventually terminates in the Fish Springs Playa. It is very similar to the Neversweat, East Skedaddle/Amedee, and Astor/Sand Pass flow paths in that there is a moderate increases in Ca^{2+} , Mg^{2+} , K^+ , HCO_3^- , SO_4^{2-} , and F^- , extremely large increases in Na^+ and Cl^- , and a decrease in SiO_2 along the flow path. This is accomplished by the dissolution of much CO_2 from the soil zone, quartz, biotite, K-feldspar, enstatite, and forsterite from the volcanics, and calcite, gypsum, halite, and some fluorite from lacustrine sediments, much ion exchange, and the production of Na-clay.

No ^3H was detected in most areas of the flow path, but some ^3H was present in the end of the flow path (maximum of 1.7 TU), adjacent to Fish Springs Playa. Thus, post-1952 recharge is present in this flow path. Mean ^{14}C ages adjacent to Fish Springs Playa are 1500-4000 years. This flow path appears to be a good mix of both modern and old groundwaters.

Carbon-13 values increase toward Fish Springs Playa, and show that the groundwater in this flow path picks up almost as much carbon from interaction with carbonates as it does from the soil zone.

Several of the $\delta^{18}\text{O}$ and δD isotopes plot close to the local meteoric water line, but the majority exhibit a consistent evaporative trend, especially those groundwaters closer to the playa.

Cottonwood Flow Path

The Cottonwood flow path begins as precipitation in the Virginia Mountains, infiltrates the ground, flows a relatively short distance, discharges as springs halfway down the mountain slope, and then either re-infiltrates the ground or flows down to the basin in streams where it then infiltrates the lacustrine sediments and flows into Fish Springs Playa. Along this path, it interacts with Tertiary volcanics and lacustrine sediments, and thus there are moderate increases in Ca^{2+} , Mg^{2+} , K^+ , HCO_3^- , SO_4^{2-} , and F^- concentrations, extremely large increases in Na^+ and Cl^- concentrations, and a slight decrease in the SiO_2 concentration along the flow path. According to the NETPATH models, this is accomplished by the dissolution of much CO_2 from the soil zone, quartz, biotite, K-feldspar, enstatite, and forsterite from the volcanics, and calcite, gypsum, halite, and some fluorite from lacustrine sediments, much ion exchange, and the production of Na-clay.

Most, if not all, of the groundwaters in the Cottonwood flow path are thought to contain post-1952 recharge. Tritium is very high (> 8 TU) at the head of the flow path, and is also found toward the end (1.2 TU). No ^{14}C ages were calculated for this flow path.

Carbon-13 measured at the head of the flow path shows addition of carbon to the system from CO_2 in the soil zone and organic matter in aerobic conditions. Values are

likely to decrease toward Fish Springs Playa as the groundwater interacts with carbonates in lacustrine sediments, but not data is available to support this assumption.

Oxygen-18 and δD isotopes plot close to the local meteoric water line, but also exhibit a slight evaporative trend.

Fort Sage Mountains Flow Path

The Fort Sage Mountains flow path begins as precipitation in the Fort Sage Mountains and flows into the basin where it terminates in Fish Springs Playa. This flow path interacts with granodiorites, some Tertiary volcanics, and lacustrine sediments. As the groundwater flows down gradient, it increases slightly in Ca^{2+} , Mg^{2+} , K^+ , HCO_3^- , SO_4^{2-} , and F^- concentrations, increases much in Na^+ and Cl^- concentrations, and decreases in SiO_2 along the flow path. According to the NETPATH models, this is accomplished by the dissolution of much CO_2 from the soil zone, quartz, biotite, K-feldspar, enstatite, and forsterite from the volcanics, and calcite, gypsum, halite, and some fluorite from lacustrine sediments, much ion exchange, and the production of Na-clay.

No 3H data was available for the groundwaters in the highlands of this flow path, and very little 3H was measured at the end of the flow path (maximum 0.5 TU). Post-1952 recharge more than likely plays a role in the recharge of this flow path much like it does in the neighboring Virginia Mountains flow path. Mean ^{14}C ages indicate that the groundwater near the middle of the flow path is modern to 2500 years old.

Carbon-13 measurements were only made on one of the samples, located in the middle of this flow path (-14.1‰). Like the Fort Sage Mountains flow path, $\delta^{13}C$ values are likely to decrease toward Fish Springs Playa as the groundwater interacts with carbonates in lacustrine sediments, but not data is available to support this assumption.

Several of the $\delta^{18}\text{O}$ and δD isotopes plot close to the local meteoric water line, but the majority exhibit a consistent evaporative trend, especially those groundwaters closer to the playa.

CONCLUSION

Groundwater flowing through granitic terrain (west-southwest Honey Lake Basin) is dominantly calcium-bicarbonate in character and has low TDS (~ 150 mg/L), whereas groundwater flowing through mafic terrain (north and east Honey Lake Basin) is dominantly sodium-bicarbonate in character with a slightly higher TDS (~ 200 mg/L; Figure 28). Once these low TDS groundwaters encounter lacustrine deposits down gradient on the basin floor, the solute load increases (~ 300 mg/L) and the groundwater becomes sodium-bicarbonate in character. Dissolution of silicate minerals, calcite, and ion exchange with clays is responsible for these geochemical changes. Further down gradient, contact with evaporite minerals, such as halite and gypsum, in the playa areas causes the evolution to sodium-chloride groundwater and dramatically increases the TDS (~ 1100 mg/L on the Honey Lake Playa and 43,000 mg/L on the Fish Springs Playa). The sharp contrast in the concentrations of evaporite minerals in the groundwater from the two separate playas seems counterintuitive since both playas have the same origin, Lake Lahontan, and should therefore exhibit the same characteristics. It is concluded that episodic post Lahontan flooding of the basin, via inflow from Susan River and Long Valley Creek on the west, dissolved evaporite minerals on Honey Lake Playa and flushed them east to Fish Springs Playa (Figure 29). Much evaporation in this area and closed basin conditions prevent groundwater out flow and effectively concentrate the solute load on the playa.

Stable isotopes show that groundwater throughout the closed basin has a meteoric origin and experiences much evaporation, especially in areas which receive little

precipitation annually (eastern Honey Lake Basin). Groundwater in areas which experience mixing with upwelling thermal groundwater have stable isotope values which show exchange with silicate minerals at high temperatures ($> 100^{\circ}\text{C}$), as well as evaporation.

Carbon -13 analysis shows increased interaction with carbonates, and possibly organic matter, in lacustrine sediments as groundwater flows down gradient to the basin floor. Tritium analysis shows that post-1952 precipitation is an important source to highland groundwater recharge, but does not greatly affect groundwater on the basin floor. Carbon-14 ages show that these geochemical evolutions occur over a long period; 1,000-5,000 years for the shorter flow paths in eastern Honey Lake Basin and 10,000-23,500 years for the longer flow paths in western Honey Lake Basin.

This investigation provides insight into the geochemical evolution of groundwater flow from both mafic and granitic terrains to lacustrine sediments with evaporite minerals, in a closed basin environment.

REFERENCES

- Adams, M.C., 1984, Geochemistry of the Wendel-Amedee geothermal system, California: Geothermal Resources Council, Transactions, Vol. 8, pp. 363-368.
- Adams, K.D., 1997, Late Quaternary pluvial history, isostatic rebound, and active faulting in the Lake Lahontan Basin, Nevada and California: Doctoral dissertation, University of Nevada-Reno, 169 p.
- Anderson, K., Nelson, S.T., Mayo, A.L., and Tingey, D.G., 2005, Interbasin flow revisited: the contribution of local recharge to high-discharge springs, Death Valley, CA: Journal of Hydrology, Vol. 323, pp. 276-302.
- Beaudoin, G. and Therrien, P., 2007, Stable isotope fractionation calculator (SIFC); Université Laval, http://www.ggl.ulaval.ca/cgi-bin/isotope/generisotope_4alpha.cgi.
- Benson, L., 1993, Carbonate deposition, Pyramid Lake Subbasin, Nevada: 1. sequence of formation and elevation distribution of carbonate deposits (tufas): Palaeogeography, Palaeoclimatology, Palaeoecology, Vol. 109, pp. 55-87.
- Benson, L., White, L.D., and Rye, R., 1996, Carbonate deposition, Pyramid Lake Subbasin, Nevada: 4. comparison of the stable isotope values of carbonate deposits (tufas) and the Lahontan lake-level record: Palaeogeography, Palaeoclimatology, Palaeoecology, Vol. 122, pp. 45-76.
- Benson, L., 2004, The tufas of Pyramid Lake, Nevada: Geological Survey Circular, Report C 1267, 14 p.
- Blackwell, D.D., Wisian, K.W., Richards, MC., and Steele, J.L., 2000, Geothermal resource/reservoir investigations based on heat flow and thermal gradient data for the United States: US Department of Energy, Technical Report 13504, 51 p.
- Bonham, H.F., 1969, Geology and mineral deposits of Washoe and Storey Counties, Nevada: Nevada Bureau of Mines and Geology, Bulletin 70, p. 140.
- California Department of Water Resources, 1962, Geographic distribution of precipitation in northeastern California: California Department of Water Resources, map.
- California Department of Water Resources, 1963, Northeastern counties ground-water investigation: California Department of Water Resources, Water Resources Bulletin 98, V. 1, 244 p.

- California Department of Water Resources, 2003, Honey Lake Valley groundwater basin: California Department of Water Resources, California's Groundwater Bulletin 118, 7 p.
- Clark, I. and Fritz, P., 1997, Environmental Isotopes in Hydrogeology: Boca Raton, Florida, Lewis Publishers, 328 p.
- Coplen, T.B., 1998, Normalization of oxygen and hydrogen isotope data: Chemical Geology, Vol. 72, pp. 293-297.
- Craig, H., 1961, Isotopic variations in meteoric waters: Science, Vol. 133, pp. 1702-1703.
- Deines, P., D. Langmuir, and R. S. Harmon, 1974, Stable carbon isotope ratios and the existence of gas phase in the evolution of carbonate ground waters: Geochimica et Cosmochimica Acta, Vol.38, no.7, pp.1147-1164.
- Domenico, P.A. and Schwartz, F. W., 1998, Physical and chemical hydrogeology: New York, New York, John Wiley & Sons, pp. 279-280 and 319-322.
- Eggett, D., 2007, Research Associate Professor of Statistics: Brigham Young University, personal communication.
- Environmental Isotopes Laboratory, 1998, Tritium analysis: technical procedure 1.0: Department of Earth Sciences, University of Waterloo.
- Faure, G. and Mensing, T.M., 2005, Isotopes: principles and applications, Third Edition: Hoboken, New Jersey, John Wiley & Sons, pp.693-744.
- Fontes, J.Ch., 1983, Dating of groundwater in guidebook on nuclear techniques in hydrology: International Atomic Energy Agency, Technical Report Services 91, p. 285-317.
- Fontes, J.Ch. and Garnier, J.M., 1979, Determination of the initial ^{14}C activity of the total dissolved carbon: a review of the existing models and a new approach: Water Resource Research, Vol. 15, n. 2, p. 399-413.
- Fournier, R.O. and Rowe, J.J., 1966, Estimation of underground temperatures from the silica content of water from hot springs and wet-steam wells: American Journal of Science, Vol. 264, pp. 685-697.
- Fournier, R.O., and Truesdell, A.H., 1973, An empirical Na-K-Ca geothermometer for natural waters: Geochimica et Cosmochimica Acta, Vol. 37, Issue 5, p. 1255-1275.

- Fournier, R.O, White, D.E., and Truesdell, A.H., 1974, Geochemical indicators of subsurface temperature; Part I, basic assumptions: U.S. Geological Survey, Open-File Report 74-1033, 384 p.
- Fournier, R.O., and Rowe, J.J., 1977, The solubility of amorphous silica in water at high temperatures and high pressures: American Mineralogist, Vol. 62, p. 1052-1056.
- Fournier, R.O., 1979, A revised equation for the Na-K geothermometer: Geothermal Resource Council, Trans., Vol. 3, p. 221-224.
- Fuis, G.S., Zucca, J.J., Mooney, W.D., and Milkereit, B., 1987, A geologic interpretation of seismic-refraction results in northeastern California: Geological Society of America Bulletin, Vol. 98, No. 1, pp. 53-65.
- Geoproducts Corporation, 1984, The Honey Lake geothermal project, Lassen County, California: U.S. Department of Energy, Final Technical Report 12262-T1, 56 p.
- Grose, T.L.T., 1984, Geologic map of the State Line Peak Quadrangle, Nevada-California: Nevada Bureau of Mines and Geology, Map 82, scale 1:24,000.
- Grose, T.L.T, Saucedo, G.J., and Wagner, D.L., 1991, Geologic Map of the Susanville Quadrangle, Lassen and Plumas Counties, California: California Division of Mines and Geology, Map 20 p., scale 1:100,000.
- Handman, E.H., Lonquist, C.J., and Maurer, D.K., 1990, Ground-water resources of Honey Lake Valley, Lassen County, California, and Washoe County, Nevada: U.S. Geological Survey, Report 90-4050, 112 p.
- Hardt, W.F., Olmsted, F.H., and Trainer, F.W., 1975, Susanville-Honey Lake geothermal reconnaissance, southern Lassen County, California: U.S. Geological Survey, Open-File Report 76-429, 73 p.
- IAEA, 2001, Global Network of Isotopes in Precipitation Maps and Animations: International Atomic Energy Agency, Vienna, Accessible at <http://isohis.iaea.org>.
- Jones, B.F., Vandeburgh, A.S., Truesdell, A.H., and Rettig, S.L., 1969, Interstitial brines in playa sediments: Chemical Geology, Vol. 4, Issue 1-2, pp. 253-262.
- Klein, C., 2002, Mineral Science: New York, New York, John Wiley & Sons, 641 p.
- Laird, L.B., Taylor, H.E., and Lombard, R.R., 1986, Data on snow chemistry of the Cascade-Sierra Nevada Mountains: U.S. Geological Survey, Open-File Report 86-61, 25 p.

- Mariner, R.H., Presser, T.S., and Evans, W.C., 1977, Chemical composition data and calculated aquifer temperature for selected wells and springs of Honey Lake Valley, California: U.S. Geological Survey, Open-File Report 76-0783, 10 p.
- Mayo, A.L. and Slosson, J.E, 1992, The application of ground-water flow models as predictive tools—a review of two ground-water models of eastern Honey Lake Valley, California-Nevada: Bulletin of the Association of Engineering Geologists, Vol. XXIX, No. 2, pp. 151-163.
- Mayo, A.L., 2005, Professor of Geology: Brigham Young University, written communication.
- McDonald, G.A., 1966, Geology of the Cascade Range and Modoc Plateau: California Division of Mines and Geology, Bulletin 190, pp. 65-96.
- Miner, R.E., Nelson, S.T., Tingey, D.G., and Murrell, M.T., 2006, Using fossil spring deposits in the Death Valley region, USA to evaluate Palaeoflowpaths: Journal of Quaternary Science, Vol. 21.
- Moll, N.E., 2000, A groundwater flow model of eastern Honey Lake Valley, Lassen County, California and Washoe County, Nevada: Abstracts with Programs - Geological Society of America, Vol. 32, Issue 7, pp.252.
- Morrison, R.B., 1991, Quaternary stratigraphic , hydrologic, and climatic history of the Great Basin, with emphasis on Lakes Lahontan, Bonneville, and Tecopa; The Geology of North America, Quaternary Nonglacial Geology: Conterminous U.S.: Geological Society of America, Vol. K-2, pp. 283-320.
- Nathenson, M. and Guffanti, M., 1988, Geothermal gradients in the conterminous United States: Journal of Geophysical Research, Vol. 93, Issue B6, p. 6437-6450.
- Neary, M.P., 1997, Tritium enrichment: to enrich or not to enrich?: Radioactivity and Radiochemistry, Vol. 8:4, pp. 23-35.
- Nelson, S.T., 2007, Associate Professor of Geology: Brigham Young University, personal communication.
- Nelson, S.T., 2000, A simple, practical methodology for routine VSMOW/SLAP normalization of water sample analyzed by continuous flow methods: Rapid Communications in Mass Spectrometry, Vol. 14, pp. 1044-1046.
- Nelson, S.T. and Dettman, D., 2001, Improving hydrogen isotope ratio measurement for on-line Cr reduction systems: Rapid Communications in Mass Spectrometry, Vol. 15, pp. 2301-2306.

- Nelson, S.T., Wood, M.J., Mayo, A.L., Tingey, D.G., and Eggett, D., 2005, Shoreline tufa and tufaglomerate from Pleistocene Lake Bonneville, Utah, USA: stable isotopic and mineralogical records of lake conditions, processes, and climate: *Journal of Quaternary Science*, Vol. 20, pp.3-19.
- Oviatt, C.G., McCoy, W.D., and Nash, W.P., 1994. Sequence stratigraphy of lacustrine deposits – a quaternary example from the Bonneville basin, Utah: *Geological Society of America, Bulletin* 106, p. 133-144.
- Pearson, F.J., Jr., and Hanshaw, B.B., 1970, Sources of dissolved carbonate species in groundwater and their effects on carbon-14 dating: *Isotope Hydrology: Proceedings Symp. IAEA, Vienna*, pp. 271-286.
- Piper, A.M., 1944, A graphic procedure in the geochemical interpretation of water analyses: *Transcripts of the American Geophysical Union*, 25, p. 914-923.
- Plummer, L.N., Jones, B.F., and Truesdell, A.H., 1976, WATEQF a Fortran version of WATEQ a computer program for calculating chemical equilibrium of natural waters: *U.S. Geological Survey Water Resources Investigation*, 76-13, 60 p.
- Plummer, L.N., Prestemon, E.C., and Parkhurst, D.L., 1994, An interactive code (NETPATH) for modeling NET geochemical reactions along a flow PATH-version 2.0: *U.S. Geological Survey Water Resources Investigation, Report 94-4169*, 130 p.
- Polach, H.A., Stipp, J.J., 1967, Improved synthesis techniques for methane and benzene radiocarbon dating: *International Journal of Applied Radiocarbon and Isotopes*, v. 18, pp. 359-364.
- Reed, M.J., 1978, Chemistry of thermal waters in selected geothermal areas of California: *California Division of Oil & Gas, Report TR15*, pp. 13-16.
- Rockwell, G.L., 1993, Surface-water hydrology of Honey Lake Valley, Lassen County, California and Washoe County, Nevada: *U.S. Geological Survey, Open-File Report 90-177*.
- Roberts, C.T., 1985, Cenozoic evolution of the Northwestern Honey Lake Basin, Lassen County, CA: *Colorado School of Mines Quarterly*, Vol. 80, No. 1, pp. 283-320.
- Rose, T.P., Davisson, M.L., Hudson, G.B., and Varian, A.R., 1997, Environmental isotope investigation of groundwater flow in the Honey Lake Basin, California and Nevada: *Lawrence Livermore National Laboratory, Technical Report UCRL-ID-127978*, 72 p.
- SAHRA, 2006, Sustainability of semi-arid hydrology and riparian areas; Oxygen: *University of Arizona*, Accessible at: www.sahra.arizona.edu/programs/isotopes/oxygen.html.

- SAS Institute Inc., 2004, SAS Version 9.1: Cary, North Carolina.
- Schimschal, U., 1991, Integrated exploration for low-temperature geothermal resources in the Honey Lake Basin, California: *Geophysical Prospecting*, Vol. 39, pp. 279-291.
- Skiba, P.A., 1985, Artesian flow testing of the geothermal production wells WEN-1 and WEN-2, Honey Lake hybrid power plant project, California: *Transactions*, V. 9, Part II, pp. 585-589.
- Stiff, H.A. Jr., 1951, The interpretation of chemical water analyses by means of patterns: *Journal of Petroleum Technology* 3, p. 15-17.
- Stuvier, M., and Polach, H.A., 1977, Discussion: reporting of ^{14}C data: *Radiocarbon*, Vol. 19, n. 3, pp. 355-363.
- Tarbet, M.E.S., 2005, Evolution of paleo-climate for the Boise area, Idaho, from the last glacial maximum to the present based on $\delta^2\text{H}$ and $\delta^{18}\text{O}$ groundwater composition: Master's thesis, Brigham Young University, 56 p.
- Taylor, K., Widmer, M., and Chesley, M., 1992, Use of transient electromagnetic to define local hydrogeology in an arid alluvial environment: *Geophysics*, Vol. 57, No. 2, pp. 343-352.
- Truesdell, A.H., 1976, GEOTHERM, a geothermometric computer program for hot spring systems: *Proceedings 2nd UN Symposium on the Development and Use of Geothermal Resources*, San Francisco, 1975, Vol. 1, p. 831-836.
- Varian, A.R., 1997, Use of environmental isotopes to investigate hydrologic processes at Honey Lake Basin, Lassen County, California and Washoe County, Nevada: Master's thesis, University of Nevada-Reno, 132 p.
- Webber, W.D., 1996, Salinization of shallow ground waters in Honey Lake Valley, California-Nevada: Master's thesis, Brigham Young University, 106 p.
- Western Regional Climate Center, 2007, Susanville Airport and Doyle 4SSE stations: <http://www.wrcc.dri.edu/summary/Climsmnca.html>.
- Wills, C.J. and Borchardt, G., 1993, Holocene slip rate and earthquake recurrence on the Honey Lake fault zone, northeastern California: *Geology*, Vol. 21, pp. 853-856.

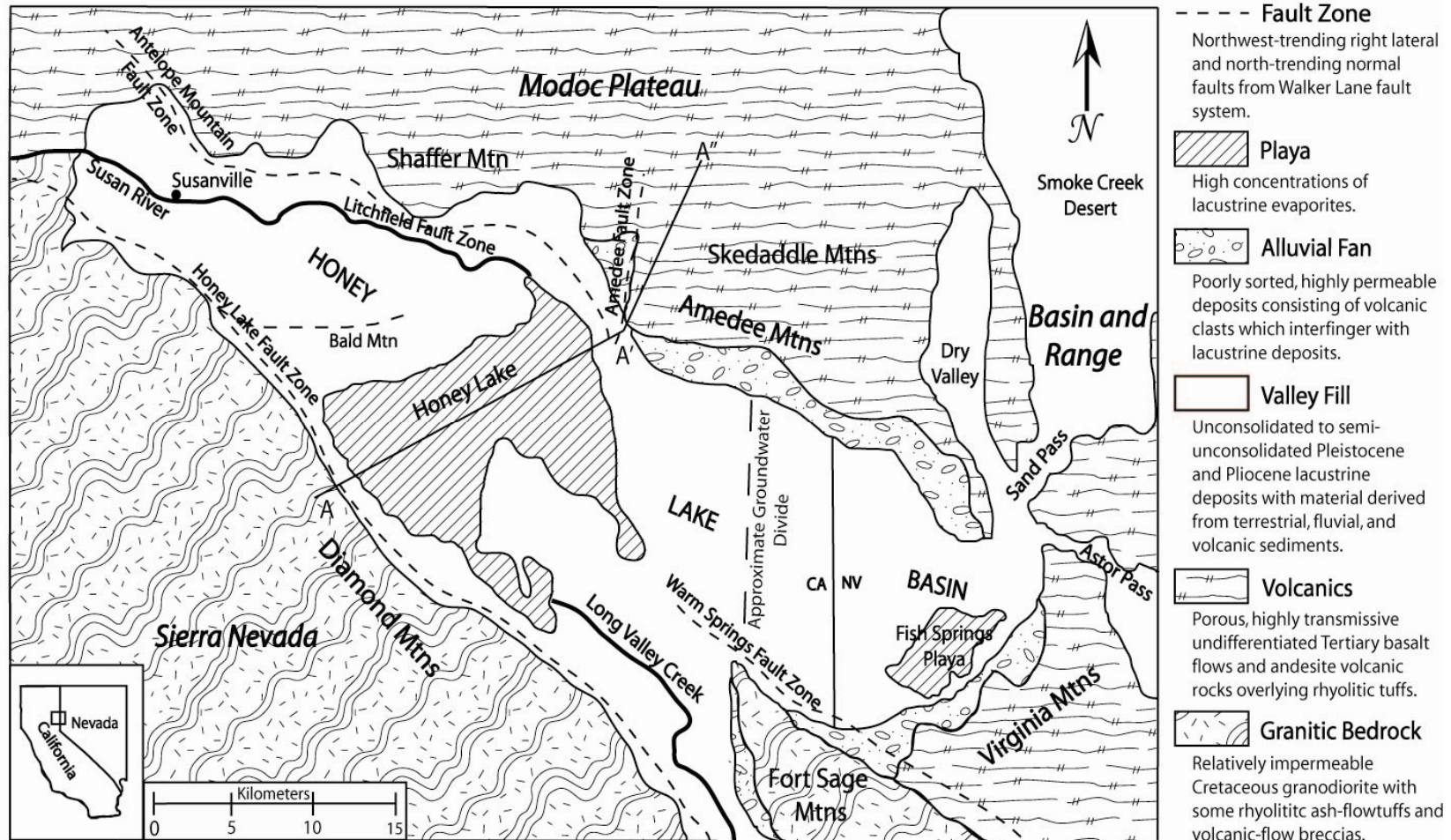


Figure 1. A simplified geologic map of the Honey Lake Basin, CA-NV. Modified from Mayo and Slosson, 1992 and Varian, 1997. Figure 3 is a cross section along A-A”.

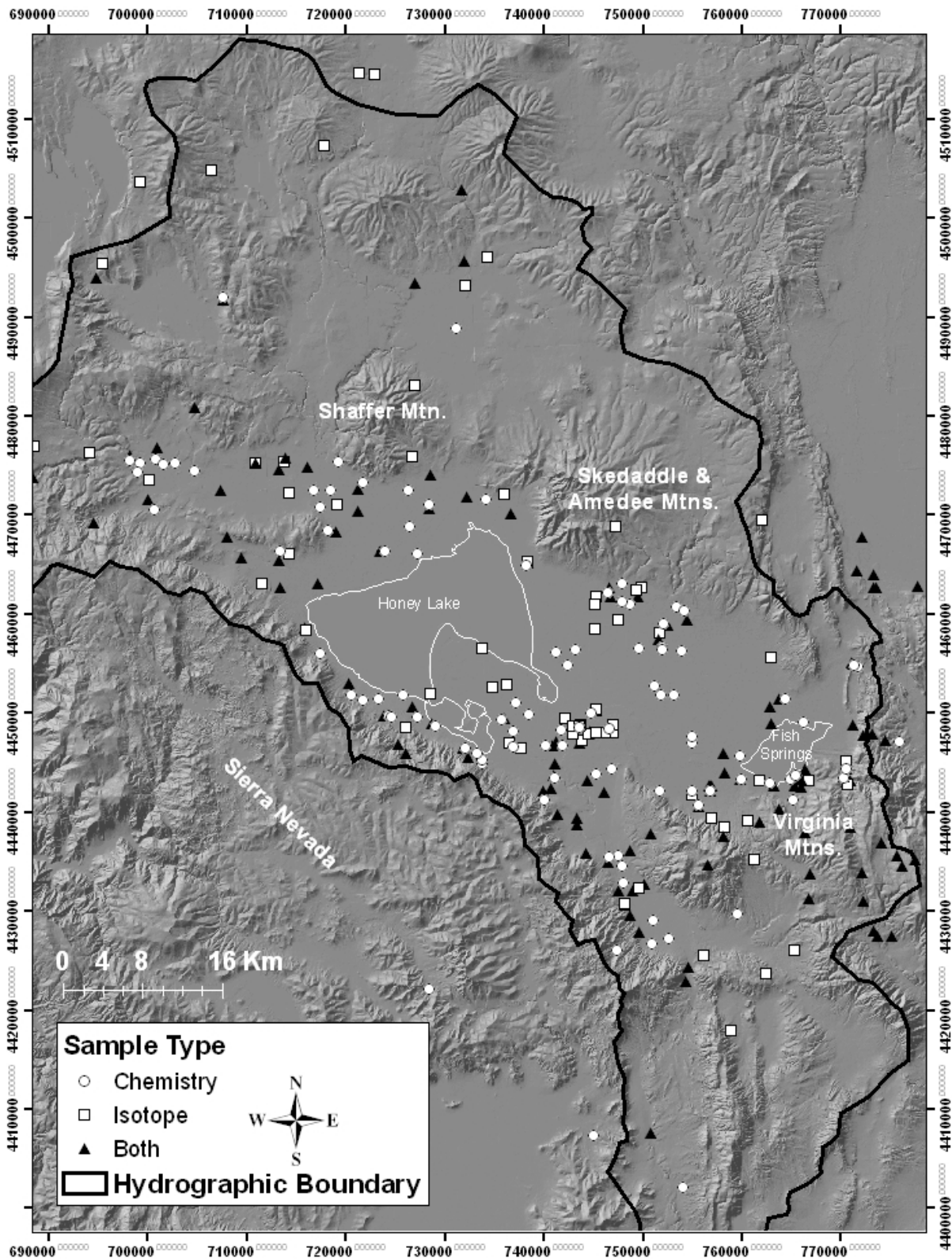


Figure 2. Honey Lake Basin sample location map. The hydrographic boundary was defined by Rockwell (1993).

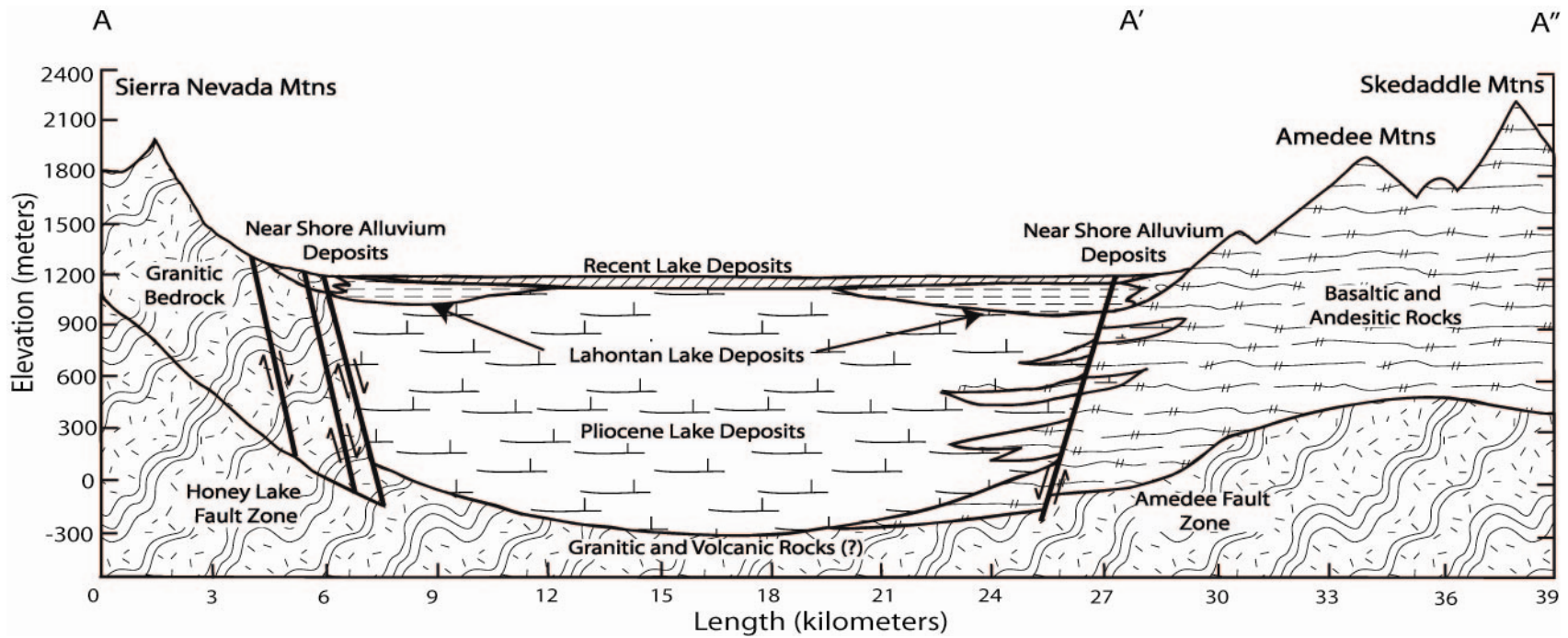


Figure 3. A simplified geologic cross section of Honey Lake Basin (Modified from California Department of Water Resource, 1963).

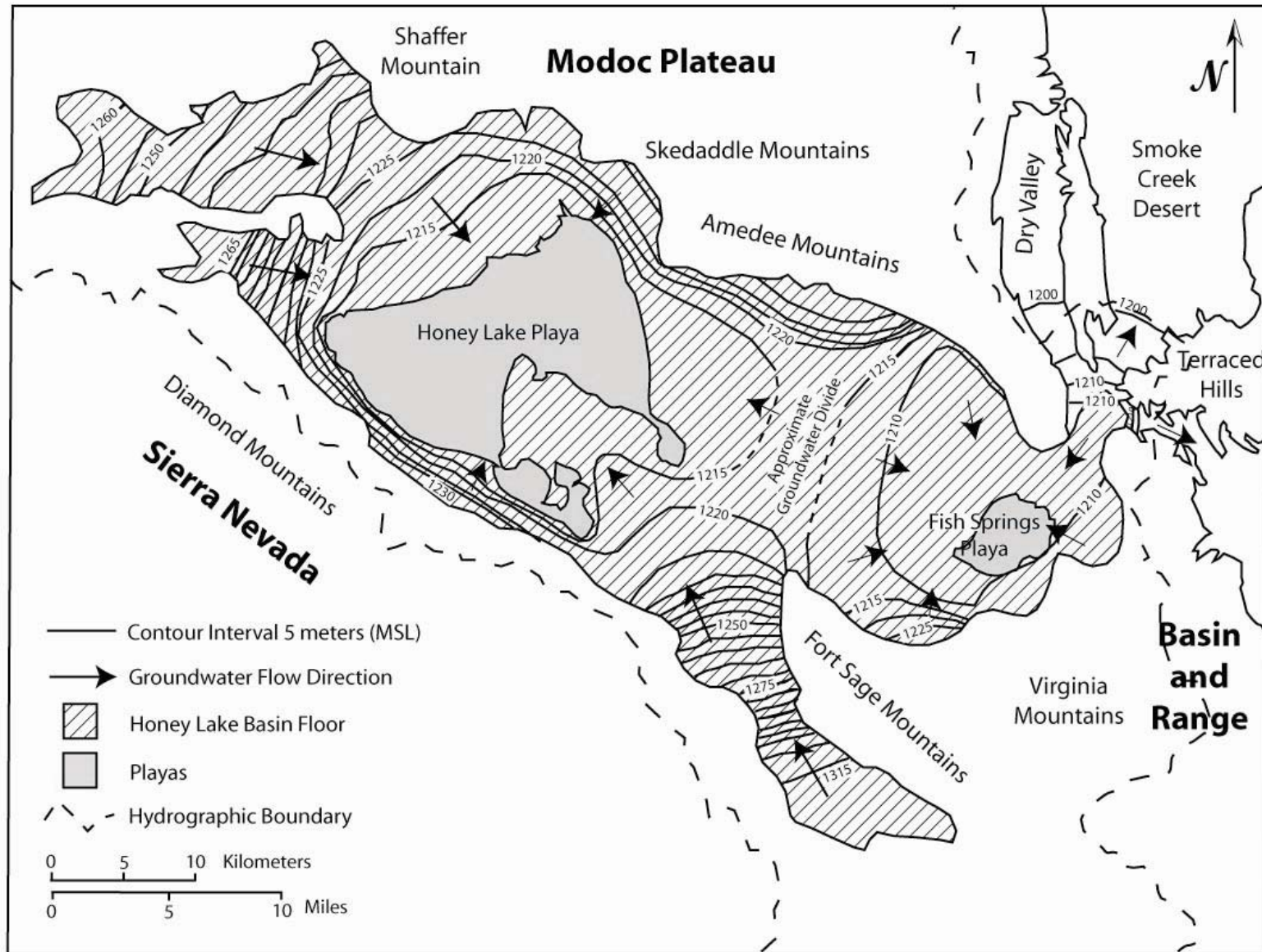


Figure 4. Groundwater level contour map. Groundwater flows from higher to lower water levels, or toward the basin floor.

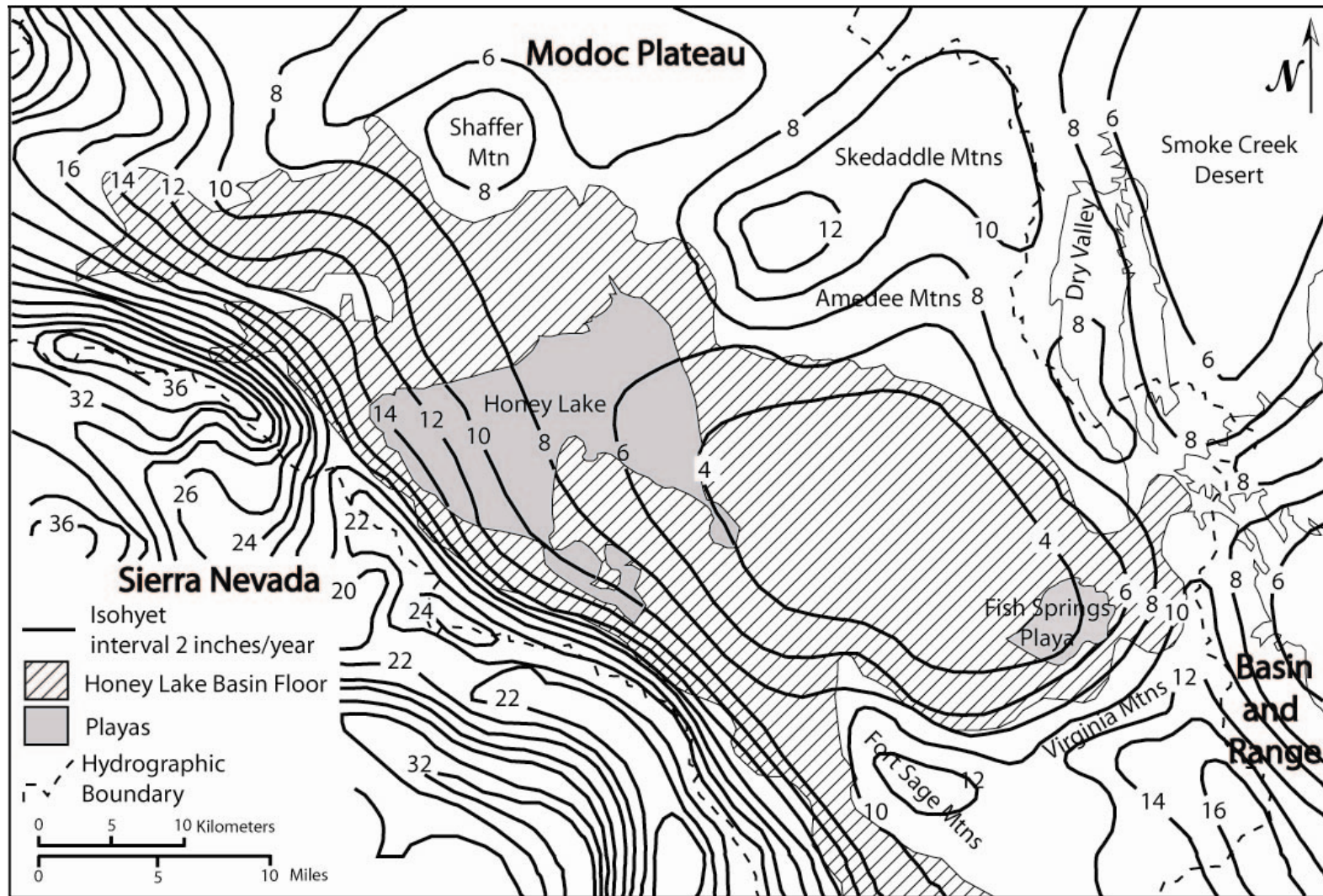


Figure 5. Isohyetal map of Honey Lake Basin. Note the large difference in the amount of precipitation between the east and west sides of the basin. Modified from Mayo and Slosson, 1992 and California Department of Water Resources, 1962.

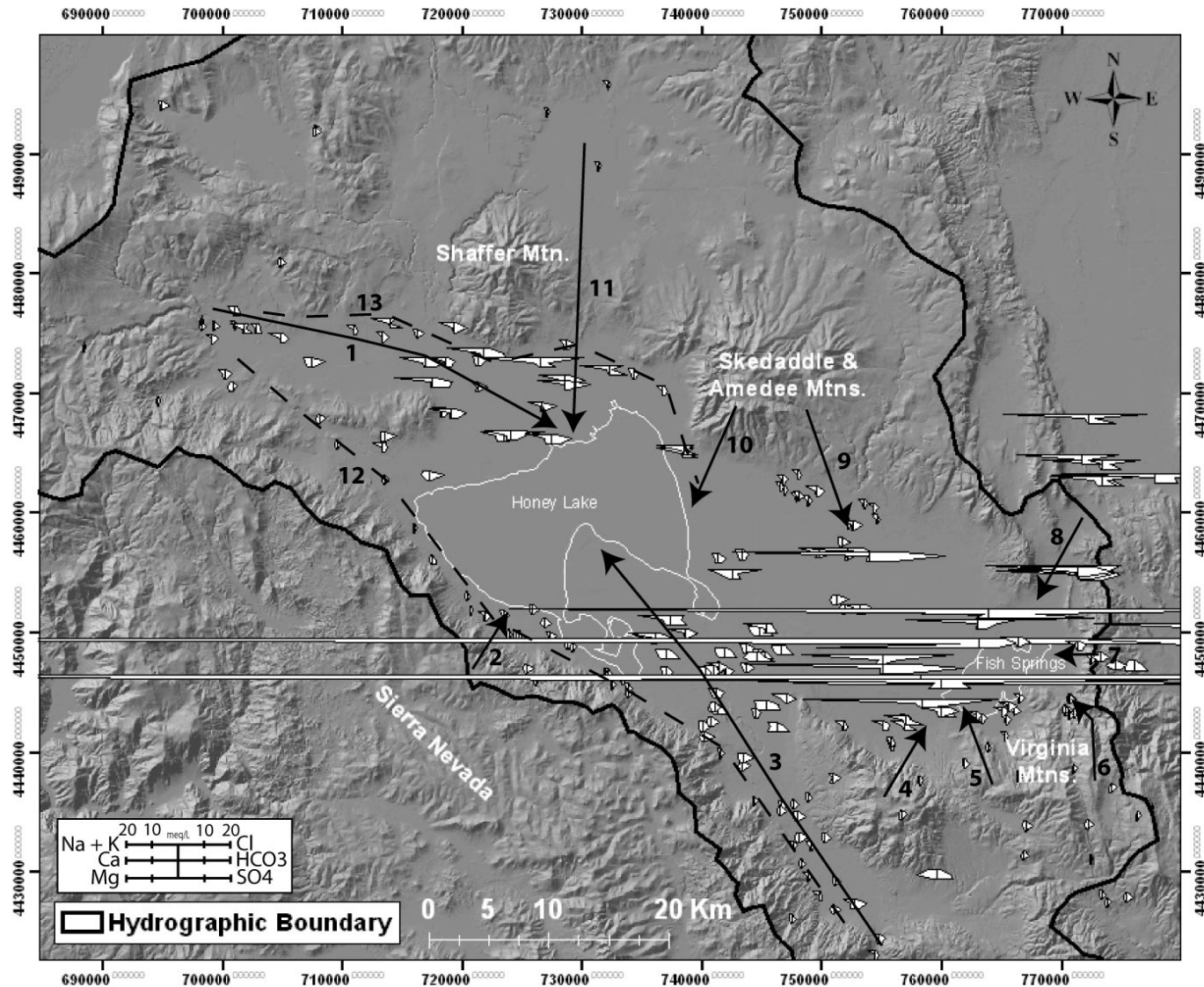


Figure 6. Stiff diagrams of all samples in Honey Lake Basin with solute chemistry data, and Honey Lake Basin flow paths. 1) Susan River path, 2) Sierra Nevada path, 3) Long Valley Creek path, 4) Fort Sage Mountains path, 5) Cottonwood path, 6) Virginia Mountains path, 7) Neversweat path, 8) Astor/Sand Pass path, 9) East Skedaddle/Amedee path, 10) West Skedaddle/Amedee path, 11) Shaffer Mountain path, 12) Honey Lake/Warm Springs Fault Zone path, and 13) Antelope Mountain/Litchfield Fault Zone path.

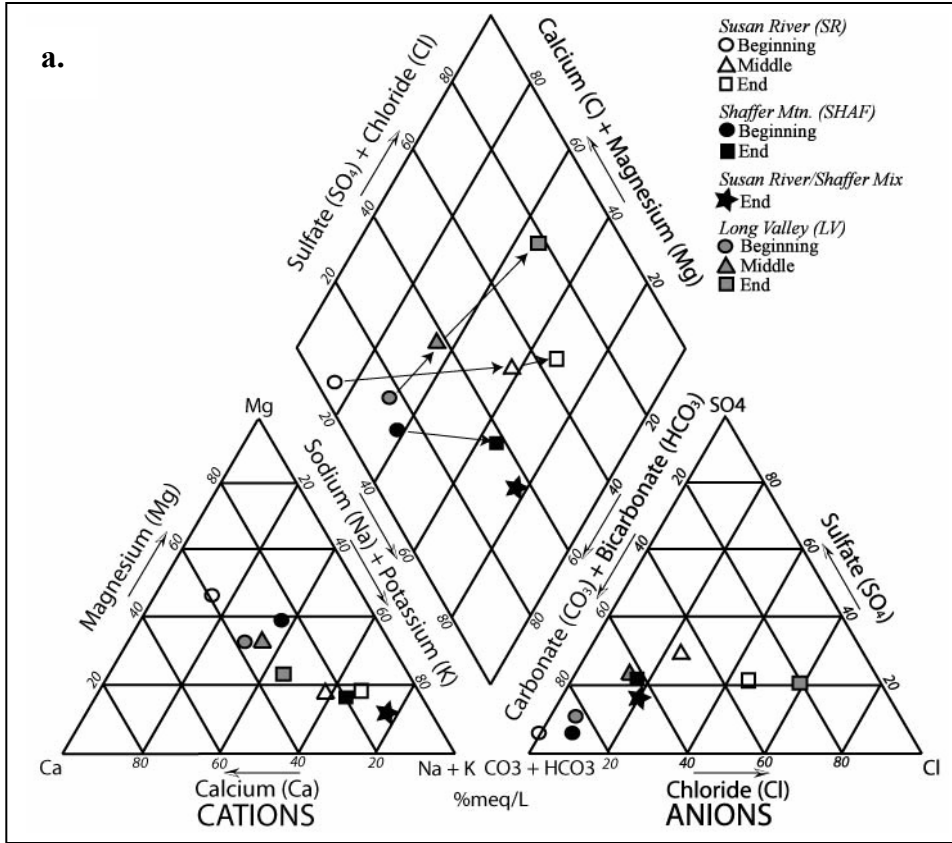
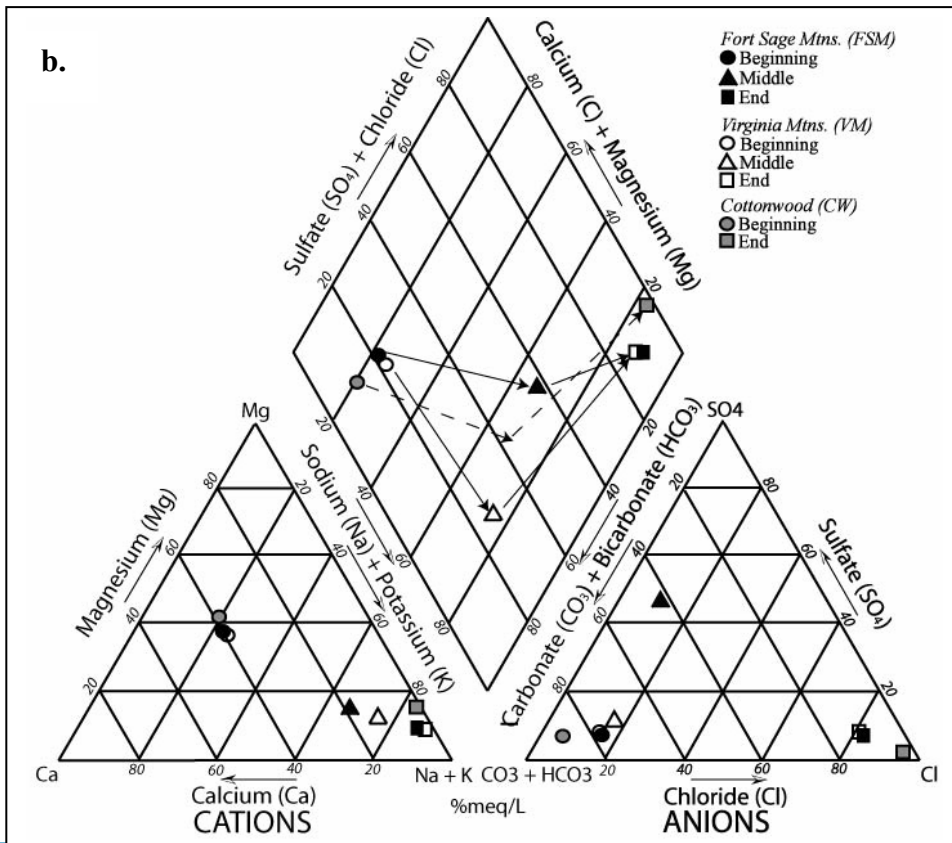


Figure 7. Piper diagrams of median solute chemistry data for the Honey Lake Basin flow paths. These diagrams illustrate how the groundwater changes chemically from the beginning to the end of each flow path. The 13 physical flow paths are grouped into 7 chemical flow paths – paths with similar chemical evolutions.



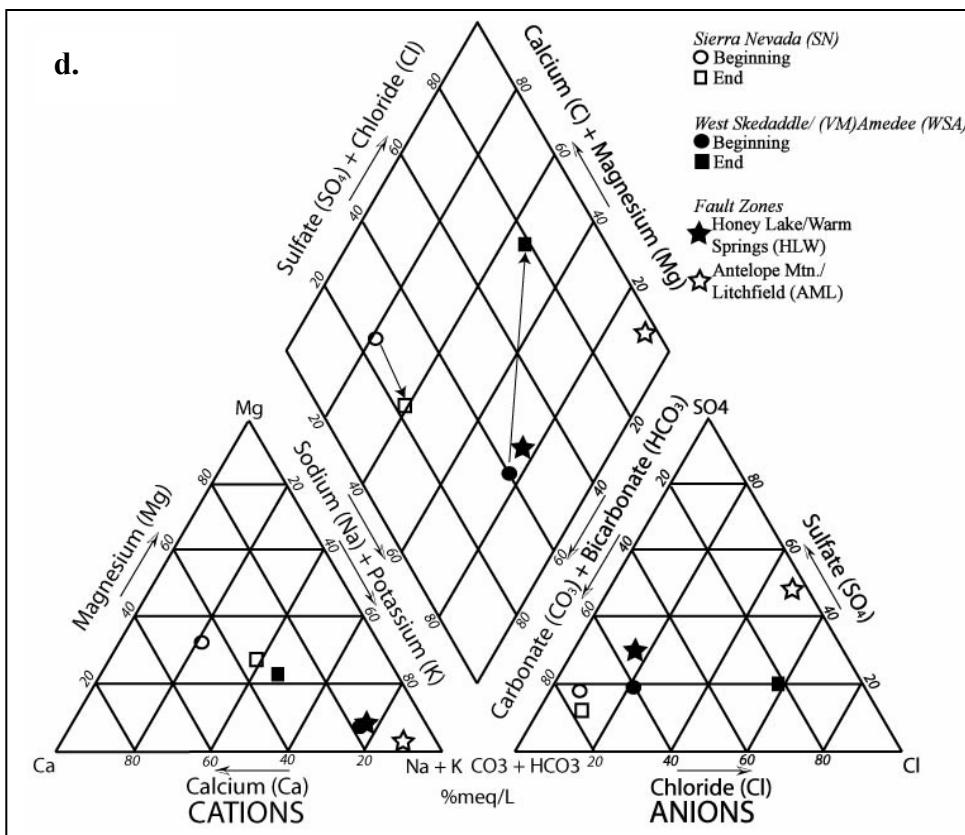
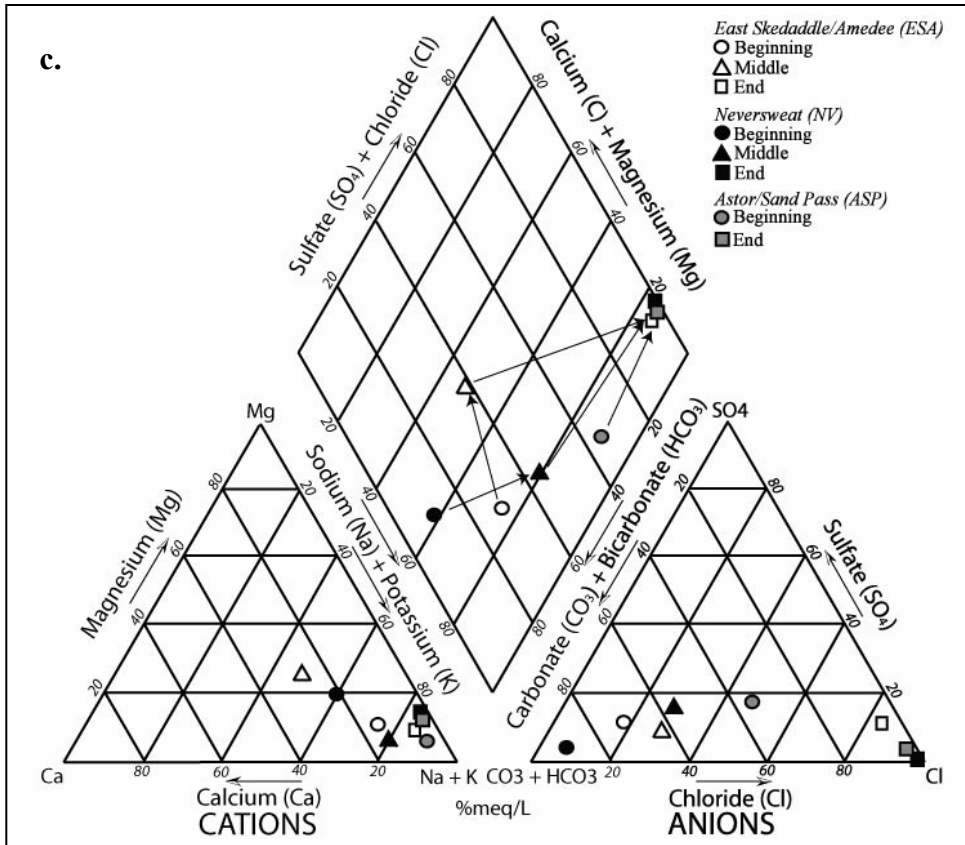


Figure 7 (continued). Piper diagrams of median solute chemistry data for the Honey Lake Basin flow paths. These diagrams illustrate how the groundwater changes chemically from the beginning to the end of each flow path. The 13 physical flow paths are grouped into 7 chemical flow paths – paths with similar chemical evolutions.

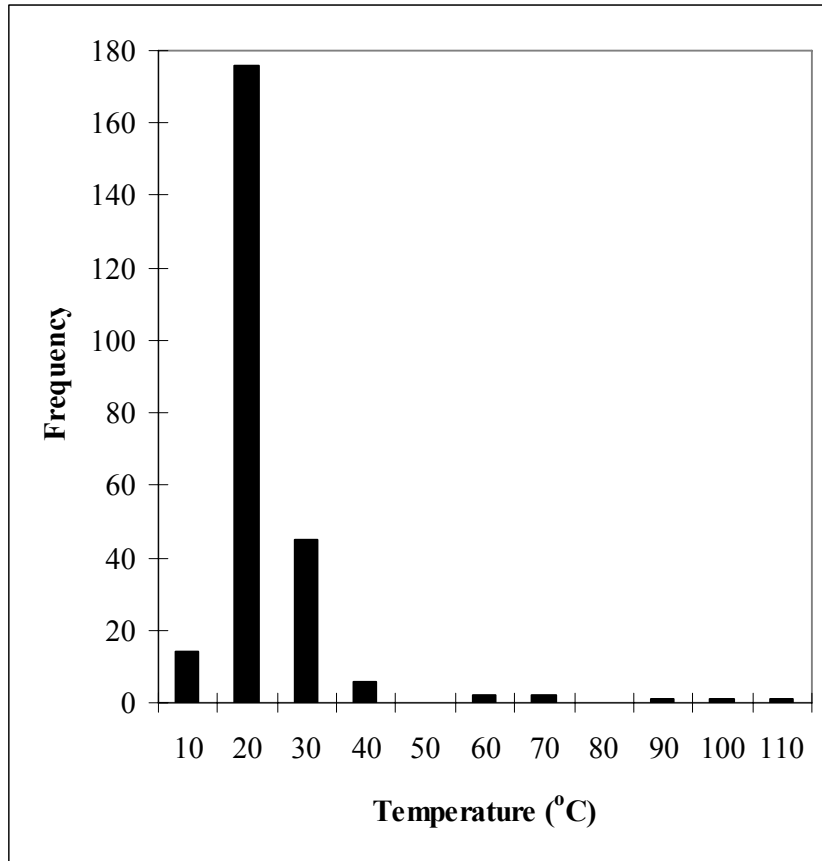


Figure 8. Histogram of groundwater temperatures in Honey Lake Basin.

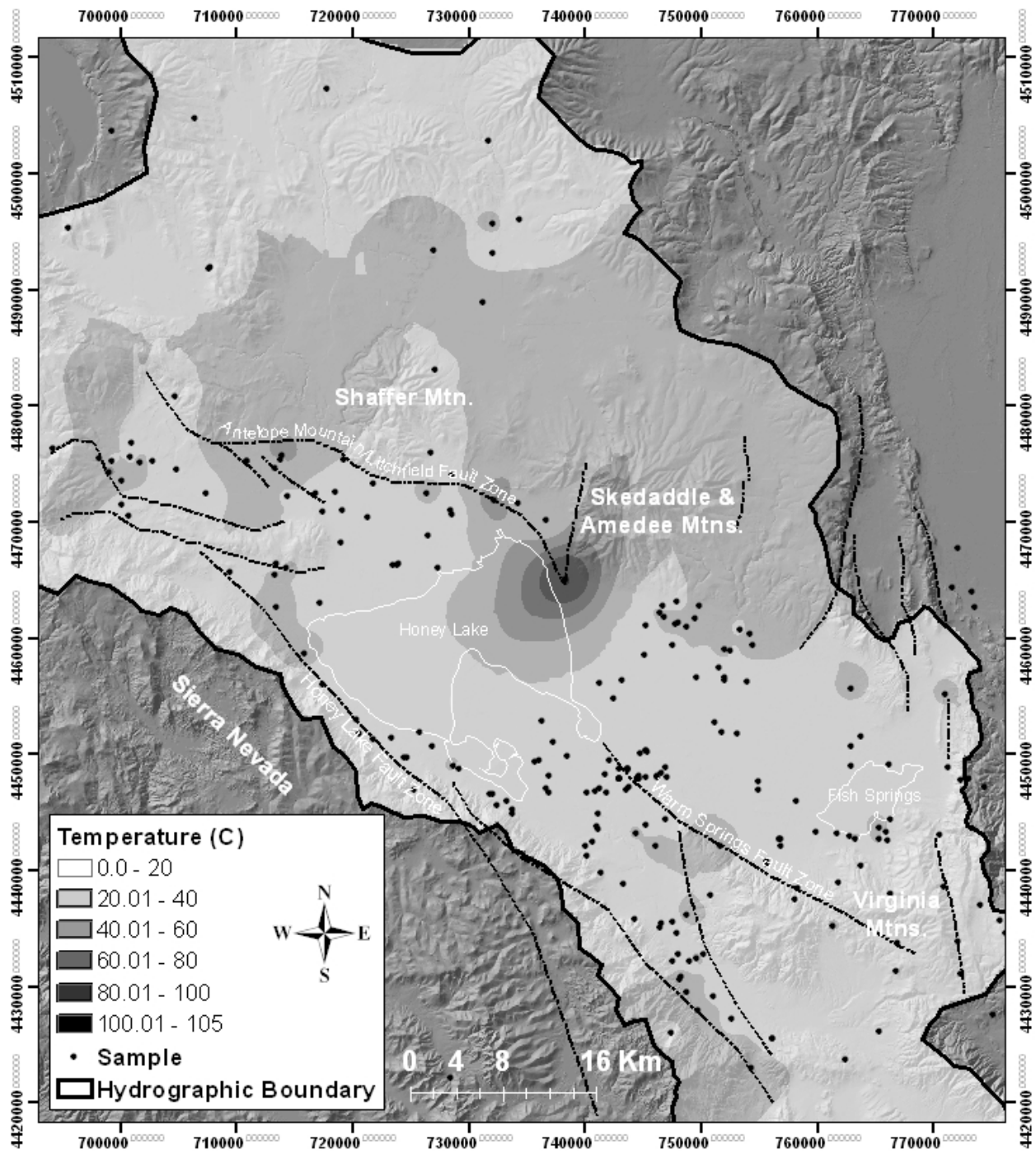


Figure 9. Contour map of groundwater temperatures in Honey Lake Basin. Note that the hottest waters are closely associated with faults zones.

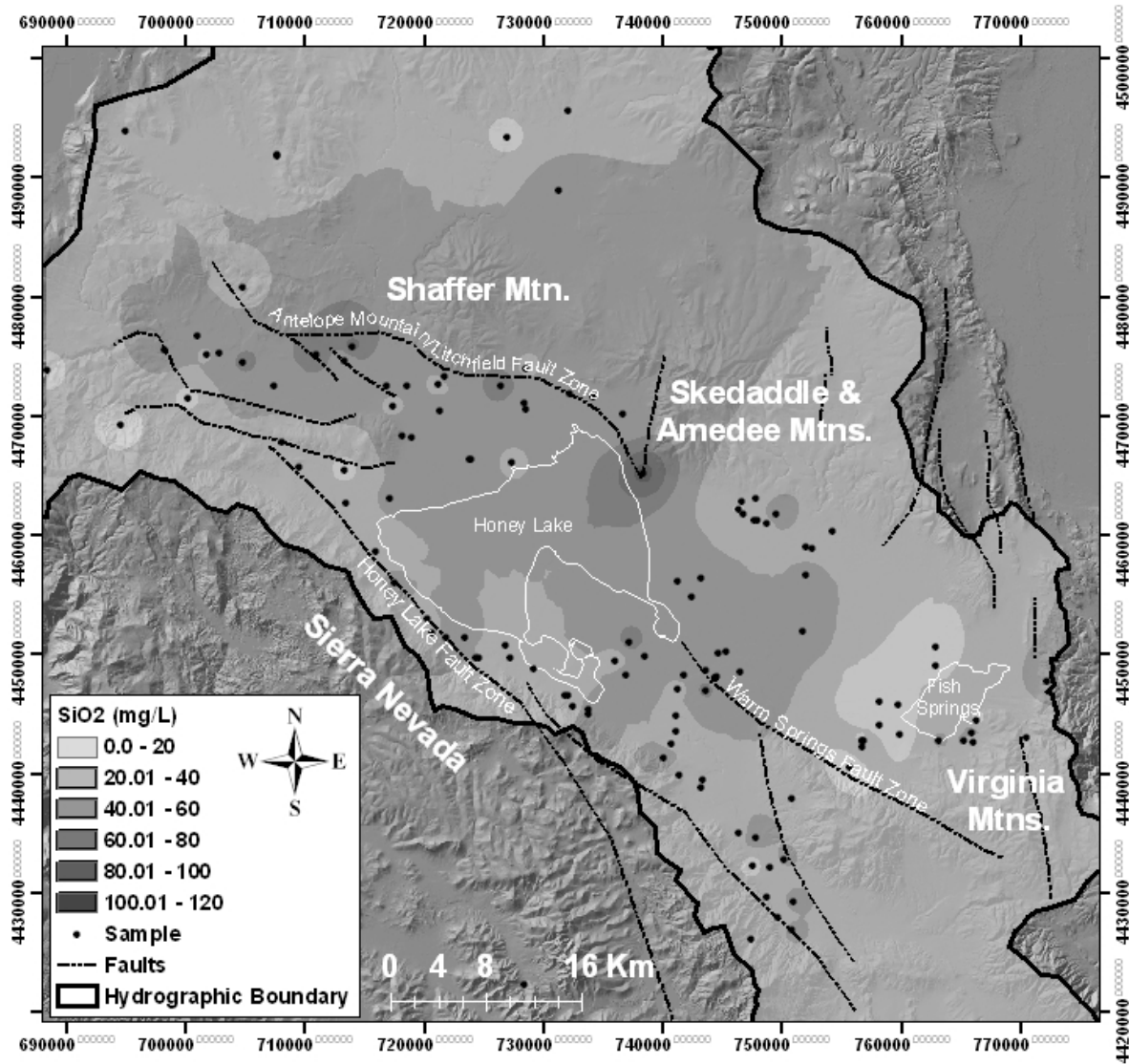


Figure 10. Contour map of silica concentrations in Honey Lake Basin groundwater. The highest concentrations of silica are associated with fault zones.

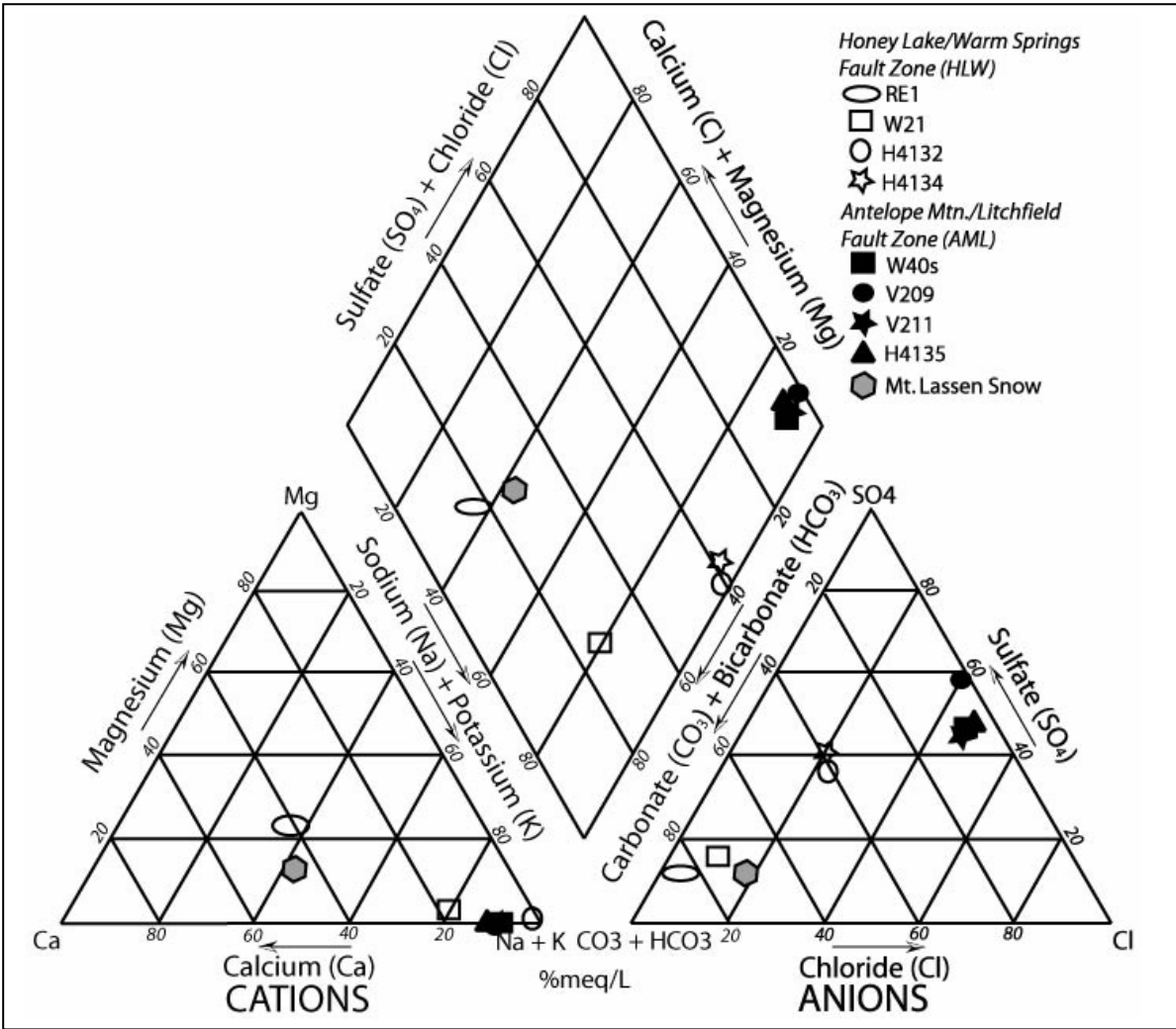


Figure 11. Piper diagram of the solute chemistry of the thermal water in Honey Lake Basin.

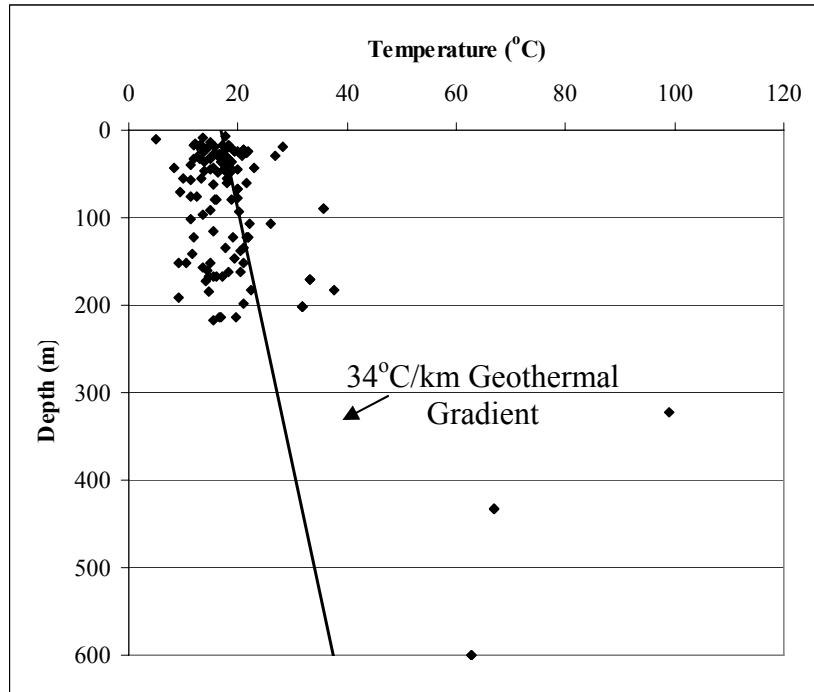


Figure 12. The geothermal gradient (34°C/km) and groundwater temperatures plotted according to depth.

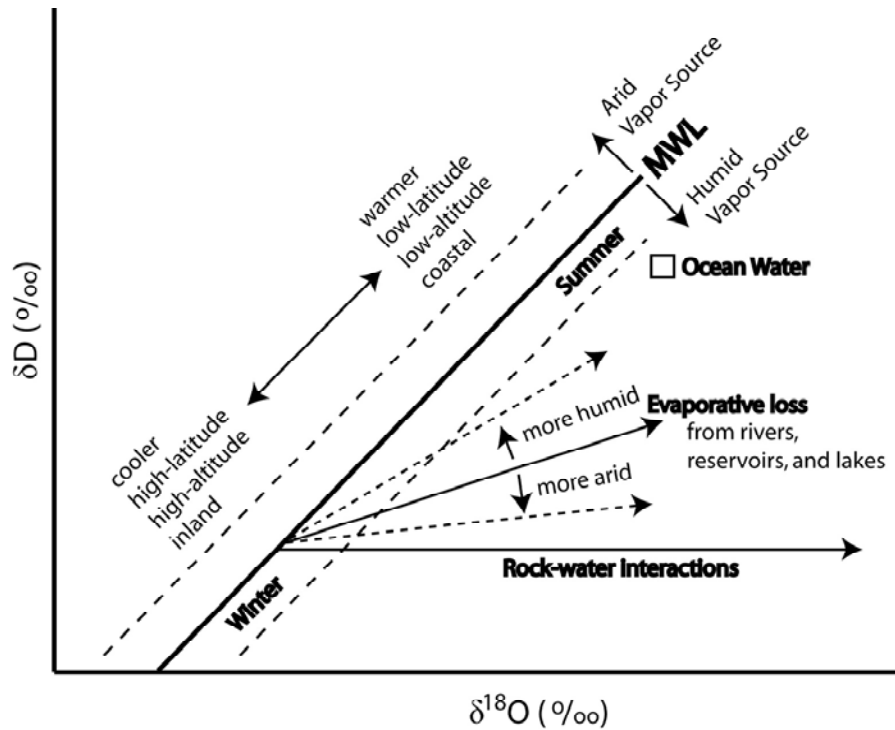


Figure 13. Oxygen-18 vs. deuterium graph showing deviations from the meteoric water line (SAHRA, 2006).

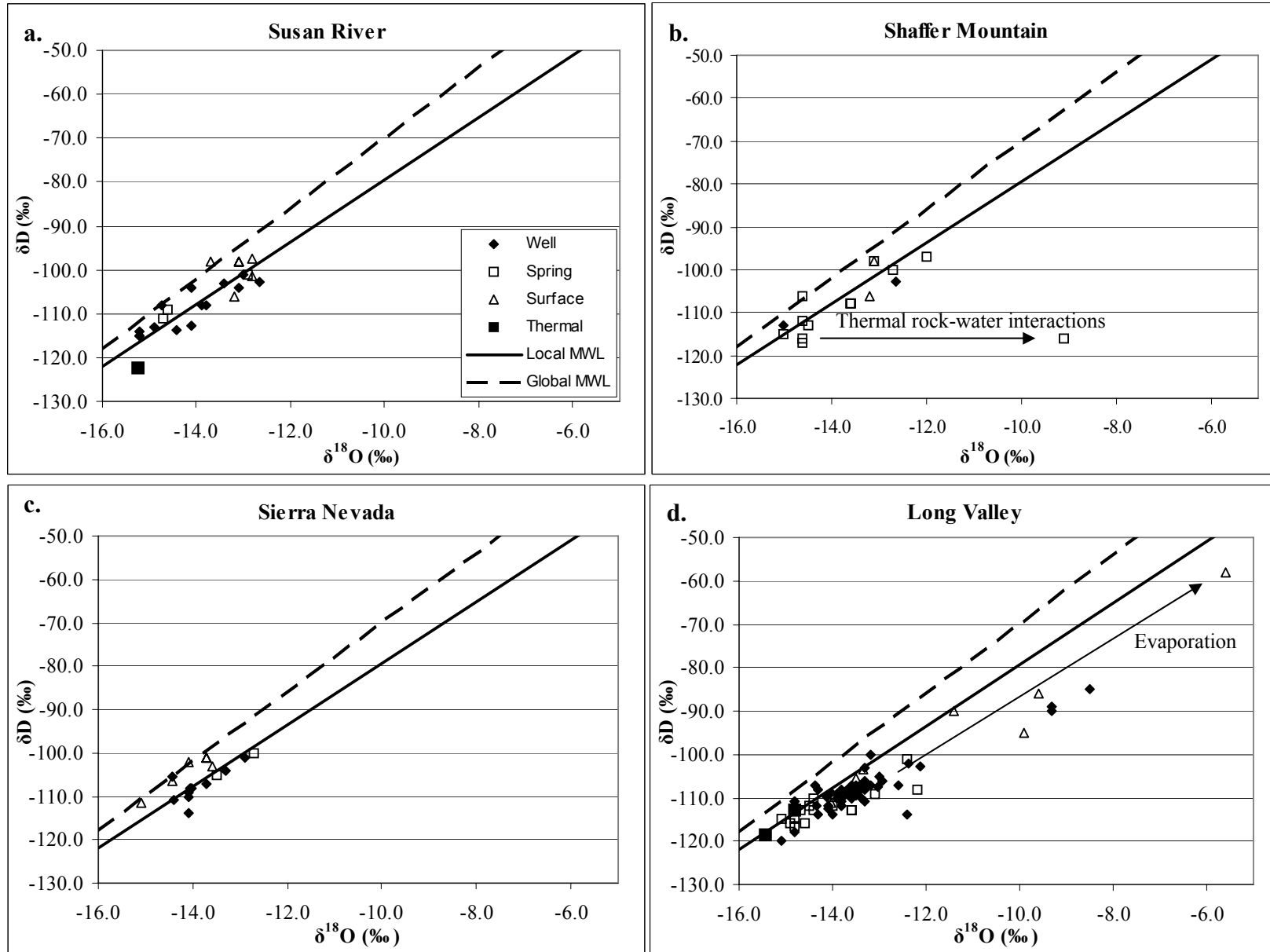


Figure 14. Oxygen-18 vs. deuterium vales for western Honey Lake Basin flow paths.

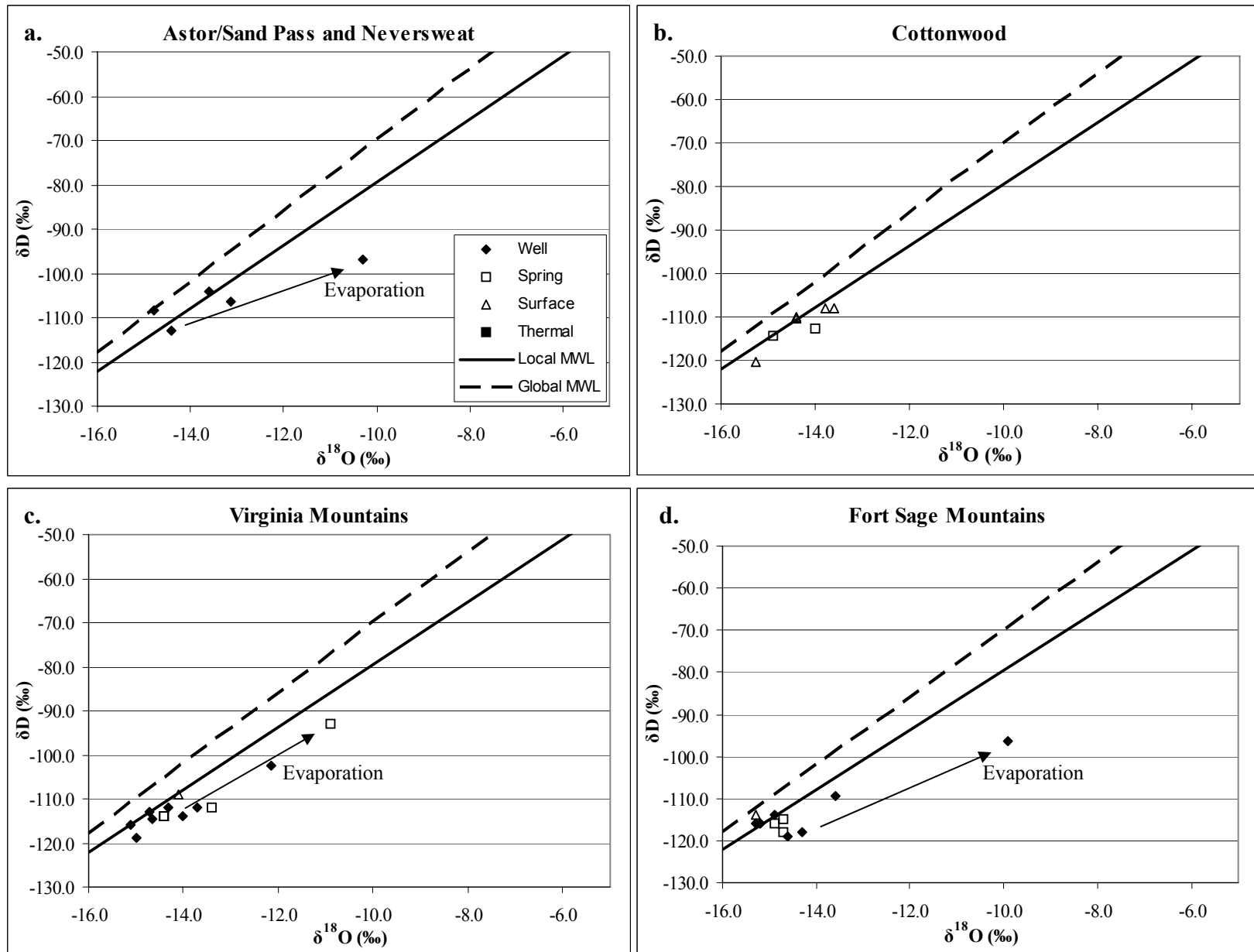


Figure 15. Oxygen-18 vs. deuterium values for eastern Honey Lake Basin flow paths.

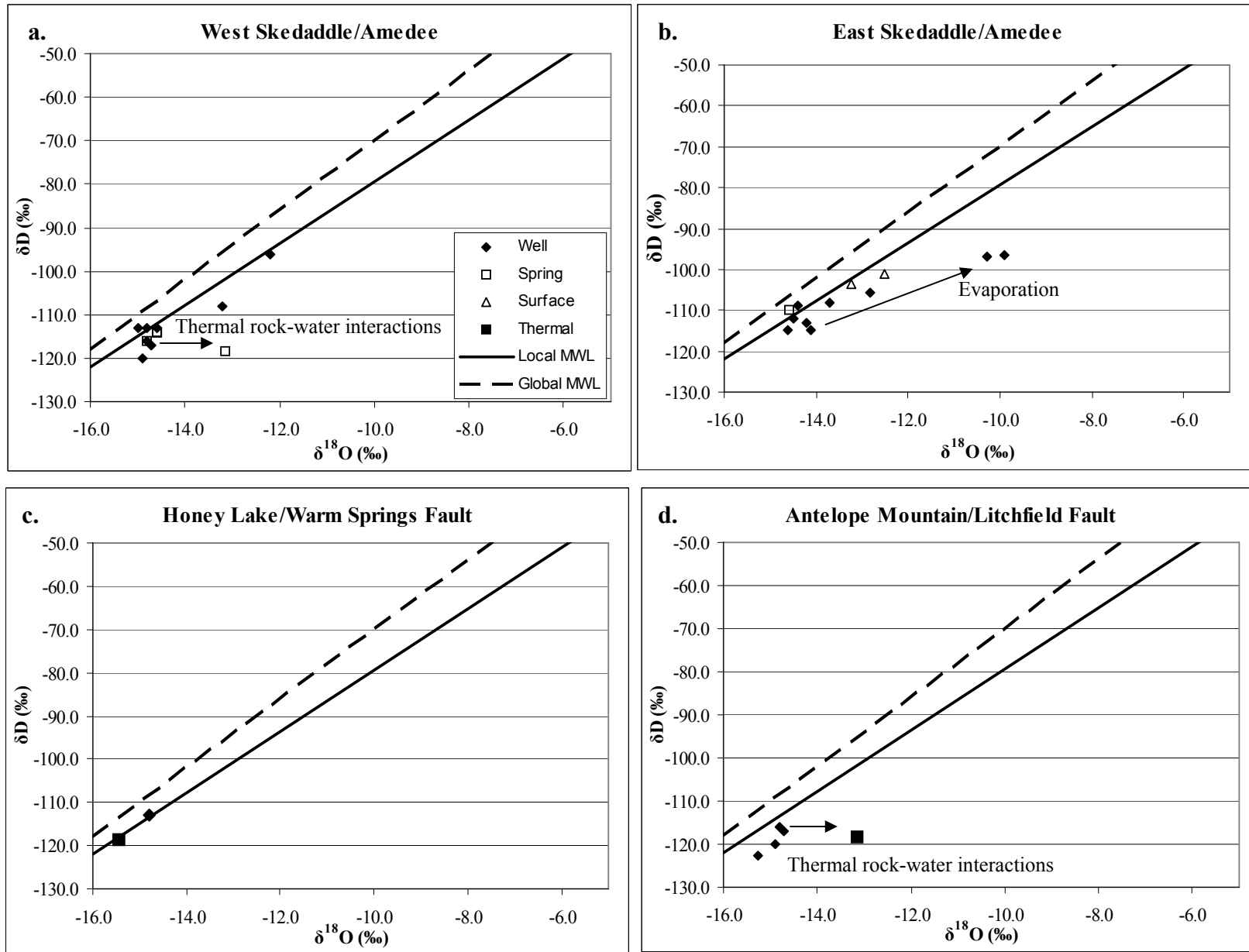


Figure 16. Oxygen-18 vs. deuterium values for central Honey Lake Basin and fault zone flow paths.

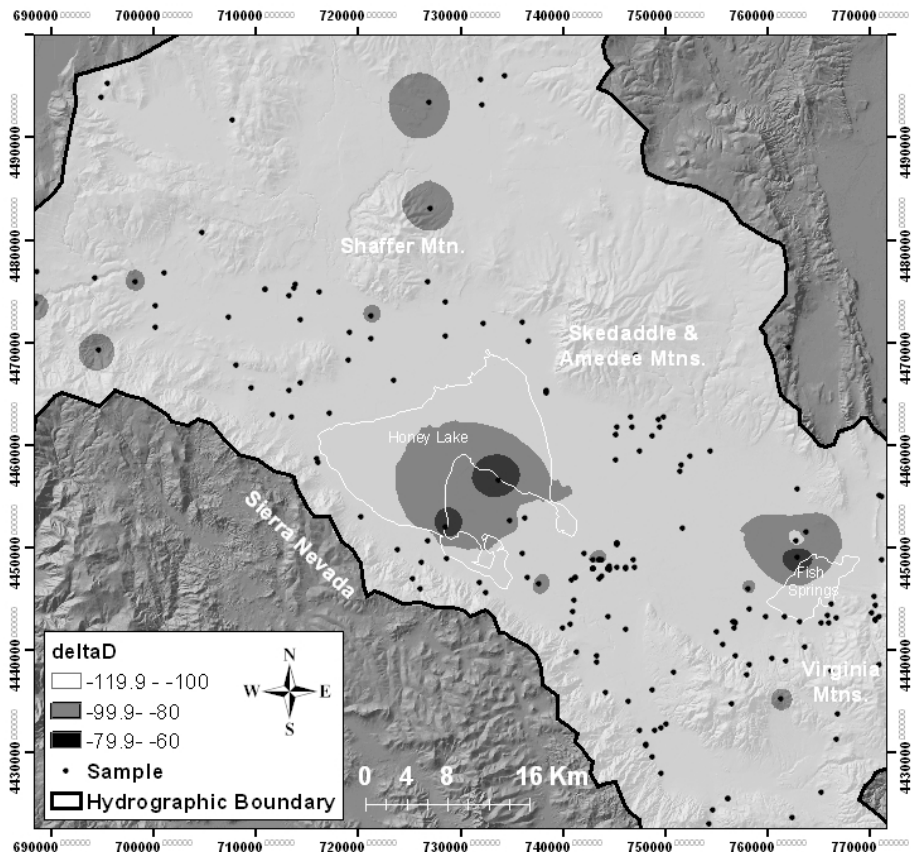
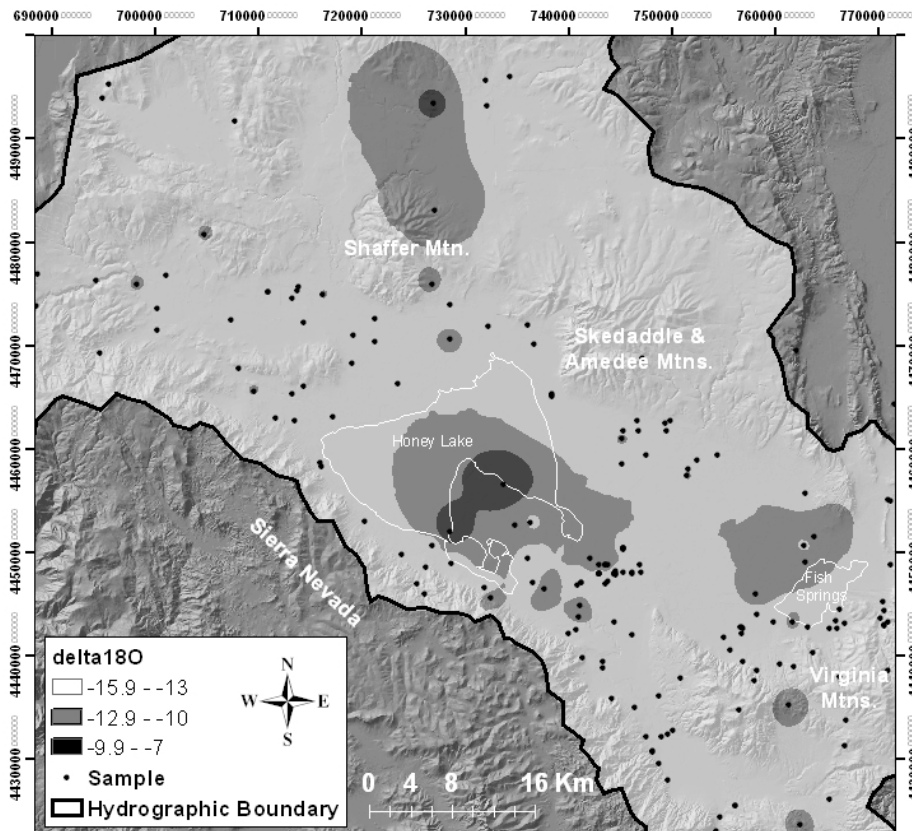


Figure 17. Contour map of $\delta^{18}\text{O}$ (top) and δD values (bottom). Both become more enriched down gradient.

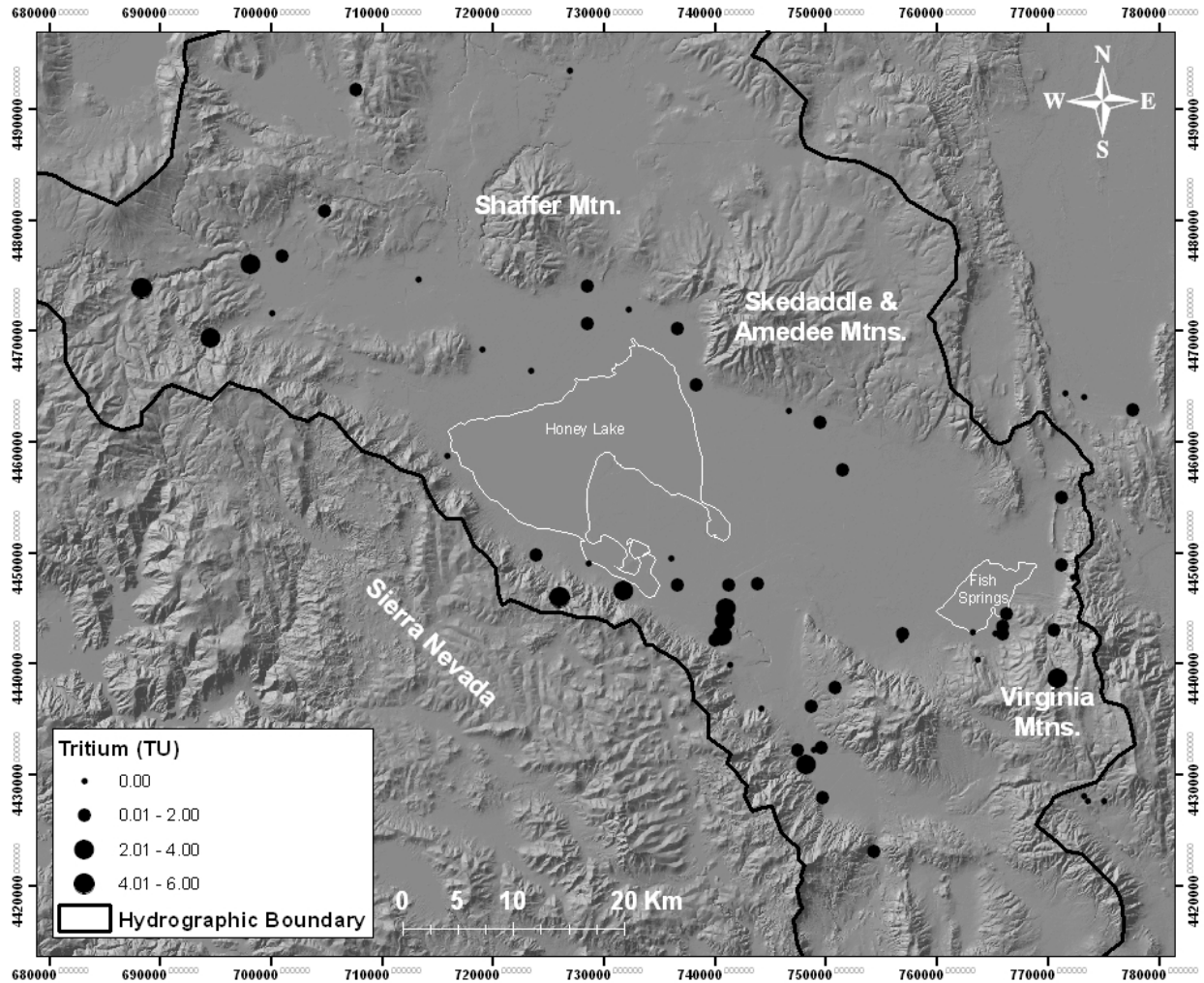


Figure 18. Tritium concentrations throughout Honey Lake Basin. The presence of ^3H in groundwater indicates some component of post-1952 recharge. Concentrations are generally highest in areas of recharge (highlands) and decrease down gradient.

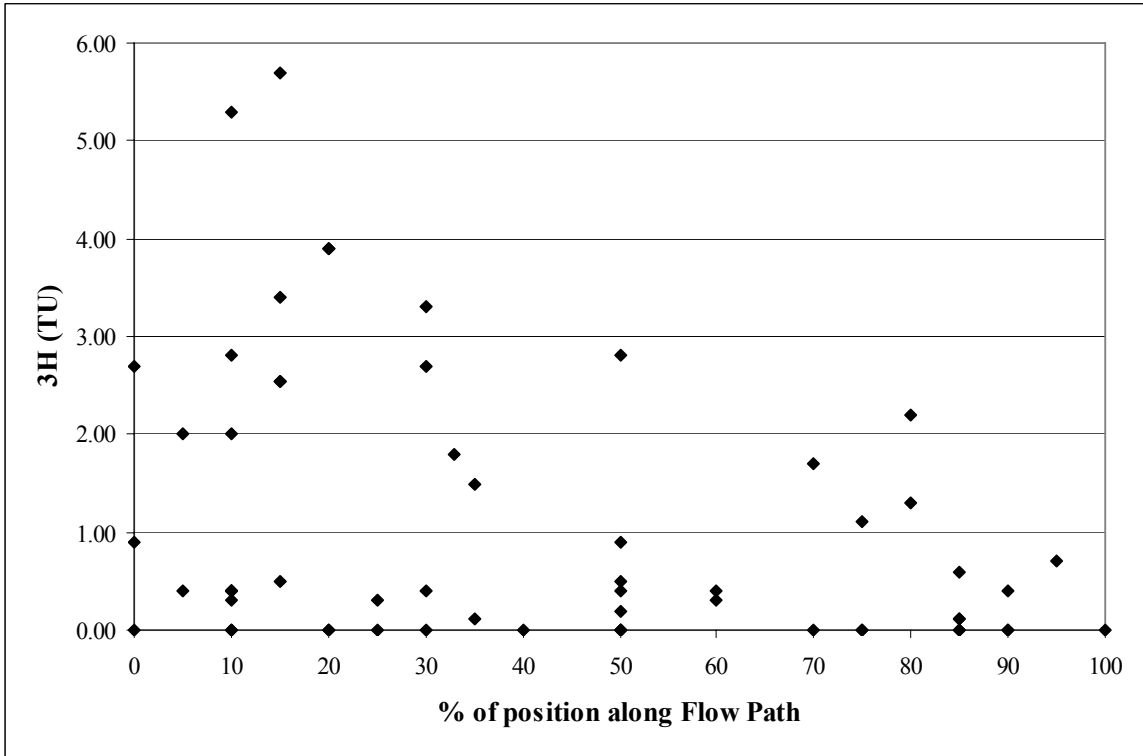


Figure 19. Tritium values in Honey Lake Basin groundwaters according to the sample's position along the flow path. Values decrease, and thus post-1952 recharge decreases, down gradient toward the end of the flow paths.

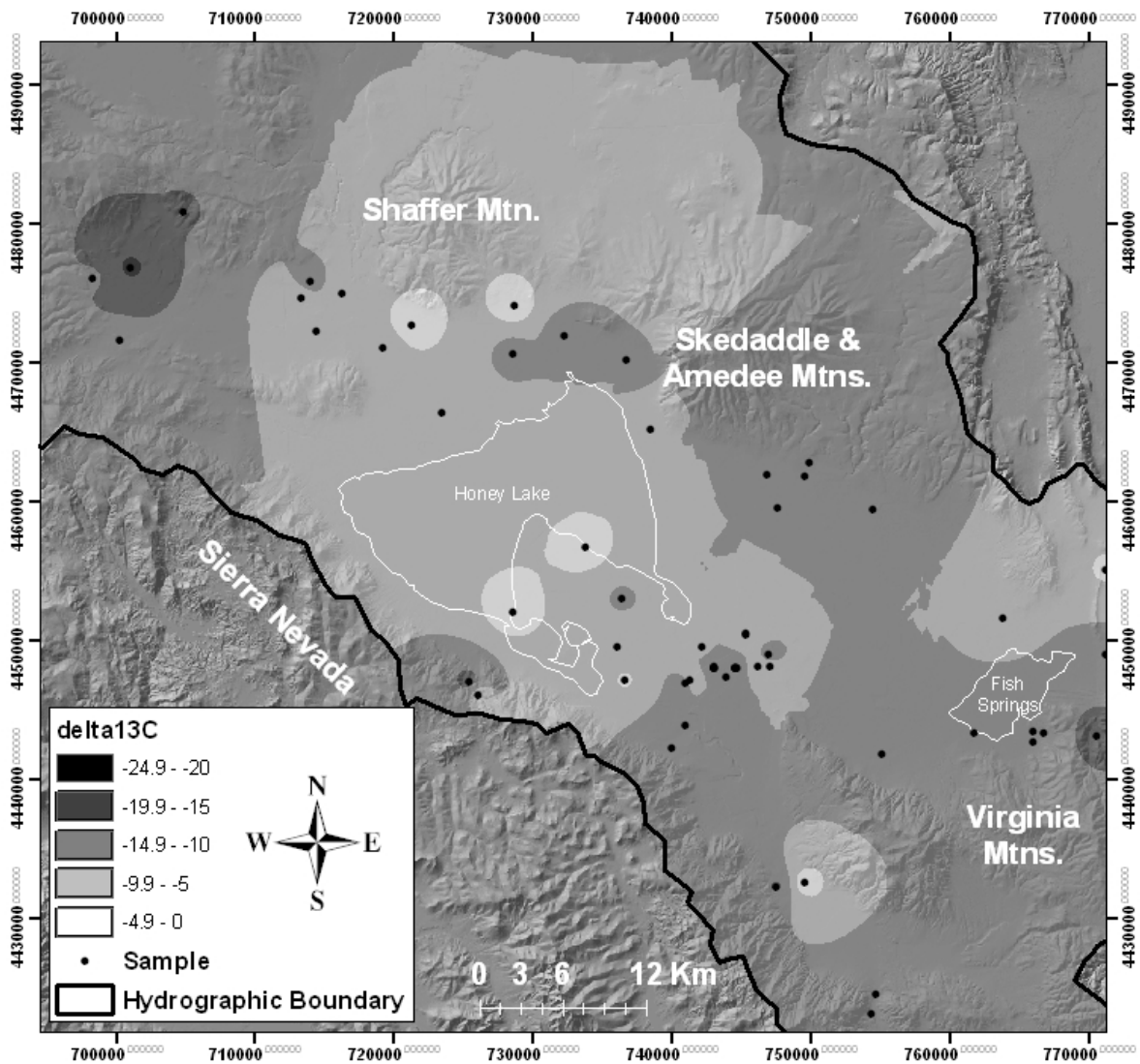


Figure 20. Contour map of groundwater carbon-13 values, which become more enriched toward the basin floor.

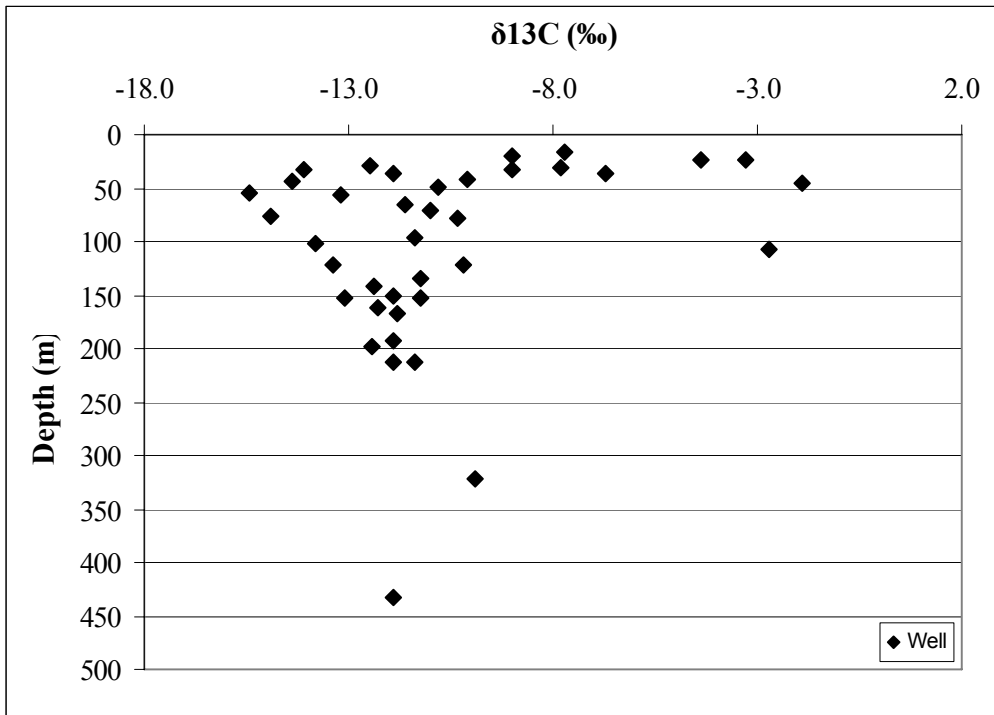


Figure 21. Carbon-13 variations with depth. Values become less variable with depth and generally range between -14 and -10‰.

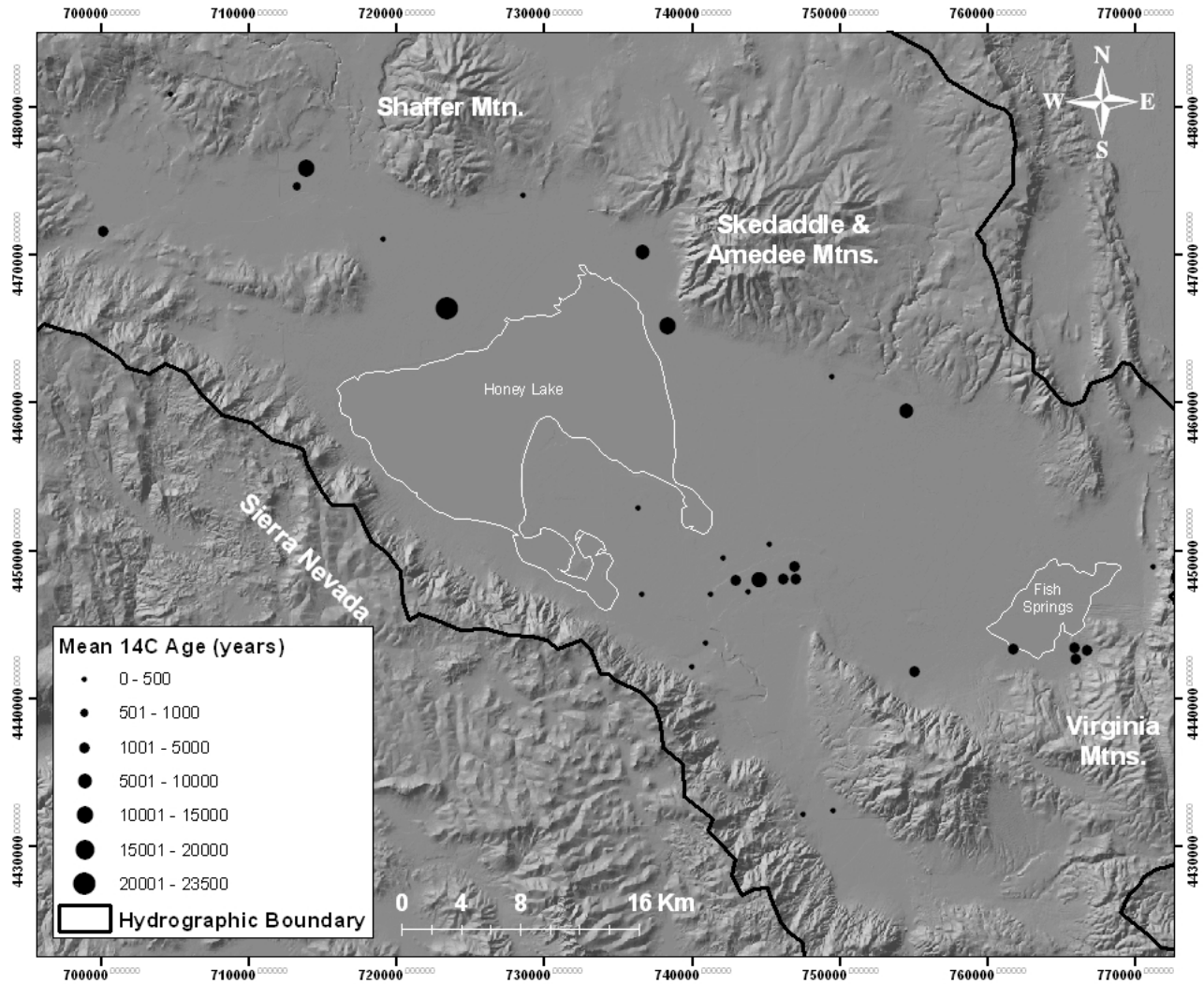


Figure 22. Mean ¹⁴C ages for Honey Lake Basin groundwaters. Deep groundwaters on the basin floor show much older ages than highland and shallow basin floor groundwaters.

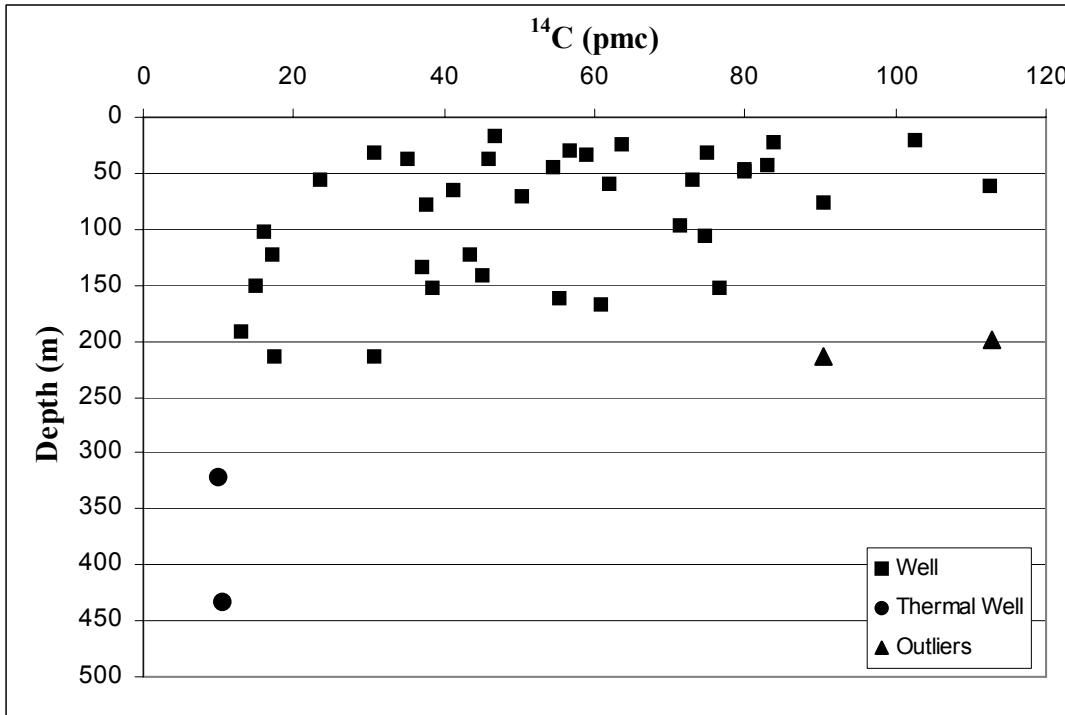


Figure 24. Carbon-14 variations with depth. Groundwaters become more depleted in ¹⁴C with depth, indicating older waters. Deep wells with high ¹⁴C pmc (outliers) have large perforation intervals that span shallow and deep aquifers and therefore do not reflect accurate measurements for the well bottom.

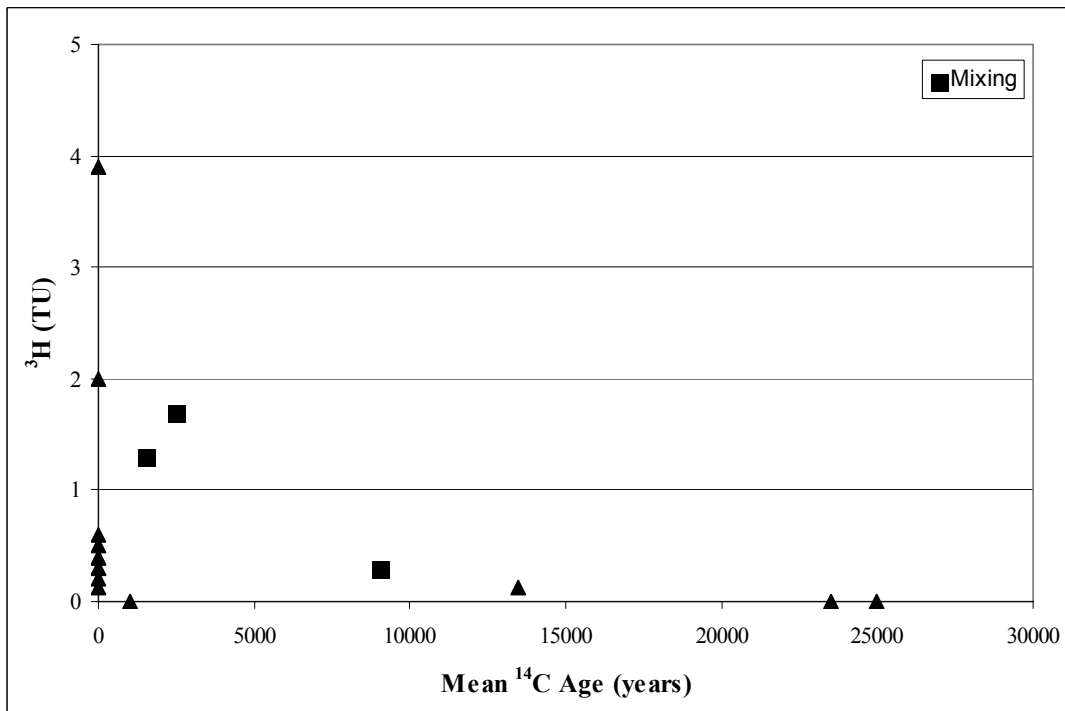


Figure 23. Mean ¹⁴C ages vs. ³H concentrations. This graph shows that little mixing occurs between groundwaters recharged by post-1952 precipitation and old groundwaters found in the center of the Basin.

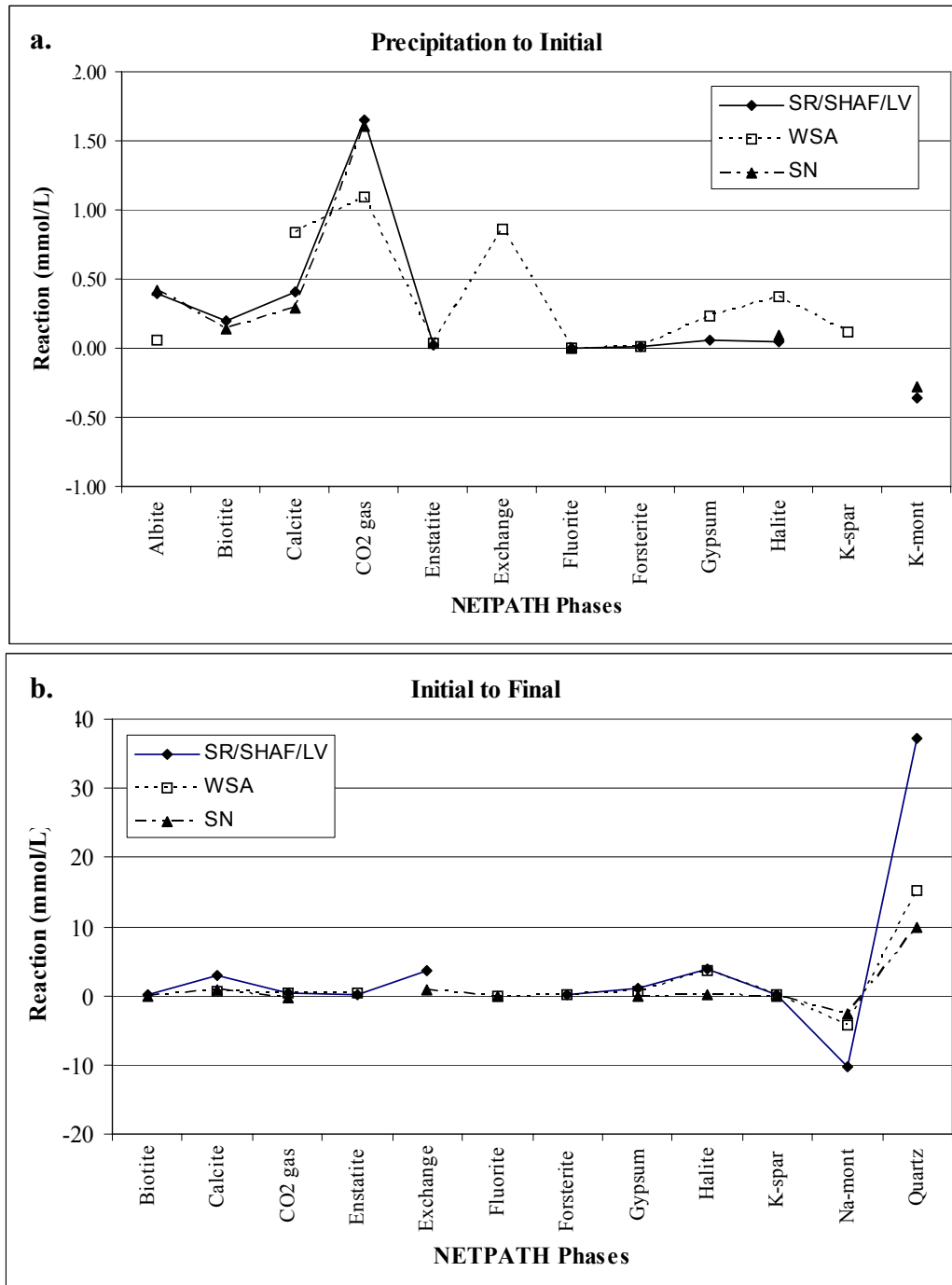


Figure 25. NETPATH geochemical evolution models for eastern Honey Lake Basin flow paths, as modeled from (a) precipitation to initial water and from (b) initial to final waters. Positive values represent dissolution and negative values represent precipitation.

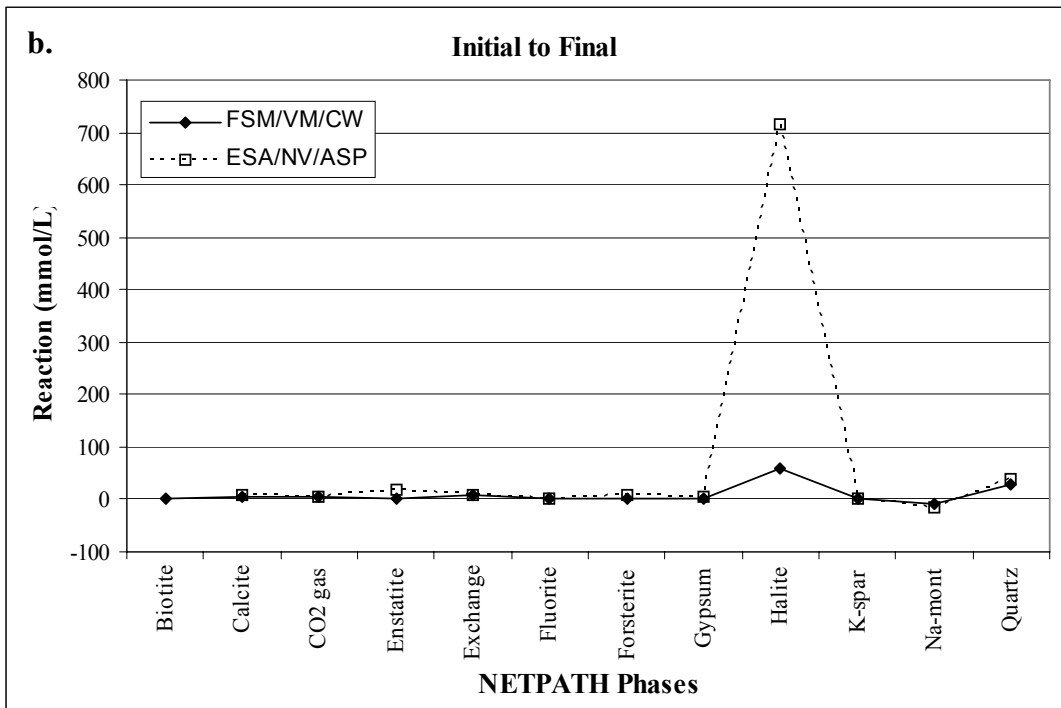
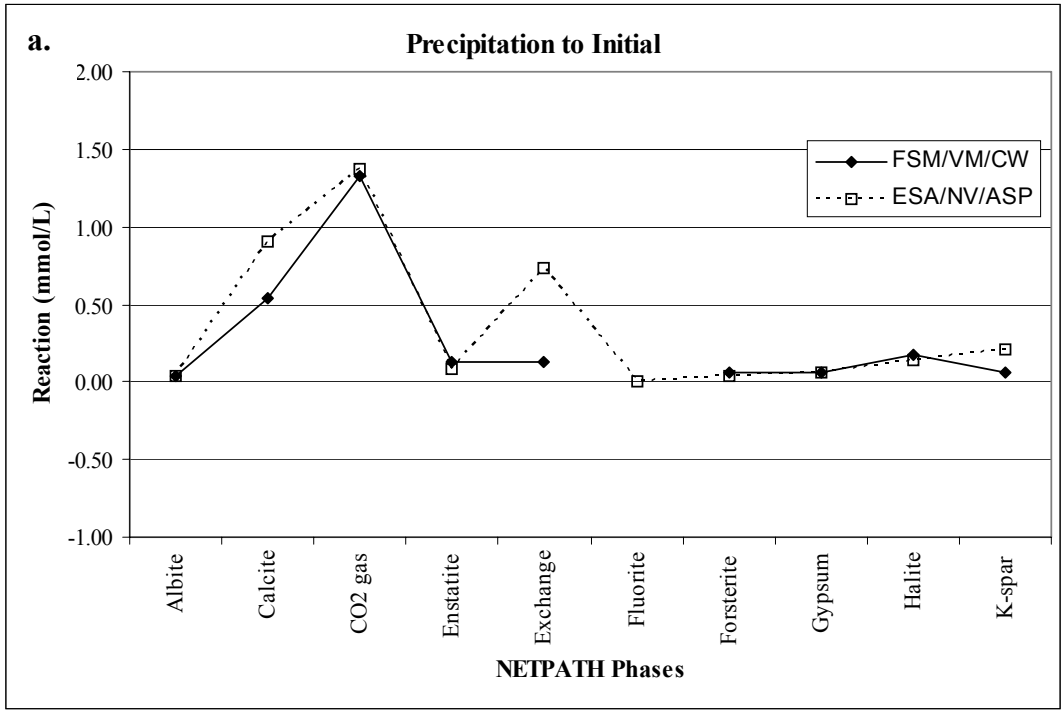


Figure 26. NETPATH geochemical evolution models for western Honey Lake Basin flow paths, as modeled from (a) precipitation to initial water and from (b) initial to final waters. Positive values represent dissolution and negative values represent precipitation.

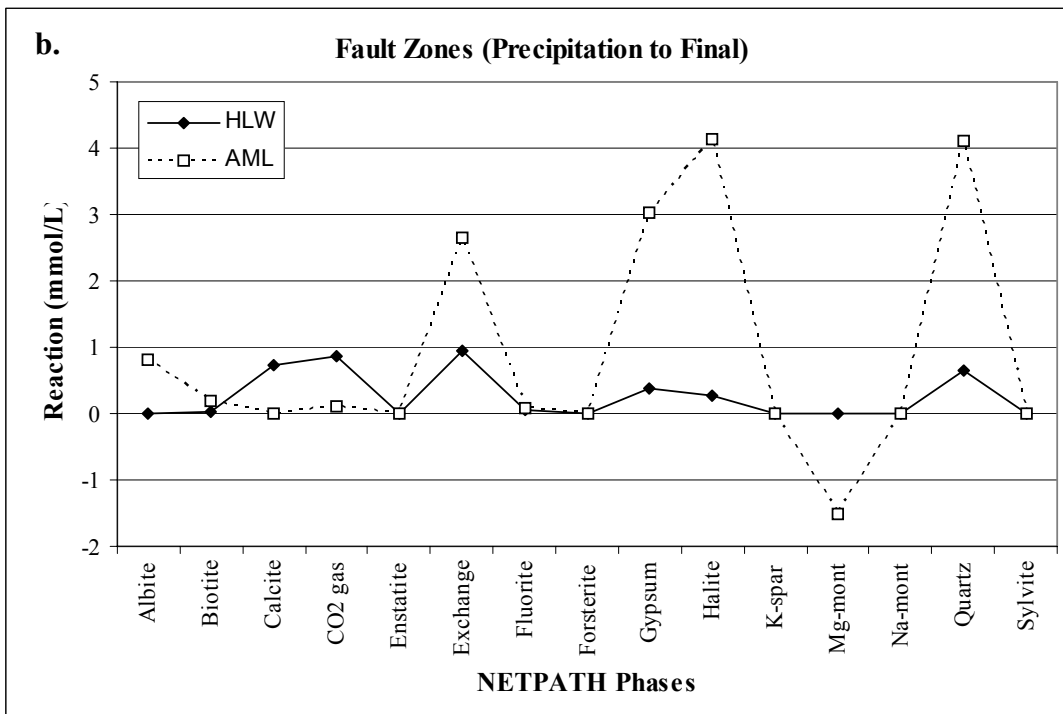
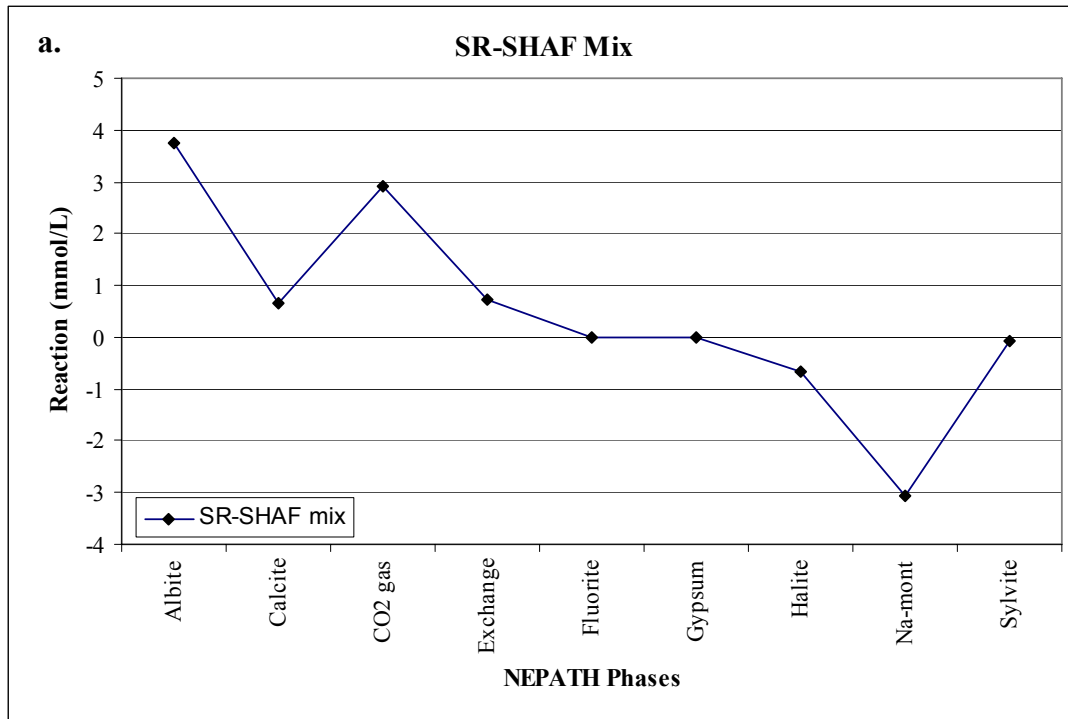


Figure 27. NETPATH geochemical evolution models for (a) groundwater mixing at the end of the Susan River and Shaffer Mountain flow paths and (b) fault zone thermal waters. Positive values represent dissolution and negative values represent precipitation.

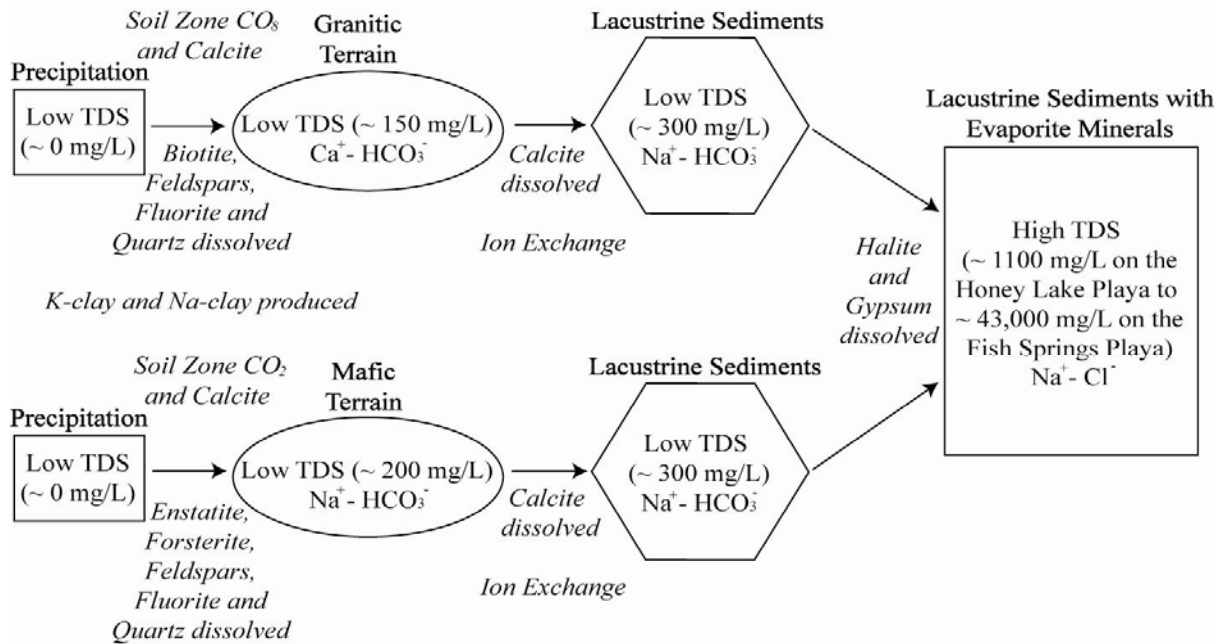


Figure 28. Summary of flow path geochemical evolution as groundwater flows through (top) granitic terrain to lacustrine sediments with evaporite minerals and (bottom) mafic terrain to lacustrine sediments with evaporite minerals.

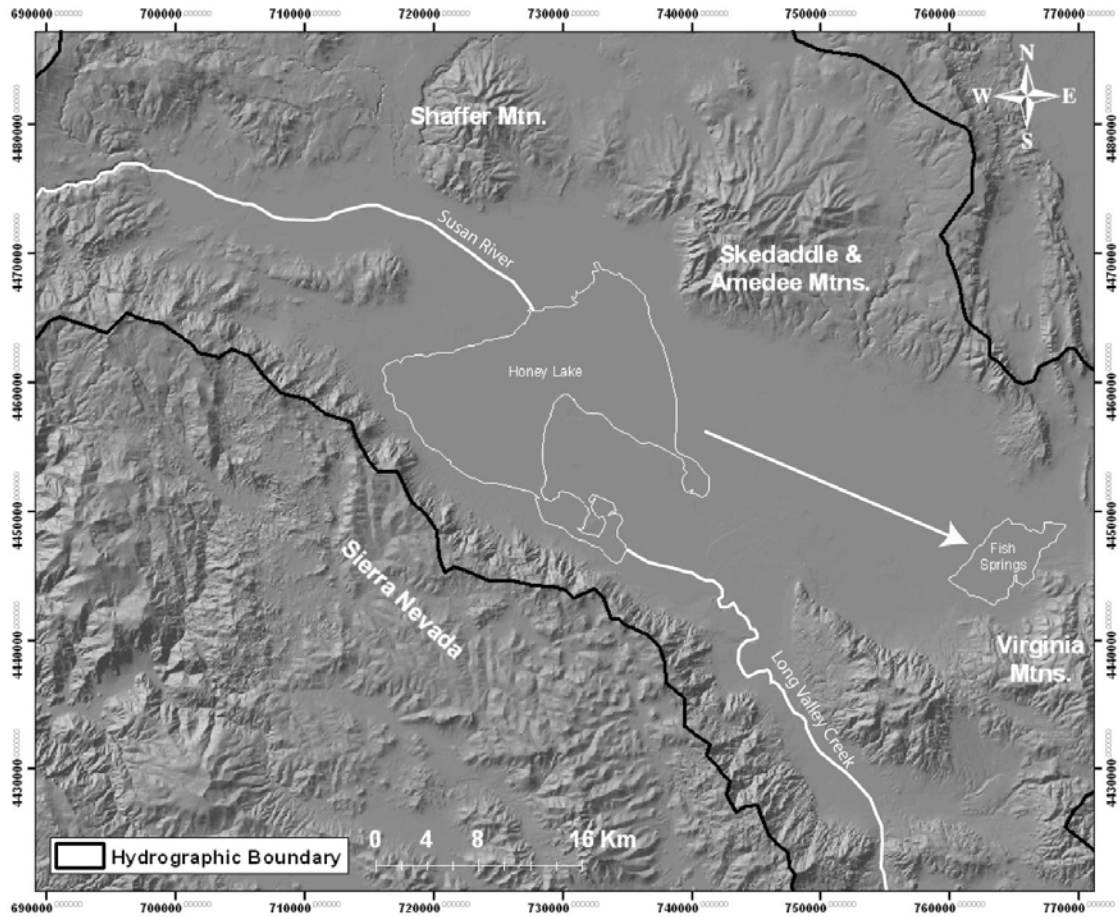


Figure 29. Post Lahontan episodic flooding of Honey Lake Playa flushes solutes east, to Fish Springs Playa.

Table 1. Total stream flow into Honey Lake Basin. Data from Rockwell (1993), table modified from Webber (1996).

	Name	Mean Annual Measurements		
		ft ³ /sec	acre-ft/yr	% Total
Susan River Area	Cascade Range and Intervening Area	28.50	20,639	9.09
	Balls Canyon Creek	26.00	18,828	8.29
	Gold Run Creek	6.10	4,417	1.94
	Hills Creek	2.20	1,593	0.7
	Lassen Creek	1.40	1,014	0.45
	Petes Creek	11.00	7,966	3.51
	Piute Creek	4.70	3,404	1.5
	Shaffer Creek	0.22	159	0.07
	Susan River	94.70	68,578	30.19
	Willow Creek near Susanville	34.70	25,128	11.06
	Total	209.52	151,726	66.8
Sierra Nevada Area	Diamond Mtns Intervening	28.50	20,639	9.09
	Bankhead Creek	0.98	710	0.31
	Baxter Creek	2.30	1,666	0.73
	Elysian Creek	4.90	3,548	1.56
	Hallet Creek	0.55	398	0.18
	McDermott Creek	1.50	1,086	0.48
	Mill Creek	2.80	2,028	0.89
	Parker Creek	0.86	623	0.27
	Sloss Creek	0.59	427	0.19
	Total	42.98	31,125	13.7
Long Valley Creek Area	Long Valley Creek and Intervening Area	24.00	17,380	7.65
	Long Valley Creek	11.00	7,966	3.51
	Willow Creek	2.90	2,100	0.92
	Total	37.90	27,446	12.08
West Skedaddle Mtn Area	Skedaddle Creek-West	3.45	2,498	1.1
	Spencer Creek	0.53	384	0.17
	Total	3.98	2,882	1.27
Fish Springs Playa Area	Virginia & Fort Sage Mtns and Intervening Area	3.30	2,390	1.05
	Shaffer Mtn to Neversweat and Intervening Area	8.20	5,938	2.61
	Antoinette Creek	0.04	29	0.01
	Butler Creek	0.04	29	0.01
	Cottonwood Creek	2.20	1,593	0.7
	Fish Springs Creek	0.43	311	0.14
	Fort Sage Creek	0.61	442	0.19
	Gasperoni Creek	0.08	58	0.03
	Milne Creek	0.27	196	0.09
	Mullen Creek	0.15	109	0.05
	Rock Springs Creek	0.29	210	0.09
	Skedaddle Creek-East	3.45	2,498	1.1
	Willow Springs Creek	0.22	159	0.07
Total	19.28	13,962	6.14	
Total Stream Flow Into Honey Lake Basin		313.66	227,141	100

Table 2. Median values for the end members of the Honey Lake Basin flow paths, arranged by chemical and physical flow paths. * Indicates estimated numbers. † Indicates the physical flow paths that are later modeled using NETPATH.

Chemical Flow Path	Physical Flow Path	n (# of samples)	Temp (°C)	pH	TDS (mg/L)	Cations (meq/L)				Anions (meq/L)				SiO ₂ (mg/L)	Balance Error %	δ ¹³ C (‰)	
						Ca ²⁺	Mg ²⁺	Na ⁺	K ⁺	HCO ₃ ⁻	SO ₄ ²⁻	Cl ⁻	F ⁻				
	Precipitation	1	0.0	5.7		0.00	0.000	0.00	0.00	0.00	0.00	0.00	0.00		0.0		
LV/SHAF/SR	SR [†]	Beginning	2	15.3	8.01	119.00	0.93	0.66	0.44	0.07	2.05	0.10	0.05	0.00	28.1	-2.8	-15.3
		Middle	10	17.1	7.81	311.71	0.95	0.55	2.96	0.10	2.44	1.23	0.70	0.06	47.0	-1.5	-14.3
		End	9	14.6	7.90	770.6	1.54	1.18	8.71	0.23	5.24	2.45	4.03	0.03	47.8	-2.2	-7.2
		Δ					0.61	0.53	8.27	0.16	3.19	2.35	3.98	0.03	19.7		
	SHAF	Beginning	6	20.6	8.07		0.51	0.53	0.92	0.07	1.83	0.09	0.11	0.00	30.4	-0.1	-15.1
		End	3	23.3	8.09	340.0	0.89	0.49	3.69	0.19	3.67	1.00	0.55	0.01	36.8	-0.20	-1.9
		Δ					0.38	-0.04	2.77	0.12	1.84	0.92	0.44	0.00	6.4		
	SR & SHAF Mix End [†]		4	14.0	8.50	654.9	1.06	0.82	9.53	0.13	8.02	1.68	1.37	0.03	43.2	-1.3	-11.9
	LV	Beginning	11	17.2	7.59	176.2	0.93	0.49	0.94	0.06	1.99	0.15	0.14	0.03	23.6	1.3	-15.4
		Middle	29	17.6	7.67	312.1	1.61	0.99	1.98	0.13	3.11	0.92	0.37	0.02	45.7	1.4	-11.3
End		10	15.4	7.74	619.5	2.84	1.34	4.82	0.28	2.68	2.03	4.24	0.02	54.1	1.5	-10.1	
Δ						1.91	0.86	3.88	0.22	0.69	1.88	4.11	-0.01	30.6			
SN	SN [†]	Beginning	7	17.5	6.93	129.7	0.91	0.41	0.52	0.04	1.58	0.32	0.10	0.00	37.1	-4.4	-16.8
		End	18	16.5	7.59	186.8	1.04	0.51	1.35	0.08	2.39	0.28	0.21	0.01	37.3	-0.6	~ -10*
		Δ					0.13	0.10	0.83	0.04	0.82	-0.03	0.11	0.01	0.2		
WSA	WSA [†]	Beginning	8	22.1	8.31	193.9	0.44	0.13	2.11	0.12	1.97	0.46	0.37	0.01	32.9	-0.6	-10.3
		End	4	15.4	7.74	619.5	2.84	1.34	4.82	0.28	2.68	2.03	4.24	0.02	54.1	1.5	-10.1
		Δ					2.40	1.22	2.71	0.16	0.71	1.57	3.87	0.01	21.2		
ASP/NV/ESA	ESA	Beginning	7	22.1	8.32	274.5	0.37	0.20	2.53	0.12	2.24	0.40	0.42	0.01	38.1	-2.2	-12.7
		Middle	5	15.4	8.23	496.1	1.80	1.23	3.98	0.20	4.85	0.62	1.34	0.05	54.0	2.2	~ -12*
		End	11	13.5	8.01	1197.3	8.60	11.02	188.44	1.08	14.32	27.44	142.00	0.14	21.1	6.4	-6.4
		Δ					8.24	10.82	185.91	0.96	12.08	27.04	141.59	0.13	-17.0		
	NV [†]	Beginning	1	18.8	7.88	199.8	0.49	0.33	1.63	0.21	2.25	0.13	0.14	0.01	51.0	1.4	~ -15*
		Middle	2	15.3	8.26	660.2	0.78	0.33	5.76	0.24	4.29	1.15	1.55	0.02		-2.5	-11.2
		End	1	12.4	7.09	42700	7.49	67.48	700.35	2.40	15.57	7.29	685.50	0.02	18.0	4.7	~ -10*
		Δ					7.00	67.15	698.72	2.20	13.32	7.16	685.36	0.02	-33.0		
	ASP	Beginning	4	21.0	8.23	2403.0	0.95	1.17	31.41	0.30	14.55	5.84	11.74	0.14	~25*	2.3	-4.5
		End	2	11.8	7.32	42700	4.64	36.43	448.71	2.61	17.71	25.51	423.38	0.23	18.0	2.7	-6.4
Δ						3.68	35.26	417.30	2.31	3.16	19.67	411.63	0.09	-7.0			

Table 2 (continued). Median values for the end members of the Honey Lake Basin flow paths, arranged by chemical and physical flow paths.
 * Indicates estimated numbers. † Indicates the physical flow paths that are later modeled using NETPATH.

Chemical Flow Path	Physical Flow Path	n (# of samples)	Temp (°C)	pH	TDS (mg/L)	Cations (meq/L)				Anions (meq/L)				SiO ₂ (mg/L)	Balance Error %	δ ¹³ C (‰)	
						Ca ²⁺	Mg ²⁺	Na ⁺	K ⁺	HCO ₃ ⁻	SO ₄ ²⁻	Cl ⁻	F ⁻				
	Precipitation	1	0.0	5.7		0.00	0.000	0.00	0.00	0.00	0.00	0.00	0.00		0.0		
CW/VM/FSM	FSM [†]	Beginning	2	15.0	7.40	156.6	0.94	0.49	0.48	0.06	1.72	0.12	0.18		~30*	-1.2	~ -15*
		Middle	10	16.9	8.23	370.9	0.92	0.45	3.62	0.12	1.93	2.50	0.45	0.05	22.1	-3.1	-14.1
		End	3	15.0	8.12	4632	2.43	2.84	68.32	0.97	11.34	4.55	57.66	0.02	15.3	0.4	~ -10*
		Δ					1.49	2.35	67.84	0.91	9.61	4.43	57.48		-14.7		
	VM	Beginning	3	14.7	7.32	166.6	0.91	0.47	0.64	0.06	1.72	0.12	0.18		~25*	1.7	~ -15*
		Middle	9	19.8	8.16	222.2	0.38	0.20	2.54	0.17	2.39	0.32	0.44	0.01	34.2	-1.1	-11.9
		End	2	14.7	8.34	4614.5	2.17	3.15	65.69	0.96	6.99	6.79	57.42	0.05	12.7	-1.4	~ -10*
		Δ					1.25	2.67	65.04	0.90	5.27	6.67	57.24		-12.3		
	CW	Beginning	4	15.0	7.49	177.3	1.10	0.65	0.59	0.13	2.19	0.13	0.14	0.01	21.7	-0.8	-19.0
		End	2	14.0	7.68	21628	4.09	33.93	353.60	1.34	10.25	4.05	343.79	0.02	18.0	4.6	~ -10*
Δ						2.99	33.27	353.01	1.21	8.06	3.92	343.64	0.01	-3.7			
HLW	HWL [†]	4	41.3	8.43		0.40	0.09	2.17	0.03	1.73	0.67	0.26	0.10	45.4	-1.7	-12.8	
AML	AML [†]	4	82.8	8.64	820.8	0.90	0.02	10.23	0.16	0.60	6.03	4.13	0.18	85.7	1.0	-11.6	

Table 3. Data for the two fault zone flow paths which used in GEOTHERM. * Indicates an estimated number.

Flow Path	Name	Sample #	Temp (°C)	pH	SiO ₂ (mg/L)	Na ⁺ (ppm)	K ⁺ (ppm)	Ca ²⁺ (ppm)	Mg ²⁺ (ppm)
HLW	Mormon Church Heating	W21	52.0	7.7	62.0	56.00	0.90	9.50	0.60
	Roosevelt Swimming Pool	RE1	35.8	8	53.0	20.00	3.80	19.00	3.40
	Rose 27	H4132	38.0	8.9	21.1*	60.70	0.30	0.71	0.06
	Zamboni Hot Spring	H4134	40.0	9.1	21.1	63.00	0.80	2.40	0.10
AML	Amedee Hot Springs	W40	103.0	8.6	95.0	238.00	6.00	16.00	0.50
	Johnston 1	V209	67.0	8.8	88.6	172.00	2.90	13.50	0.00
	Norcal2	V211	99.0	8.9	106.0	254.00	7.00	17.60	0.00
	HL Power Plant	H4135	63.0	8.3	53.0	277.00	11.70	25.30	0.10

Table 4. GEOTHERM results. All geothermometers in grey were eliminated based on the criteria listed. * Temperatures less than the measured reservoir temperature were automatically eliminated. A geothermal gradient of 34°C/Km was used to determine circulation depths (Nathenson and Guffanti, 1988). ⁺ Mayo, written personal communication (2005). [#] Fournier and Rowe (1977). [^] Fournier and Truesdell (1973). [%] Fournier (1979).

Flow Path	Name	Sample #	Temp (°C)	Silica Conductive (good for reservoir temps <100°C) ⁺	Silica Adiabatic (good for reservoir temps >100°C) ⁺	Silica Chalcedony (good for reservoir temps <150-225°C) ⁺	Silica Cristobalite (good for reservoir temps <150-225°C) ⁺	Silica Amorphous (good for reservoir temps <150-225°C) ^{+#}	Na-K (good for reservoir temps >100-150°C) [^]	Na-K-Ca (1/3) ^{+^} (good for -β and temps >100°C)	Na-K-Ca (4/3) ^{+^} (good for +β and temps >100°C)	Average GEOTHERM Temp (°C)	Depth of Circulation (km)
HLW	Mormon Church Heating	W21	52.0	112.00	111.00	83.00	62.00	-5.00*	74.00	90.00	36.00*	112	3.00
	Roosevelt Swimming Pool	RE1	35.8	105.00	105.00	75.00	54.00	-12.00*	227.00	177.00	53.00	105	2.79
	Rose 27	H4132	38.0	65.00	71.00	33.00*	16.00*	-44.00*	-31.00*	9.00*	0.00*	65	1.62
	Zamboni Hot Spring	H4134	40.0	65.00	71.00	33.00	16.00*	-44.00*	64.00*	91.00	58.00	65	1.62
AML	Amedee Hot Springs	W40	103.0	140.00	135.00	114.00	90.00*	20.00*	94.00*	122.00	97.00*	117	3.15
	Johnston 1	V209	67.0	131.00	127.00	103.00	80.00	11.00*	76.00	103.00	73.00	131	3.56
	Norcal2	V211	99.0	140.00	135.00	114.00	90.00*	20.00*	99.00	126.00	101.00	140	3.82
	HL Power Plant	H4135	63.0	105.00	150.00	75.00	54.00*	-12.00*	121.00	144.00	113.00	105	2.79

Table 5. Published maximum temperature results based on geothermometers for the Antelope Mountain/Litchfield Fault Zone.

Author	Estimated Groundwater Temp (°C)	Notes
This Investigation	117-133	Silica conductive, silica adiabatic, and Na-K-Ca (1/3) geothermometers
Hardt et. al. (1975)	100-120 or 150-200	Maximum range calculated for mixing with shallow, cool waters
Reed (1978)	140	
Adams (1984)	150-160	Silica geothermometer
Geoproducts Corporation (1984)	110-141	Na-K-Ca, silica chalcedony, and quartz geothermometers

Table 6. Approximate mixing ratios for the groundwater (>17°C) in Honey Lake Basin based on mixing with thermal waters from the Antelope Mountain/Litchfield Fault Zone (123°C average maximum temperature) and Honey Lake/Warm Springs Fault Zone (87°C average maximum temperature).

"Thermal" Component (%)	"Cold" Component (%)	Resulting Temperature (°C)	
		AML	HLW
100	0	123	87
90	10	112.4	80
80	20	101.8	73
70	30	91.2	66
60	40	80.6	59
50	50	70	52
40	60	59.4	45
30	70	48.8	38
20	80	38.2	31
10	90	27.6	24
0	100	17	17

Table 7. Mean ¹⁴C age data. + indicates and estimated value.

Flow Path	Sample #	Temp (°C)	pH	HCO ₃ ⁻ (meq/L)	Activity of HCO ₃ ⁻	δ ¹³ C (‰)	¹⁴ C (pmc)	¹⁴ C Age (years) Fonts	¹⁴ C Age (years) Pearson	³ H (TU)
ESA	W32*	24.00	7.70	1.40	0.971	-12.80	21.60	7500		
ESA	V194*	20.60	9.00	3.60	0.953	-12.50	56.80	modern		0.5
FSM	V165*	17.80 ⁺	8.25 ⁺	1.70	0.968	-14.10	59.00		2500	
LV	V195*	9.10	8.10	3.25	0.958	-11.90	13.10	1100		
LV	V196*	9.00	8.10	3.54	0.956	-11.90	15.00	10000		
LV	V197*	11.30	8.30	3.41	0.956	-13.80	16.10	9500		
LV	V203*	16.90	8.20	3.25 ⁺	0.957	-11.40	17.50	9000		
LV	V198*	11.30	8.10	3.25	0.957	-13.20	23.40	6500		
LV	V206*	16.70	8.30	3.25 ⁺	0.957	-11.90	30.70	4000		
LV	V178*	18.30	7.40	3.62	0.955	-9.00	30.70	5000		
LV	V180*	18.10	7.70	1.61	0.969	-6.70	35.00	3500		
LV	V199*	10.40	7.83 ⁺	3.11 ⁺	0.958	-13.10	38.50	2500		
LV	V200*	11.60	7.83 ⁺	3.11 ⁺	0.958	-12.40	45.20	modern		
LV	V177*	18.90	7.30	7.38	0.938	-11.90	46.00	1500		
LV	V202*	9.40	7.60	3.11 ⁺	0.959	-11.00	50.30	500		
LV	V207*	18.30	8.10	3.11 ⁺	0.958	-12.30	55.40	modern		0.2
LV	V205*	17.10	8.50	3.49	0.955	-11.80	60.90	modern		
LV	H4115*	21.85	8.46	3.56	0.955	-3.30	63.60	modern		0.4
LV	V201*	13.60	7.70	3.11 ⁺	0.958	-11.40	71.40	modern		
LV	H4130*	18.00	8.42	1.79	0.967	-15.43	73.13		modern	0.3
LV	V174*	22.20	7.40	2.88 ⁺	0.959	-2.70	74.60	modern	modern	0.9
LV	V192*	14.80	8.10	4.90 ⁺	0.948	-7.80	75.00	modern		
LV	V141*	18.20	8.60	11.31	0.924	-10.80	79.80	modern		
LV	V168*	20.90	7.30	3.02 ⁺	0.958	-4.40	83.80	modern	modern	0.3
LV	W127*	11.25	7.31	3.02	0.959	-14.91	90.50		modern	4.1
LV	V183*	18.60	8.20	3.34 ⁺	0.956	-9.00	102.60	modern		
LV	H4084*	21.00	7.35	2.60	0.961	-12.45	112.84	modern		3.9
NV	W102*	14.90	8.25	3.66	-	-11.23	76.70	modern	modern	
SM	H4106*	17.10	7.82	1.80	0.967	-15.10	72.74		modern	
SM	H4092*	18.70	7.76	3.19	0.957	-1.90	79.90	modern		0.6
SR	W43*	14.10	6.90	5.76	0.945	-7.19	2.80	25500	21500	0
SR	H4096*	17.10	7.92	2.35	0.963	-7.70	46.70	1000		0.0
SR	H4114*	17.37	7.99	2.90	0.959	-14.40	54.50		2500	0.0
SR	H4097*	17.40	7.92	2.04	0.965	-15.28	74.72		modern	0.4
SR	V111*	15.60	7.50	7.54	0.938	-10.10	83.00	modern		
SR/AML	V209*	66.95	8.75	0.19	0.985	-11.90	10.60	13000		
VM	V153*	17.70	8.10	1.88	0.967	-11.25	37.00	3000		
VM	H4136*	15.85	8.67	3.04	0.958	-10.32	37.60	2500		1.7
VM	V145*	15.85 ⁺	8.67 ⁺	1.69	0.968	-11.60	41.30	1500		
VM	W93*	19.17	8.30	2.55	0.961	-13.40	43.48	1500		1.4
WSA	H4116*	21.85	8.25	2.06	0.965	-10.20	17.10	9000		0.3
WSA/AML	V211*	98.90	8.90	1.00	0.964	-9.90	10.00	13500		0.2

Table 8. The constraints and phases used in each NEPTPATH model.

Constraint (used in ALL models)	Phase	SR for SR/SHAF/LV		SR-SHAF	SN		WSA		NV for ESA/NV/ASP		FSM for FSM/VM/CW		HLW	AML
		Precip. to Initial	Initial and Thermal Mix to Final	Mix	Precip. to Initial	Initial to Final	Precip. to Initial	Initial and Thermal Mix to Final	Precip. to Initial	Initial to Final	Precip. to Initial	Initial to Final	Precip. to Median Chem.	Precip. to Median Chem.
Sulfur	Albite	x		x	x		x		x		x		x	x
Calcium	Biotite	x	x		x	x						x	x	x
Magnesium	Calcite	x	x	x	x	x	x	x	x	x	x	x	x	x
Sodium	CO ₂ gas	x	x	x	x	x	x	x	x	x	x	x	x	x
Potassium	Enstatite	x	x				x	x	x	x	x	x		
Chloride	Exchange		x	x		x	x	x	x	x	x	x	x	x
Carbon	Fluorite	x	x	x	x	x	x	x	x	x		x	x	x
Silica	Forsterite	x	x				x	x	x	x	x	x		
	Gypsum	x	x	x	x	x	x	x	x	x	x	x	x	x
	Halite	x	x	x	x	x	x	x	x	x	x	x	x	x
	K-spar		x			x	x	x	x	x	x	x	x	
	Mg-mont	x			x									x
	Na-mont		x	x	x	x		x		x		x		
	Quartz		x			x		x		x		x	x	x
	Sylvite			x										

Table 9. NETPATH geochemical evolution model results. Positive numbers represent dissolution and negative numbers represent precipitation. These results are graphed in Figures 24 and 25.

	SR for SR/SHAF/LV		SR-SHAF Mix (mmol/L)	SN		WSA		NV for ESA/NV/ASP		FSM for FSM/VM/CW		HLW	AML
	Precip. to Initial (mmol/L)	Initial and Thermal Mix to Final (mmol/L)		Precip. to Initial (mmol/L)	Initial to Final (mmol/L)	Precip. to Initial (mmol/L)	Initial and Thermal Mix to Final (mmol/L)	Precip. to Initial (mmol/L)	Initial to Final (mmol/L)	Precip. to Initial (mmol/L)	Initial to Final (mmol/L)		
Phase													
Albite	0.40		3.74	0.42		0.06		0.04		0.04			0.80
Biotite	0.20	0.09		0.14	0.03						0.26	0.03	0.18
Calcite	0.41	2.91	0.65	0.30	0.89	0.84	0.56	0.91	9.78	0.54	5.22	0.74	
CO2 gas	1.65	0.49	2.92	1.61	-0.28	1.10	0.35	1.38	5.75	1.33	4.27	0.86	0.10
Enstatite	0.02	0.15				0.03	0.30	0.08	17.54	0.13	0.40		
Exchange		3.62	0.73		0.81	0.86		0.73	9.86	0.13	6.70	0.96	2.65
Fluorite	0.002		0.01	0.002	0.00	0.003	0.001	0.003	0.01		0.01	0.05	0.09
Forsterite	0.01	0.09				0.02	0.15	0.04	8.77	0.06	1.97		
Gypsum	0.05	1.09	-0.001		-0.02	0.23	0.63	0.06	3.74	0.06	2.22	0.37	3.02
Halite	0.05	3.92	-0.66	0.10	0.11	0.37	3.67	0.14	715.91	0.18	57.74	0.26	4.13
K-spar		0.09			0.004	0.12	0.16	0.21	2.30	0.06	0.91	0.01	
Mg-mont	-.37			0.00									-1.52
Na-mont		-10.22	-3.05	-0.28	-2.71		-4.34		-17.10		-9.05		
Quartz		37.16			9.84		15.15		37.78		29.64	0.65	4.10
Sylvite			-0.07										
Mix													
% Initial		0.72	0.44				0.95						
% Thermal		0.28	0.56				0.05						
$\delta^{13}\text{C}$													
Observed		-7.19	-11.87		-10.40		-10.10		-10.00		-10.00		
Computed		-7.19	-11.87		-10.00		-10.10		-10.00		-10.00		

APPENDIX A

Table 2. Honey Lake Basin groundwater temperature data. * indicates a sample location with more than one sampling event.

Flow Path	Name	Sample #	Water Source	Depth Interval (m)	Temp (°C)	pH	SiO ₂ (mg/L)
FSM	Hell Dom. Well	W117*	well	10.668	5.00	8.60	8.00
SR	P. Milton Dom.	W17	well		5.10	7.10	
LV	Mad Spring	W146*	spring		6.00	6.90	
DLT	Upper Adobe Spring	W89*	spring		7.00	7.5	
OUT	Upper Jumper Spring	W99*	spring		8.00	7.5	
SHAF	Shafter Spring	W45*	spring		8.30		
LV	Beebeers Well	W688	well	42.672	8.40	6.83	
SR	Spring S. Raop Min.	W13*	spring		8.50	8.62	
LV	SIAD PSW PZ-1	V198*	well	150.876	9.00	8.10	45.10
LV	SIAD PSW PZ-4	V195*	well	192.024	9.10	8.10	47.40
USA	Parkie Ranch	W59	well		9.20	7.60	
LV	SIAD PSW PZ-1	V202*	well	70.5612	9.40	7.60	
LV	August Spring	W80*	spring		9.60	8.59	
SN	Phoma National Forest	W682	well	54.864	10.00	6.38	
FSM	Spring N. Ft. Snow Min.	W58*	spring		10.30	8.02	
LV	SIAD PSW PZ-4	V199*	well	152.4	10.40		
SR	Cady Spring	W40*	spring		10.50	8.16	
EXPRESA	Stone Well	W687	well	39.824	11.20	7.54	42.00
LV	Gianted Well #2	W125*	well	76.2	11.25	7.31	
LV	SIAD PSW PZ-1	V198*	well	56.388	11.30	8.10	42.60
LV	SIAD PSW PZ-2	V199*	well	102.108	11.30	8.30	38.20
LV	SIAD PSW PZ-3	V200*	well	141.21384	11.60		
LV	SIAD STP-4-PZ	W186*	well	17.3736	11.80	6.70	
SHAF	SIAD ILE-AMWA	W128*	well	33.228	11.80	7.60	
SN	27N14E06B01M	W85	well	121.92	12.00	6.60	41.00
LV	Horse Spring	W141*	spring		12.00	7.3	
LV	Cald Spring	W130*	spring		12.00	7.30	
OUT	Fale Spring	W142*	spring		12.00	7.2	
USA	27N17E15P02 M	W56	well	16.1544	12.20	8.60	
SN	27N15E08B01M	W72	well		12.20	7.60	40.00
ESAC/WASP	May Well	W116*	well	76.2	12.40	7.09	18.00
SR/SHAF	F. Dewey Dom.	W4	well		12.50	8.50	
VM	Shoop Spring	W126*	spring		12.50	7.20	
LV	SAID ALF-3	V175*	well	32.1088	12.90	7.70	
FSM	McCorle Dom. Well	W104*	well	19.812	13.00	7.36	12.00
SR	Ca Fish & Game Ir.	W4	well		13.00	8.35	46.00
LV	STP-03-PZ	V185*	well	17.0688	13.10	7.20	
SR	SIAD STP-3-PZ	V187*	well	27.7368	13.10	7.70	
LV	MacDonald Dom.	W20	well		13.11	8.10	
LV	Johnstonville	W113*	well	21.9456	13.20	7.28	52.05
SR	Hagen Well	W52*	well	54.864	13.30	8.40	
USA	H&H Dom. Well	W163	well	156.2624	13.50	6.95	37.00
SN	Humphries #1	W4086*	well	13.55	8.12	37.00	
WSA	SIAD ILE-AMWA	V182*	well	8.8392	13.60	8.30	
LV	SIAD PSW PZ-2	V201*	well	96.012	13.60	7.70	
LV	Spring N. Seven Lakes Min.	V77*	spring		13.60	7.71	
LV	Spr. N. Seven Lakes Min.	W109*	well		13.60	7.80	
ES/FSM	Assan North Dom. Well	W114*	well	13.60	7.80	5.30	
SR	E. Grant Dom.	W12	well	26.2128	13.61	8.25	33.50
SR/SHAF	Tanner Ranch Dom.	W41	well		13.61	8.30	24.50
WSA	Johnson Ranch Dom.	W19	well	18.288	13.69	7.97	46.50
SR	SIAD STP-7	V188*	well	20.7264	13.70	7.90	
SR	I. Swain Dom.	W13	well		13.72	8.30	42.50
SR	Ca Fish & Game Ir.	W42	well	45.72	13.75	7.45	50.50
USA	27N17E04A02 M	W87	well	36.576	13.95	8.56	
LV	Duper Scott Spring	W141*	spring		14.00	7.70	
LV	Lower Scott Spring	W144*	spring		14.00	7.80	
LV	Upper Road Spring	W146*	spring		14.00	7.93	
CH	Black Canyon	W179*	spring		14.00	7.80	
SR	Darken Well	W43*	well		14.10	6.90	
SN	27N14E22A01M	W82	well	171.6024	14.20	7.10	46.00
LV	Haugen Spring	W75*	spring		14.30	7.87	
OUT	Soda Springs	W2756	spring		14.30	8.53	
SR/SHAF	Frab & Game Well	W4093*	well	160.02	14.33	8.40	44.00
LV	SIAD ILE-AMWA	V191*	well	20.94208	14.40	9.10	54.00
SN	27N14E26C01M	W78	well		14.40	7.80	34.00
SN	26N15E11B01M	W137	well		14.40	7.50	50.00
SN	27N16E26B01M	W66	well		14.40	8.00	56.00
SN	SE of Otis Canyon	spring/well		14.50	7.78	35.50	
SR	Trussell Well	W4099*	well	14.54	7.78	44.50	
SN	Newkirk Dom.	W45	well		14.56	7.80	
LV	27N17E30B01M	W176	well		14.60	7.43	
VM	Ford #1 Well	W112*	well	184.404	14.70	8.37	5.30
SR/SHAF	B. Pomeroy	W15	well	161.24	14.72	8.25	60.00
LV	Cottonwood Springs	W96*	spring		14.77	7.77	21.67
LV	SIAD INT-AMWB	V192*	well	31.568126	14.80	8.10	
LV	SIAD INT-AMWC	V193*	well	44.8066	14.80	7.90	
NV	Never Sweat Ranch	W102*	well	152.4	14.90	8.25	
USA	27N17E31D01M	W54	well	13.4112	15.00	8.60	
ES/FSM	Frank Whit	W60	well	13.232	15.00	9.00	
SR	B. Vanders Ir. Well	W124	well	91.44	15.00	7.85	
SR	J. Ferris Dom.	W14	well		15.00	8.10	51.00
LV	25N17E14B01M	W157	well		15.00	7.50	48.00
LV	22N17E14B01M	W177	well		15.00		62.00
LV	Spring A. Seven Lakes Min.	W76*	spring		15.00	8.33	
USA	Sand A. Well	W19	well		15.00	9.00	29.00
WSA	Spr. N. of Stacy	W90	spring		15.00	8.90	
ES/FSM	26N17E01P01 M	W120	well		15.00	8.30	
FSM	Red Spring	W125*	spring		15.00	7.50	
VM	Mustang Spring	W151*	spring		15.00	7.30	
LV	26N14E21B01M	W126	well		15.25	8.05	57.50
SN	27N14E26B01M	W71	well	61.5696	15.25	6.78	43.00
WSA	27N16E03B01M	W70	well	167.64	15.50	7.50	54.00
OUT	Sand Pines East Well	W46*	well	217.076	15.50	8.7	
SR/SHAF	Ca Fish & Game Ir.	W8	well		15.50	8.80	51.00
SN	27N14E24B01M	W80	well		15.50	7.00	
SN	26N17E08B01M	W136	well		15.50	7.90	51.00
LV	27N16E34B01M	W63	well		15.50	7.60	47.00
LV	27N16E31M	W64	well		15.50	7.40	46.00
LV	27N16E25M	W67	well		15.50	7.40	49.00
LV	27N16E19M	W68	well		15.50	7.70	71.00
LV	26N16E04B01M	W134	well		15.50	8.10	
WSA	27N16E02M	W71*	well		15.50	7.40	55.00
WSA	27N16E11E01Mk	W69*	well	115.824	15.50	7.47	53.36
SR	Lassen County Well	W111*	well	42.672	15.60	7.50	
CH/ASH/NNV	BRE-C	W10*	well	25.908	15.67	8.27	
SHAF	Spring NW Five Spring Min.	V35*	spring		15.70	7.96	
SHAF	Murrers Meadow Spring	V33*	spring		15.80	7.64	
VM	Frab Spring Ranch Dom. Well	W4106*	well	78.6384	15.85	8.61	17.40
LV	26N16E15E01M	W129	well	18.288	15.87	7.72	36.43
FSM	Austin Dom. Well	W105*	well		16.00	8.10	8.00
FSM	Willow Well	W108*	well		16.00	8.15	18.50
LV	27N16E35P01M m	W62	well	167.64	16.07	7.46	55.23
LV	25N17E30B01M	W161	well	79.248	16.10	7.55	
LV	25N17E17A01M	W162	well		16.10	7.60	60.00
LV	25N17E07B01	W165	well		16.10	8.57	
LV	25N17E02B01M	W175	well		16.10	7.03	
LV	27N16E36B01M	W61*	well	48.1584	16.30	7.51	46.65
LV	Webber 167	W421*	well		16.30	7.57	
LV	27N15E25B01M	W75	well		16.35	8.05	
SR	Gen. Well	W4095*	well		16.50	8.20	56.00
SHAF	Spring E. Horse Lake Min.	W4101*	spring		16.60	7.77	23.70
VM	Willow Spring	W103*	spring		16.60	7.47	
USA	25N17E01B01 M	W58	well		16.65	8.40	48.00
SR	Ca Conserv. Chr. Dom.	W18	well		16.67	8.00	
WSA	Abraham Jensen Ir.	W23	well		16.67	7.20	52.00
SR	Lemley Location	W4117*	spring		16.69	8.27	36.50
SR	SE of Standsah	V110*	well	27.82824	16.70	7.50	49.80
LV	SIAD PSW #5	V206*	well	213.36	16.70	8.30	49.00
SN	27N14E23B01M	W81	well		16.70	8.60	43.00
OUT	Heming Spring	V29*	spring		16.80	8.29	
LV	SIAD PSW #2	V203*	well	213.36	16.90	8.30	
LV	S of Doble	W166*	well	36.576	16.90	7.31	24.50
OUT	Suzie Spring	W168*	spring		17.00	7.70	
OUT	Ragle Lake Spring	V25*	spring		17.00		
SR	NW of Spanish	W4096*	well	17.0688	17.10	7.92	38.10
LV	SIAD PSW #5	V205*	well	167.64	17.10	8.50	
SHAF	Fale Patch Spring	W4106*	spring		17.10	7.82	15.70
USA	Shil Dom. Well	W70	well		17.15	8.25	38.50
SN	Orin Canyon	W4091*	spring/surface		17.15	7.49	25.90
SR	Rainwood School	W4114*	well	44.196	17.17	7.99	
SR	Plumtree Spring	W4097*	spring		17.40	7.92	28.10
USA	Droeger Well	W4118*	well		17.55	8.48	40.55
LV	SIAD ILE-AMWA	V181*	well	33.228	17.60	7.50	
USA	Harding Well	W4119*	well	46.3296	17.60	8.07	
SHAF	Spr. S. Horse Min.	W95	spring		17.60	8.30	
SHAF	Spring N. Horse Min.	W98	spring		17.60	8.25	
SHAF	Spring S. of Snowsystem Min.	V34*	spring		17.60	7.68	
LV	26N17E18B01M	W122	well		17.60	7.30	
LV	Cowboy Joe Spring	W4089*	spring		17.65	7.46	20.70
VM	Frab Spring Irrigation Well-SW	V153*	well	134.112	17.70	8.10	
LV	22N17E08B01M	W178	well		17.75	7.65	32.50

Flow Path	Name	Sample #	Water Source	Depth Interval (m)	Temp (°C)	pH	SiO ₂ (mg/L)
LV	26N14E06B01 M	W133	well	22.86	17.77	7.10	
FSM	W. Hurd Dom. Well	W110	well	7.62	17.80	8.25	
SN	Basler Well	W4110*	well	30.48	17.85	7.46	43.50
USA	SW of Bass Hill	W4112*	well	60.96	17.95	6.90	38.90
LV	Harden Place - Constanta Rd.	W4130*	well	54.864	18.00	8.42	7.20
SN	Duck Lake Imp. Well	W55*	well		18.00	7.70	54.00
OUT	24N15E20A02M	W174	well		18.00	7.90	50.00
LV	SIAD ILE-AMWA	V180*	well	36.5712	18.10	7.70	
LV	JDS Wetlands	V141*	well	48.768	18.20	8.60	
SN	Webber 84	W4108*	well		18.20	7.54	40.00
LV	SIAD ILE-AMWA	V184*	well	17.526	18.30	8.90	
LV	SIAD R21-S-PZ	V178*	well	32.004	18.30	7.40	
LV	Webber 159	W159*	well	36.576	18.30	7.15	46.00
LV	SIAD PSW #9	V207*	well	161.544	18.30	8.10	
LV	27N17E13K01M	W53	well		18.30	7.40	48.00
LV	26N15E03B01M	W139	well		18.44	7.73	32.25
SN	Stanford	V112*	well	43.8912	18.50	8.00	
LV	SIAD ILE-AMWA	V183*	well	19.812	18.60	8.20	
SHAF	BLM Horse Corral Well	W4092*	well	45.72	18.70	7.76	33.55
LV	Webber 125	W4120*	well		18.70	7.54	42.00
NV	Hodges Well						

Table 3. Heavy Metals chemical data, in mg/L. * indicates a sample location with more than one sampling event.

Flow Path	Name	Sample	Water Source	Depth (m)	Temp (°C)	pH	Cond (µS/cm)	Soluble Chemistry (mg/L)												NO ₃ -N (mg/L)
								Ca ²⁺	Mg ²⁺	Na ⁺	K ⁺	Fe ²⁺	CaCO ₃	CO ₃ ²⁻	HCO ₃ ⁻	SO ₄ ²⁻	Cl ⁻	NO ₂ ⁻	F ⁻	
BS/STAF	El-Dokki Dam	814	well	11.30	8.50	77.0	12.0	2.2	2782	2.2	0.0	18.0	11.0	2.0	0.1	0.1	14.00			
BS/STAF	El-Dokki Dam	815	well	11.30	8.50	78.0	12.0	2.2	2848	2.2	0.0	18.0	11.0	2.0	0.1	0.1	14.00			
BS/STAF	El-Dokki Dam	816	well	11.30	8.50	79.0	12.0	2.2	2914	2.2	0.0	18.0	11.0	2.0	0.1	0.1	14.00			
BS/STAF	El-Dokki Dam	817	well	11.30	8.50	80.0	12.0	2.2	2980	2.2	0.0	18.0	11.0	2.0	0.1	0.1	14.00			
BS/STAF	El-Dokki Dam	818	well	11.30	8.50	81.0	12.0	2.2	3046	2.2	0.0	18.0	11.0	2.0	0.1	0.1	14.00			
BS/STAF	El-Dokki Dam	819	well	11.30	8.50	82.0	12.0	2.2	3112	2.2	0.0	18.0	11.0	2.0	0.1	0.1	14.00			
BS/STAF	El-Dokki Dam	820	well	11.30	8.50	83.0	12.0	2.2	3178	2.2	0.0	18.0	11.0	2.0	0.1	0.1	14.00			
BS/STAF	El-Dokki Dam	821	well	11.30	8.50	84.0	12.0	2.2	3244	2.2	0.0	18.0	11.0	2.0	0.1	0.1	14.00			
BS/STAF	El-Dokki Dam	822	well	11.30	8.50	85.0	12.0	2.2	3310	2.2	0.0	18.0	11.0	2.0	0.1	0.1	14.00			
BS/STAF	El-Dokki Dam	823	well	11.30	8.50	86.0	12.0	2.2	3376	2.2	0.0	18.0	11.0	2.0	0.1	0.1	14.00			
BS/STAF	El-Dokki Dam	824	well	11.30	8.50	87.0	12.0	2.2	3442	2.2	0.0	18.0	11.0	2.0	0.1	0.1	14.00			
BS/STAF	El-Dokki Dam	825	well	11.30	8.50	88.0	12.0	2.2	3508	2.2	0.0	18.0	11.0	2.0	0.1	0.1	14.00			
BS/STAF	El-Dokki Dam	826	well	11.30	8.50	89.0	12.0	2.2	3574	2.2	0.0	18.0	11.0	2.0	0.1	0.1	14.00			
BS/STAF	El-Dokki Dam	827	well	11.30	8.50	90.0	12.0	2.2	3640	2.2	0.0	18.0	11.0	2.0	0.1	0.1	14.00			
BS/STAF	El-Dokki Dam	828	well	11.30	8.50	91.0	12.0	2.2	3706	2.2	0.0	18.0	11.0	2.0	0.1	0.1	14.00			
BS/STAF	El-Dokki Dam	829	well	11.30	8.50	92.0	12.0	2.2	3772	2.2	0.0	18.0	11.0	2.0	0.1	0.1	14.00			
BS/STAF	El-Dokki Dam	830	well	11.30	8.50	93.0	12.0	2.2	3838	2.2	0.0	18.0	11.0	2.0	0.1	0.1	14.00			
BS/STAF	El-Dokki Dam	831	well	11.30	8.50	94.0	12.0	2.2	3904	2.2	0.0	18.0	11.0	2.0	0.1	0.1	14.00			
BS/STAF	El-Dokki Dam	832	well	11.30	8.50	95.0	12.0	2.2	3970	2.2	0.0	18.0	11.0	2.0	0.1	0.1	14.00			
BS/STAF	El-Dokki Dam	833	well	11.30	8.50	96.0	12.0	2.2	4036	2.2	0.0	18.0	11.0	2.0	0.1	0.1	14.00			
BS/STAF	El-Dokki Dam	834	well	11.30	8.50	97.0	12.0	2.2	4102	2.2	0.0	18.0	11.0	2.0	0.1	0.1	14.00			
BS/STAF	El-Dokki Dam	835	well	11.30	8.50	98.0	12.0	2.2	4168	2.2	0.0	18.0	11.0	2.0	0.1	0.1	14.00			
BS/STAF	El-Dokki Dam	836	well	11.30	8.50	99.0	12.0	2.2	4234	2.2	0.0	18.0	11.0	2.0	0.1	0.1	14.00			
BS/STAF	El-Dokki Dam	837	well	11.30	8.50	100.0	12.0	2.2	4300	2.2	0.0	18.0	11.0	2.0	0.1	0.1	14.00			
BS/STAF	El-Dokki Dam	838	well	11.30	8.50	101.0	12.0	2.2	4366	2.2	0.0	18.0	11.0	2.0	0.1	0.1	14.00			
BS/STAF	El-Dokki Dam	839	well	11.30	8.50	102.0	12.0	2.2	4432	2.2	0.0	18.0	11.0	2.0	0.1	0.1	14.00			
BS/STAF	El-Dokki Dam	840	well	11.30	8.50	103.0	12.0	2.2	4498	2.2	0.0	18.0	11.0	2.0	0.1	0.1	14.00			
BS/STAF	El-Dokki Dam	841	well	11.30	8.50	104.0	12.0	2.2	4564	2.2	0.0	18.0	11.0	2.0	0.1	0.1	14.00			
BS/STAF	El-Dokki Dam	842	well	11.30	8.50	105.0	12.0	2.2	4630	2.2	0.0	18.0	11.0	2.0	0.1	0.1	14.00			
BS/STAF	El-Dokki Dam	843	well	11.30	8.50	106.0	12.0	2.2	4696	2.2	0.0	18.0	11.0	2.0	0.1	0.1	14.00			
BS/STAF	El-Dokki Dam	844	well	11.30	8.50	107.0	12.0	2.2	4762	2.2	0.0	18.0	11.0	2.0	0.1	0.1	14.00			
BS/STAF	El-Dokki Dam	845	well	11.30	8.50	108.0	12.0	2.2	4828	2.2	0.0	18.0	11.0	2.0	0.1	0.1	14.00			
BS/STAF	El-Dokki Dam	846	well	11.30	8.50	109.0	12.0	2.2	4894	2.2	0.0	18.0	11.0	2.0	0.1	0.1	14.00			
BS/STAF	El-Dokki Dam	847	well	11.30	8.50	110.0	12.0	2.2	4960	2.2	0.0	18.0	11.0	2.0	0.1	0.1	14.00			
BS/STAF	El-Dokki Dam	848	well	11.30	8.50	111.0	12.0	2.2	5026	2.2	0.0	18.0	11.0	2.0	0.1	0.1	14.00			
BS/STAF	El-Dokki Dam	849	well	11.30	8.50	112.0	12.0	2.2	5092	2.2	0.0	18.0	11.0	2.0	0.1	0.1	14.00			
BS/STAF	El-Dokki Dam	850	well	11.30	8.50	113.0	12.0	2.2	5158	2.2	0.0	18.0	11.0	2.0	0.1	0.1	14.00			
BS/STAF	El-Dokki Dam	851	well	11.30	8.50	114.0	12.0	2.2	5224	2.2	0.0	18.0	11.0	2.0	0.1	0.1	14.00			
BS/STAF	El-Dokki Dam	852	well	11.30	8.50	115.0	12.0	2.2	5290	2.2	0.0	18.0	11.0	2.0	0.1	0.1	14.00			
BS/STAF	El-Dokki Dam	853	well	11.30	8.50	116.0	12.0	2.2	5356	2.2	0.0	18.0	11.0	2.0	0.1	0.1	14.00			
BS/STAF	El-Dokki Dam	854	well	11.30	8.50	117.0	12.0	2.2	5422	2.2	0.0	18.0	11.0	2.0	0.1	0.1	14.00			
BS/STAF	El-Dokki Dam	855	well	11.30	8.50	118.0	12.0	2.2	5488	2.2	0.0	18.0	11.0	2.0	0.1	0.1	14.00			
BS/STAF	El-Dokki Dam	856	well	11.30	8.50	119.0	12.0	2.2	5554	2.2	0.0	18.0	11.0	2.0	0.1	0.1	14.00			
BS/STAF	El-Dokki Dam	857	well	11.30	8.50	120.0	12.0	2.2	5620	2.2	0.0	18.0	11.0	2.0	0.1	0.1	14.00			
BS/STAF	El-Dokki Dam	858	well	11.30	8.50	121.0	12.0	2.2	5686	2.2	0.0	18.0	11.0	2.0	0.1	0.1	14.00			
BS/STAF	El-Dokki Dam	859	well	11.30	8.50	122.0	12.0	2.2	5752	2.2	0.0	18.0	11.0	2.0	0.1	0.1	14.00			
BS/STAF	El-Dokki Dam	860	well	11.30	8.50	123.0	12.0	2.2	5818	2.2	0.0	18.0	11.0	2.0	0.1	0.1	14.00			
BS/STAF	El-Dokki Dam	861	well	11.30	8.50	124.0	12.0	2.2	5884	2.2	0.0	18.0	11.0	2.0	0.1	0.1	14.00			
BS/STAF	El-Dokki Dam	862	well	11.30	8.50	125.0	12.0	2.2	5950	2.2	0.0	18.0	11.0	2.0	0.1	0.1	14.00			
BS/STAF	El-Dokki Dam	863	well	11.30	8.50	126.0	12.0	2.2	6016	2.2	0.0	18.0	11.0	2.0	0.1	0.1	14.00			
BS/STAF	El-Dokki Dam	864	well	11.30	8.50	127.0	12.0	2.2	6082	2.2	0.0	18.0	11.0	2.0	0.1	0.1	14.00			
BS/STAF	El-Dokki Dam	865	well	11.30	8.50	128.0	12.0	2.2	6148	2.2	0.0	18.0	11.0	2.0	0.1	0.1	14.00			
BS/STAF	El-Dokki Dam	866	well	11.30	8.50	129.0	12.0	2.2	6214	2.2	0.0	18.0	11.0	2.0	0.1	0.1	14.00			
BS/STAF	El-Dokki Dam	867	well	11.30	8.50	130.0	12.0	2.2	6280	2.2	0.0	18.0	11.0	2.0	0.1	0.1	14.00			
BS/STAF	El-Dokki Dam	868	well	11.30	8.50	131.0	12.0	2.2	6346	2.2	0.0	18.0	11.0	2.0	0.1	0.1	14.00			
BS/STAF	El-Dokki Dam	869	well	11.30	8.50	132.0	12.0	2.2	6412	2.2	0.0	18.0	11.0	2.0	0.1	0.1	14.00			
BS/STAF	El-Dokki Dam	870	well	11.30	8.50	133.0	12.0	2.2	6478	2.2	0.0	18.0	11.0	2.0	0.1	0.1	14.00			
BS/STAF	El-Dokki Dam	871	well	11.30	8.50	134.0	12.0	2.2	6544	2.2	0.0	18.0	11.0	2.0	0.1	0.1	14.00			
BS/STAF	El-Dokki Dam	872	well	11.30	8.50	135.0	12.0	2.2	6610	2.2	0.0	18.0	11.0	2.0	0.1	0.1	14.00			
BS/STAF	El-Dokki Dam	873	well	11.30	8.50	136.0	12.0	2.2	6676	2.2	0.0	18.0	11.0	2.0	0.1	0.1	14.00			
BS/STAF	El-Dokki Dam	874	well	11.30	8.50	137.0	12.0	2.2	6742	2.2	0.0	18.0	11.0	2.0	0.1	0.1	14.00			
BS/STAF	El-Dokki Dam	875	well	11.30	8.50	138.0	12.0	2.2	6808	2.2	0.0	18.0	11.0	2.0	0.1	0.1	14.00			
BS/STAF	El-Dokki Dam	876	well	11.30	8.50	139.0	12.0	2.2	6874	2.2	0.0	18.0	11.0	2.0	0.1	0.1	14.00			
BS/STAF	El-Dokki Dam	877	well	11.30	8.50	140.0	12.0	2.2	6940	2.2	0.0	18.0	11.0	2.0	0.1	0.1	14.00			
BS/STAF	El-Dokki Dam	878	well	11.30	8.50	141.0	12.0	2.2	7006	2.2	0.0	18.0	11.0	2.0	0.1	0.1	14.00			
BS/STAF	El-Dokki Dam	879	well	11.30	8.50	142.0	12.0	2.2	7072	2.2	0.0	18.0	11.0	2.0	0.1	0.1	14.00			
BS/STAF	El-Dokki Dam	880	well																	

Table 5. Honey Lake Basin isotope data. * indicates a sample location with more than one sampling event.

Flow Path	Name	Sample #	Source	Depth (m)	Temp (°C)	pH	T (°C)	δ ¹⁸ O (‰)	δ ² H (‰)	δ ³⁴ S (‰)	δ ³³ S (‰)	‰C (ppm)
ASB	Amor Pass	H0101*	well	134.11	21.00	7.90	2.1	-106.3	-11.1	-2.5		
ASP	Aspen Pass West	W51*	well	134.11	21.00	7.90		-104.0	-13.6			
ASP/ESA	Stone Well	B087*	well	39.62	11.20	7.54		-96.8	-10.3	-6.4		
ESW/ASW	Wells Well	W110*	well	96.20	12.40	7.99		-89.0	-10.9			
CW	Cottonwood Springs	W36*	spring	14.77	7.77	1.2		-114.3	-14.9	-19.0		
CW	Cottonwood Creek South	W95*	surface	12.20	8.40			-110.4	-14.4			
CW	Cold Spring	W506*	spring	12.00	7.30	8.44		-112.5	-14.0			
CW	Cottonwood Creek	V97*	surface	15.00	7.90			-110.0	-14.4			
CW	E. Cottonwood Canyon Creek	V98*	surface	14.10	8.29			-108.0	-13.8			
CW	Cottonwood Spring	B088*	none					-120.2	-15.3			
CW	Cottonwood Creek	B1992*	surface	6.50				-107.9	-13.6			
USA	Hack Rock Ranch	W131*	well	24.00	7.70			-112.0	-14.5	-13.8	21.6	
USA	SIAD LIR-LEADWA	V194*	well	39.41	20.60	9.00	0.5	-109.0	-14.4	-12.5	56.8	
USA	SIAD DEMO-1	V139*	well	28.65	26.70			-115.0	-14.1	-10.2		
USA	Spencer Spring	W12*	spring					-110.0	-14.6			
USA	Lipson Well	W52*	well	54.80	13.30	8.46		-108.0	-13.7			
USA	Duck Lake Irrig. Well	W55*	well	18.00	7.70			-101.6				
USA	Shoshone Creek	V93*	surface					-103.5	-13.2			
USA	Spencer Creek	V99*	surface					-101.0	-12.5			
USA	Fanagan Ranch Well	V139*	well	22.00				-113.0	-14.2			
USA	Diageo Well	H4118*	well	17.55	8.48			-114.9	-14.6			
USA	Harding Well	H4119*	well	46.33	17.60	8.07	0.9	-105.9	-12.8			
ESAFSM	Austin North Dom. Well	W114*	well	13.60	7.80			-96.5	-9.9			
FSM	Cap Nera Rd. - DWK West	V165*	well	12.21				-116.1	-15.7	-14.1	39.0	
FSM	McKenzie Dom. Well	W101*	well	19.81	13.00	7.36		-116.0	-15.2			
FSM	Austin Dom. Well	W105*	well	16.00	8.10			-114.0	-14.9			
FSM	Wilson Well	W109*	well	16.00	8.15	0		-118.0	-14.2			
FSM	Prickie Dom. Well	W113*	well	8.20				-109.5	-13.6			
FSM	Hall Dom. Well	W117*	well	5.00	8.60			-116.0	-15.3			
FSM	EIF Spring	W125*	spring					-115.0	-14.7			
FSM	Rat Spring	W133*	spring	15.00	7.30			-118.0	-14.7			
FSM	Mullen Creek	W134*	surface					-114.0	-15.3			
FSM	Spring V. T. Sage Mtn	V103*	spring	10.30	8.02			-116.0	-14.9			
FSM	Neck/Fanstone Well	H4128*	well	22.35	7.88	0.5		-119.0	-14.6			
LV	SIAD PSW PZ-4	V195*	well	192.02	9.10	8.10		-120.0	-15.1	-11.9	13.1	
LV	SIAD PSW PZ-1	V196*	well	150.88	9.60	8.10		-118.0	-14.8	-11.9	15.0	
LV	SIAD PSW PZ-2	V197*	well	102.11	11.30	8.30		-114.0	-14.3	-13.8	16.1	
LV	SIAD PSW PZ-2	V203*	well	213.36	16.90	8.20		-112.0	-14.1	-11.4	17.5	
LV	SIAD PSW PZ-1	V199*	well	111.30	11.30	8.10		-116.0	-13.8	-11.2	23.4	
LV	SIAD PSW PZ-5	V206*	well	213.36	16.70	8.30		-112.0	-13.8	-11.9	30.7	
LV	SIAD PZ1-4PZ	V178*	well	32.00	18.30	7.40		-109.0	-13.5	-9.0	30.7	
LV	SIAD DM0-3	V180*	well	16.21	18.10	7.70		-107.0	-13.5	-8.7	35.0	
LV	SIAD PSW PZ-4	V199*	well	152.40	10.40			-108.0	-13.8	-13.1	38.5	
LV	SIAD PSW PZ-3	V200*	well	141.21	11.60			-108.0	-13.7	-12.4	45.2	
LV	SIAD ELS-MWB	V175*	well	35.51	18.90	7.30		-103.0	-13.3	-11.9	46.0	
LV	SIAD PSW PZ-1	V202*	well	70.56	9.40	7.60		-110.0	-13.9	-11.0	50.3	
LV	SIAD PSW PZ-9	V207*	well	161.54	18.30	8.10	0.2	-111.0	-13.8	-12.3	55.4	
LV	SIAD PSW PZ-5	V205*	well	167.44	17.10	8.50		-109.0	-13.6	-11.8	60.8	
LV	W of Herlong	H4115*	well	24.38	21.85	8.46	0.4	-107.0	-13.6	-3.3	63.6	
LV	SIAD PSW PZ-2	V201*	well	96.01	13.60	7.70		-110.0	-13.6	-11.4	71.4	
LV	Buchanan Place - Constantia Rd.	H4116*	well	54.80	18.00	8.42	0.3	-109.0	-13.7	-15.4	73.1	
LV	E of Doyle	V174*	well	106.68	22.20	7.40	0.9	-108.0	-13.3	-2.7	74.6	
LV	SIAD TN1-MWB	V192*	well	31.57	14.80	8.10		-108.0	-13.4	-7.8	75.0	
LV	JDS Wetlands	V141*	well	48.17	18.20	8.60		-108.0	-13.6	-10.8	78.8	
LV	NE of Herlong Junction	V168*	well	22.80	20.90	7.30	0.3	-114.0	-14.0	-4.4	83.8	
LV	Garred Well #2	W127*	well	76.20	11.25	7.31	4.1	-108.7	-14.0	-14.9	80.5	
LV	Bad Flat Ranch #2	H4085*	well	71.36	19.55	7.25	3.55	-110.0	-13.9			
LV	SIAD LF-1	V183*	well	19.81	18.60	8.20		-107.0	-12.6	-9.0	102.6	
LV	Bad Flat Ranch #1	H4084*	well	198.12	21.00	7.35	3.9	-102.7	-12.1	-12.5	112.8	
LV	Beebees Well	B088*	well	42.67	8.40	8.83		-109.5	-13.5	-14.4		
LV	Long Valley Creek-HU	H4133*	surface	8.60	8.00	2.7		-103.4	-13.4	-12.0		
LV	Long Valley Creek, S. of Doyle	B090*	surface	7.30	7.73			-111.3	-14.0	-11.0		
LV	SIAD TN1-MWA	V191*	well	30.94	14.40	9.10		-107.0	-13.4	-11.9		
LV	Long Valley Creek, N. of Doyle	H4127*	surface	16.63	8.13			-105.4	-13.5	-7.5		
LV	JDS Wetland Dom. Well	H4129*	well	92.66	20.20	8.80	0.0	-112.0	-13.8	-6.8		
LV	Honey Lake E. arm	V94*	surface	21.90	9.03			-88.0	-5.6	-2.6		
LV	Honey Lake-W. arm	V93*	surface	24.40	8.80			-57.0	-4.9	-2.0		
LV	S of Doyle	V176*	well	24.38	21.40	6.80	4.7	-108.0	-14.1		0.4	
LV	27N16@300M	W11*	well	16.19	7.51			-112.5	-14.1			
LV	20N16@300M	W136*	well	161.54	20.37	7.83		-109.0	-13.9			
LV	Horse Spring	W141*	spring		12.0	7.3		-112.0	-14.7			
LV	Upper Scott Spring	W143*	spring		14.00	7.19		-110.0	-14.4			
LV	Lower Scott Spring	W144*	spring		14.00	7.80		-115.0	-14.8			
LV	Mad Spring	W145*	spring		6.00	6.96		-108.0	-12.7			
CW	Upper Red Spring	W146*	spring		14.00	7.93		-116.5	-14.8			
CW	Black Canyon	W147*	spring		14.00	7.40		-115.0	-15.1			
LV	Newcombe Spring	W148*	spring		2.0			-116.0	-14.9			
LV	Webber 19	W159*	well	36.58	18.30	7.15		-111.0	-14.8			
LV	S of Doyle	W160*	well	36.58	16.96	7.31	0	-111.0	-14.8			
LV	Spencer	W161*	well		9.60			-113.0	-14.4			
LV	Higgins Spring	V72*	spring		14.30	7.87		-116.0	-14.6			
LV	Spring E. Seven Lakes Mtn.	V76*	spring		15.00	8.33		-101.0	-12.4			
LV	Spring S. Seven Lakes Mtn.	V75*	spring		13.60	7.71		-113.0	-13.8			
LV	August Spring	V80*	spring		9.60	8.59		-112.0	-14.5			
LV	Long Valley Creek, Herlong	V99*	surface		28.66	8.21		-96.0	-11.4			
LV	SIAD Swamp Treatment Plant	V106*	surface		6.80			-86.0	-9.6			
LV	JDS Wetlands - surface water	V105*	surface		26.10	9.70		-95.0	-9.9			
LV	SIAD AL1-3	V170*	well	182.88	22.40	8.10		-113.0	-14.8			
LV	SIAD AL1-B-MWA	V176*	well	33.53	11.80	7.60		-107.0	-13.2			
LV	SIAD DM0-11-A	V181*	well	33.53	17.60	7.50		-106.0	-13.3			
LV	SIAD MKP-2	V184*	well	17.53	18.30	6.90		-89.0	-9.3			
LV	STP-03-PZ	V185*	well	17.07	13.10	7.20		-96.0	-9.3			
LV	SIAD STP-4-PZ	V186*	well	17.37	11.80	6.70		-85.0	-8.5			
LV	SIAD STP-8-PZ	V187*	well	27.71	13.10	7.70		-106.0	-13.2			
LV	SIAD TN1-MWB	V189*	well	31.39				-111.0	-13.3			
LV	SIAD TN1-MWC	V190*	well	44.81				-114.0	-12.4			
LV	SIAD TN1-MWB	V195*	well	44.81	14.90	1.90		-107.0	-13.4			
LV	Spz. - N Seven Lakes Mtn.	R107*	spring		13.60	7.70		-113.0	-13.6			
LV	Corbow Joe Spring	H4088*	spring		17.65	7.40	0.0	-112.0	-14.0			
LV	N of Old Flat Ranch	H4089*	well		18.85	7.23	2.7	-102.3	-12.4			
LV	Webber 125	H4120*	well		18.70	7.54		-109.8	-14.1			
LV	Webber 167	H4121*	well		48.16	16.30	7.57	0.0	-111.9	-14.3		
LV	Bugie Well	H4122*	well		19.05	7.24		-109.2	-13.9			
LV	Indian Spring	H4123*	spring		18.75	8.78	2.0	-109.0	-13.1			
LV	Rat Auto Salvage	H4124*	well		20.58	7.64		-106.3	-13.0			
LV	Higid Well	H4125*	well		21.53	7.61		-110.1	-13.4			
LV	Bell's Ranch	H4126*	well		106.68	26.00	7.54	0.4	-107.4	-13.0		
LV	Webber 158	H4131*	well		24.38	20.04	7.99		-107.1	-14.4		
LV/H/W	Zamboni Hat Spring	H4134*	spring		39.46	9.13	0.4	-118.5	-15.4	-13.8		
LV/H/W	Rose 21	H4132*	well		37.60	8.90	0.4	-113.0	-14.8			
NV	Never Sweated Ranch	W102*	well		152.40	14.90	8.25	1	-108.5	-14.8	-11.2	76.7
NV	Hedges Well	W109*	well		92.24	18.75	7.88	0	-113.0	-14.4		
OUT	Pape Spring	W2*	spring					-110.0	-14.3			
OUT	Well 3801	W24*	well		22.2	8.4		-112.0	-13.0			
OUT	Well 3802	W25*	well		60.90	20.0	8.1	0	-114.0	-13.3		
OUT	Bonham Ranch 1	W26*	well		23.3	8		-115.5	-13.7			
OUT	Sand Pass 1st Well	W46*	well		217.01	15.5	8.1		-106.0	-13.6		
OUT	Sand Pass 2nd Well	W47*	well		176.78			-106.0	-13.6			
OUT	Upper Adobe Spring	W89*	spring		7.0	7.5		-104.0	-12.7			
OUT	Upper Amaret Spring	W90*	spring		8.0	7.5		-105.0	-12.8			
OUT	Tree Spring	W123*	spring		1.2	7.2		-113.0	-14.4			
OUT	Sarie Spring	W168*	spring		17.00	7.70	0	-118.0	-15.2			
OUT	ADF Spring	W170*	spring			8.00	0	-116.0	-14.2			
OUT	Spring de Cas	W171*	spring									

Table 6. Honey Lake Basin ³H data. Data was normalized to 2005 based on the 12 year half life of ³H. * indicates a sample location with more than one sampling event.

Flow Path	Name	Sample #	Sample Year	³ H (TU)	³ H Normalized to 2005 (TU)
SR	NW of Standish	H4096*	2005	0.00	0.00
LV	NE of Herlong Junction	V168*	1995	0.30	0.20
LV	W of Herlong	H4115*	2005	0.40	0.40
LV	S of Doyle	V171*	1995	4.70	2.80
ESA	SIAD UBG-4-MWA	V194*	1995	0.50	0.30
WSA	Tinsley Fountain	H4117*	2005	0.00	0.00
LV	S of Doyle	W160*	1995	0.00	0.00
SN	Reinhart Well	H4090*	2005	0.00	0.00
SR	Richmond School	H4114*	2005	0.00	0.00
SHAF	BLM Horse Corral Well	H4092*	2005	0.60	0.60
ESA	Harding Well	H4119*	2005	0.90	0.90
LV	Webber 167	H4121*	2005	0.00	0.00
LV	Burkhard Place - Constantia Rd.	H4130*	2005	0.30	0.30
LV	Garrod Well #2	W127*	1990	4.10	2.00
VM	Fish Springs Ranch Dom. Well	H4136*	2005	1.70	1.70
NV	Hodges Well	W100*	1989	0.00	0.00
LV	JDS Wetland Dom. Well	H4129*	2005	0.00	0.00
LV	Bell's Ranch	H4126*	2005	0.40	0.40
LV	E of Doyle	V174*	1995	0.90	0.50
WSA	Lee Rd	H4116*	2005	0.30	0.30
VM	Headquarters	W93*	2004	1.40	1.30
VM	Ferrel Test Well	W109*	1990	0.00	0.00
VM	Jarboe Well	W91*	1989	0.00	0.00
NV	Never Sweat Ranch	W102*	2003	1.00	0.90
SR/SHAF	Fish & Game Well	H4093*	2005	0.40	0.40
LV	SIAD PSW #9	V207*	1995	0.20	0.12
LV/HLW	Rose 27	H4132*	2005	0.40	0.40
WSA/AML	Norcal2	V211*	1995	0.20	0.12
LV	Bird Flat Ranch #1	H4084*	2005	3.90	3.90
LV	Bird Flat Ranch #2	H4085*	2005	2.55	2.55
ASP	Astor Pass	B2041	2001	2.10	1.80
OUT	Soda Springs	B2756	2002	0.80	0.70
SR	Gold Run Creek	H4081*	2005	3.40	3.40
SR	Susan River in Susanville	H4082*	2005	3.30	3.30
SN	Mill Creek	H4083*	2005	0.40	0.40
SN	Humphries #2	H4087*	2005	0.00	0.00
LV	Cowboy Joe Spring	H4088*	2005	0.00	0.00
LV	N of Bird Flat Ranch	H4089*	2005	2.70	2.70
SN	Ottis Canyon	H4091*	2005	2.20	2.20
SR	Goni Well	H4095*	2005	0.00	0.00
SR	Plummer Spring	H4097*	2005	0.40	0.40
SR	Susan River North of Susanville	H4098*	2005	5.70	5.70
SR	Trussell Well	H4099*	2005	1.50	1.50
SHAF	Spring E. Horse Lake Mtn.	H4101*	2005	0.40	0.40
SHAF	Railroad Spring	H4105*	2005	0.00	0.00
LV	Indian Spring	H4123*	2005	2.00	2.00
FSM	Nork/Francone Well	H4128*	2005	0.50	0.50
LV	Long Valley Creek-HJ	H4133*	2005	2.70	2.70
LV/HLW	Zamboni Hot Spring	H4134*	2005	0.40	0.40
WSA/AML	HL Power Plant	H4135*	2005	0.00	0.00
VM	Fish Spring Ranch Irrigation Well	H4137	2005	0.70	0.70
SN	"McDermott" Creek	V95*	1995	9.20	5.30
VM	Willow Spring	W103*	1989	0.00	0.00
FSM	Wilson Well	W108*	1989	0.00	0.00
CW	Cold Spring	W150*	1989	8.44	2.80
OUT	Suzie Spring	W168*	1989	0.00	0.00
LV	Sugarcane	W169*	1989	0.00	0.00
OUT	ADP Spring	W170*	1989	0.00	0.00
OUT	Spring de Casa	W171*	1989	0.00	0.00
OUT	Well 3891	W24*	1989	0.00	0.00
OUT	Well 3902	W25*	1989	0.00	0.00
SR	Darkin Well	W43*	1990	0.00	0.00
CW	Cottonwood Springs	W96*	2002	1.20	1.10

Table 7. Honey Lake Basin $\delta^{13}\text{C}$ data. * indicates a sample location with more than one sampling event.

Flow Path	Name	Sample #	Source	Depth (m)	Temp (°C)	pH	HCO ₃ (mg/L)	HCO ₃ (meq/L)	$\delta^{13}\text{C}$ (‰)	¹⁴ C (pmc)
ASP/ESA	Stone Well	B687	well		11.20	7.54	1211	19.85	-6.4	
ASP	Astor Pass	B2041	well				876.00	14.36	-4.5	
LV	JDS Wetlands	V141*	well	48.77	18.20	8.60	690.00	11.31	-10.8	79.8
SR/SHAF	Fish & Game Well	H4093*	well		14.33	8.40	664.50	10.89	-11.9	
SR	Lassen County Well	V111*	well	42.67	15.60	7.50	460.00	7.54	-10.1	83.0
LV	SIAD B21-3-MW	V177*	well	36.58	18.90	7.30	450.00	7.38	-11.9	46.0
LV	Honey Lake-E. arm	V94*	surface		23.90	9.03	422.00	6.92	-2.6	
LV	JDS Wetland Dom. Well	H4129*	well		20.20	8.80	352.55	7.49	-6.8	
SR	Darkin Well	W43*	well		14.10	6.90	351.50	5.76	-7.2	2.8
LV	SIAD TNT-7-MWA	V191*	well		14.40	9.10	298.71	4.90	-7.9	
LV	Honey Lake-W. arm	V93*	surface		24.40	8.80	287.00	4.70	-2.0	
LV	Breshears Well	B688	well		8.40	6.83	256	4.20	-14.4	
NV	Never Sweat Ranch	W102*	well	152.40	14.90	8.25	223.13	3.66	-11.2	76.7
LV	SIAD B21-5-PZ	V178*	well	32.00	18.30	7.40	221.00	3.62	-9.0	30.7
LV	W of Herlong	H4115*	well	24.38	21.85	8.46	220.05	3.56	-3.3	63.6
ESA	SIAD UBG-4-MWA	V194*	well	29.41	20.60	9.00	219.46	3.60	-12.5	56.8
ESA	SIAD DEMO-1	V179*	well		26.70		218.00	3.57	-10.2	
LV	SIAD PSW8 PZ-3	V196*	well	150.88	9.00	8.10	216.00	3.54	-11.9	15.0
LV	SIAD PSW #5	V205*	well	167.64	17.10	8.50	213.00	3.49	-11.8	60.9
LV	SIAD PSW8 PZ-2	V197*	well	102.11	11.30	8.30	208.00	3.41	-13.8	16.1
LV	Long Valley Creek, N of Doyle	H4127*	surface		16.63	8.13	200.55	3.81	-7.5	
LV	SIAD PSW8 PZ-4	V195*	well	192.02	9.10	8.10	198.00	3.25	-11.9	13.1
LV	SIAD PSW8 PZ-1	V198*	well	56.39	11.30	8.10	198.00	3.25	-13.2	23.4
VM	Fish Springs Ranch Dom. Well	H4136*	well	78.64	15.85	8.67	185.11	3.04	-10.3	37.6
LV	Garrod Well #2	W127*	well	76.20	11.25	7.31	184.00	3.02	-14.9	90.5
LV	Long Valley Creek-HJ	H4133*	surface		8.60	8.00	163.57	2.68	-12.0	
LV	Long Valley Creek, S of Doyle	B690*	surface		7.30	7.73	162.93	2.67	-11.0	
SHAF	BLM Horse Corral Well	H4092*	well	45.72	18.70	7.76	162.70	3.19	-1.9	79.9
SR	Pete's Creek	V84*	surface		13.30	8.18	162.50	2.66	-8.2	
VM	Headquarters	W93*	well	121.92	19.17	8.30	155.57	2.55	-13.4	43.5
LV	Bird Flat Ranch #1	H4084*	well	198.12	21.00	7.35	155.33	2.60	-12.5	112.8
SN	Pluma National Forest	B682	well		10.00	6.38	155	2.54	-16.8	
SR	Richmond School	H4114*	well	44.20	17.37	7.99	134.45	2.90	-14.4	54.5
WSA	Spr. NE of Stacy	R90	spring		15.00	8.90	134.11	2.20	-10.1	
SR	Standish	V112*	well		18.50	8.00	132.00	2.16	-8.0	
SR/SHAF	Susan River at Litchfield	H4094*	surface		25.15	8.54	128.00	3.61	-0.3	
SR	Plummer Spring	H4097*	spring		17.40	7.92	124.30	2.04	-15.3	74.7
SR	Trussell Well	H4099*	well		14.54	7.78	122.50	2.01	-20.7	
VM	Fish Springs Irrigation Well-SW	V153*	well	134.11	17.70	8.10	115.00	1.88	-11.3	37.0
SR	NW of Standish	H4096*	well	17.07	17.10	7.92	114.60	2.35	-7.7	46.7
SHAF	Tule Patch Spring	H4106*	spring		17.10	7.82	109.60	1.80	-15.1	72.7
LV	Burkhard Place - Constantia Rd.	H4130*	well	54.86	18.00	8.42	109.50	1.79	-15.4	73.1
WSA	Lee Rd	H4116*	well	121.92	21.85	8.25	105.90	2.06	-10.2	17.1
FSM	Cal Neva Rd. - DWR West	V165*	well	33.22			104.00	1.70	-14.1	59.0
VM	Fish Springs Irrigation Well-SE	V145*	well	65.53			103.00	1.69	-11.6	41.3
LV	SIAD DMO-13-A	V180*	well	36.27	18.10	7.70	98.00	1.61	-6.7	35.0
CW	Cottonwood Springs	W96*	spring		14.77	7.77	95.02	1.56	-19.0	
ESA	High Rock Ranch	W32*	well		24.00	7.70	85.00	1.40	-12.8	21.6
LV/HLW	Zamoni Hot Spring	H4134*	spring		39.46	9.13	70.21	1.26	-12.8	
LV/HLW	Zamoni Hot Spring	H4134*	spring		39.46	9.13	70.21	1.26	-12.8	
SN	"McDermott" Creek	V95*	surface		17.80	8.24	64.93	1.41	-7.9	
WSA/AML	Norcal2	V211*	geo well	322.48	98.90	8.90	60.96	1.00	-9.9	10.0
SR	Susan River in Susanville	H4082*	surface		10.73	7.68	59.60	0.98	-14.7	
WSA/AML	HL Power Plant	H4135*	spring/well		62.71	8.30	49.25	0.81	-12.9	
WSA/AML	HL Power Plant	H4135*	spring/well		62.71	8.30	49.25	0.81	-12.9	
SR	Susan River North of Susanville	H4098*	surface		20.90	7.62	25.80	0.65	-2.4	
LV	S of Doyle	V171*	well		21.40	6.80	25.00	0.41	0.4	
SR/AML	Johnston 1	V209*	geo well	432.82	66.95	8.75	11.50	0.19	-11.9	10.6
LV	SIAD PSW #8	V206*	well	213.36	16.70	8.30			-11.9	30.7
LV	SAID PSW #2	V203*	well	213.36	16.90	8.20			-11.4	17.5
LV	SIAD PSW #9	V207*	well	161.54	18.30	8.10			-12.3	55.4
LV	SIAD PSW5 PZ-4	V199*	well	152.40	10.40				-13.1	38.5
LV	SIAD PSW5 PZ-3	V200*	well	141.21	11.60				-12.4	45.2
LV	E of Doyle	V174*	well	106.68	22.20	7.40			-2.7	74.6
LV	SIAD PSW5 PZ-2	V201*	well	96.01	13.60	7.70			-11.4	71.4
LV	SIAD PSW5 PZ-1	V202*	well	70.56	9.40	7.60			-11.0	50.3
LV	SIAD TNT-7-MWB	V192*	well	31.57	14.80	8.10			-7.8	75.0
LV	NE of Herlong Junction	V168*	well	22.86	20.90	7.30			-4.4	83.8
LV	SIAD LF-1	V183*	well	19.81	18.60	8.20			-9.0	102.6
WSA	Artesian Well #2	W36*	well		22.93	8.55		1.61	-10.4	

Table 8. Honey Lake Basin ¹⁴C data. * indicates a sample location with more than one sampling event.

Flow Path	Name	Sample #	δ ¹³ C (‰)	¹⁴ C (pmc)
LV	SIAD PSW #8	V206*	-11.9	30.7
LV	SAID PSW #2	V203*	-11.4	17.5
LV	SIAD PSW8 PZ-4	V195*	-11.9	13.1
LV	SIAD PSW #5	V205*	-11.8	60.9
LV	SIAD PSW #9	V207*	-12.3	55.4
LV	SIAD PSW5 PZ-4	V199*	-13.1	38.5
LV	SIAD PSW8 PZ-3	V196*	-11.9	15.0
LV	SIAD PSW5 PZ-3	V200*	-12.4	45.2
VM	Fish Springs Irrigation Well-SW	V153*	-11.3	37.0
VM	Headquarters	W93*	-13.4	43.5
WSA	Lee Rd	H4116*	-10.2	17.1
LV	E of Doyle	V174*	-2.7	74.6
LV	SIAD PSW8 PZ-2	V197*	-13.8	16.1
LV	SIAD PSW5 PZ-2	V201*	-11.4	71.4
VM	Fish Springs Ranch Dom. Well	H4136*	-10.3	37.6
LV	Garrod Well #2	W127*	-14.9	90.5
LV	SIAD PSW5 PZ-1	V202*	-11.0	50.3
VM	Fish Springs Irrigation Well-SE	V145*	-11.6	41.3
SN	SW of Bass Hill	H4112*		112.4
SN		V134*		62.0
LV	SIAD PSW8 PZ-1	V198*	-13.2	23.4
LV	Burkhard Place - Constantia Rd.	H4130*	-15.4	73.1
LV	JDS Wetlands	V141*	-10.8	79.8
SHAF	BLM Horse Corral Well	H4092*	-1.9	79.9
SR	Richmond School	H4114*	-14.4	54.5
SR	Lassen County Well	V111*	-10.1	83.0
LV	SIAD B21-3-MW	V177*	-11.9	46.0
LV	SIAD DMO-13-A	V180*	-6.7	35.0
FSM	Cal Neva Rd. - DWR West	V165*	-14.1	59.0
LV	SIAD B21-5-PZ	V178*	-9.0	30.7
LV	SIAD TNT-7-MWB	V192*	-7.8	75.0
ESA	SIAD UBG-4-MWA	V194*	-12.5	56.8
LV	W of Herlong	H4115*	-3.3	63.6
LV	NE of Herlong Junction	V168*	-4.4	83.8
LV	SIAD LF-1	V183*	-9.0	102.6
SR	NW of Standish	H4096*	-7.7	46.7
SR/AML	Johnston 1	V209*	-11.9	10.6
WSA/AML	Norcal2	V211*	-9.9	10.0
LV	Bird Flat Ranch #1	H4084*	-12.5	112.8
LV	Bird Flat Ranch #2	H4085*		90.5
NV	Never Sweat Ranch	W102*	-11.2	76.7
SR	Plummer Spring	H4097*	-15.3	74.7
SHAF	Tule Patch Spring	H4106*	-15.1	72.7
ESA	High Rock Ranch	W32*	-12.8	21.6
SR	Darkin Well	W43*	-7.2	2.8

Table 9. Mean solute chemistry values for beginning, middle, and end of the 13 flow paths in Honey Lake Basin. See Table 10 for calculations.

† indicates a flow path that was modeled with NETPATH.

* indicates an estimated value

Chemical Flow Path	Physical Flow Path	n (# of samples)	Temp (°C)	pH	TDS (mg/L)	Cations (meq/L)				Anions (meq/L)				SiO2 (mg/L)	Balance Error %	δ ¹³ C (‰)	
						Ca ²⁺	Mg ²⁺	Na ⁺	K ⁺	HCO ₃ ⁻	SO ₄ ²⁻	Cl ⁻	F ⁻				
	Precipitation	1	0.0	5.7		0.00	0.000	0.00	0.00	0.00	0.00	0.00	0.00	0.0			
LV/SHAF/SR	SR†	Beginning	2	15.3	8.01	119.00	0.93	0.66	0.44	0.07	2.05	0.10	0.05	0.00	28.1	-2.8	-15.3
		Middle	10	17.1	7.81	311.71	0.95	0.55	2.96	0.10	2.44	1.23	0.70	0.06	47.0	-1.5	-14.3
		End	9	14.6	7.90	770.6	1.54	1.18	8.71	0.23	5.24	2.45	4.03	0.03	47.8	-2.2	-7.2
		Δ					0.61	0.53	8.27	0.16	3.19	2.35	3.98	0.03	19.7		
	SHAF	Beginning	6	20.6	8.07		0.51	0.53	0.92	0.07	1.83	0.09	0.11	0.00	30.4	-0.1	-15.1
		End	3	23.3	8.09	340.0	0.89	0.49	3.69	0.19	3.67	1.00	0.55	0.01	36.8	-0.20	-1.9
		Δ					0.38	-0.04	2.77	0.12	1.84	0.92	0.44	0.00	6.4		
	SR & SHAF Mix End†	4	14.0	8.50	654.9	1.06	0.82	9.53	0.13	8.02	1.68	1.37	0.03	43.2	-1.3	-11.9	
	LV	Beginning	11	17.2	7.59	176.2	0.93	0.49	0.94	0.06	1.99	0.15	0.14	0.03	23.6	1.3	-15.4
		Middle	29	17.6	7.67	312.1	1.61	0.99	1.98	0.13	3.11	0.92	0.37	0.02	45.7	1.4	-11.3
End		10	15.4	7.74	619.5	2.84	1.34	4.82	0.28	2.68	2.03	4.24	0.02	54.1	1.5	-10.1	
Δ						1.91	0.86	3.88	0.22	0.69	1.88	4.11	-0.01	30.6			
SN	SN†	Beginning	7	17.5	6.93	129.7	0.91	0.41	0.52	0.04	1.58	0.32	0.10	0.00	37.1	-4.4	-16.8
		End	18	16.5	7.59	186.8	1.04	0.51	1.35	0.08	2.39	0.28	0.21	0.01	37.3	-0.6	~-10*
		Δ					0.13	0.10	0.83	0.04	0.82	-0.03	0.11	0.01	0.2		
WSA	WSA†	Beginning	8	22.1	8.31	193.9	0.44	0.13	2.11	0.12	1.97	0.46	0.37	0.01	32.9	-0.6	-10.3
		End	4	15.4	7.74	619.5	2.84	1.34	4.82	0.28	2.68	2.03	4.24	0.02	54.1	1.5	-10.1
		Δ					2.40	1.22	2.71	0.16	0.71	1.57	3.87	0.01	21.2		
ASP/NV/ESA	ESA	Beginning	7	22.1	8.32	274.5	0.37	0.20	2.53	0.12	2.24	0.40	0.42	0.01	38.1	-2.2	-12.7
		Middle	5	15.4	8.23	496.1	1.80	1.23	3.98	0.20	4.85	0.62	1.34	0.05	54.0	2.2	~-12*
		End	11	13.5	8.01	11973	8.60	11.02	188.44	1.08	14.32	27.44	142.00	0.14	21.1	6.4	-6.4
		Δ					8.24	10.82	185.91	0.96	12.08	27.04	141.59	0.13	-17.0		
	NV†	Beginning	1	18.8	7.88	199.8	0.49	0.33	1.63	0.21	2.25	0.13	0.14	0.01	51.0	1.4	~-15*
		Middle	2	15.3	8.26	660.2	0.78	0.33	5.76	0.24	4.29	1.15	1.55	0.02		-2.5	-11.2
		End	1	12.4	7.09	42700	7.49	67.48	700.35	2.40	15.57	7.29	685.50	0.02	18.0	4.7	~-10*
		Δ					7.00	67.15	698.72	2.20	13.32	7.16	685.36	0.02	-33.0		
	ASP	Beginning	4	21.0	8.23	2403.0	0.95	1.17	31.41	0.30	14.55	5.84	11.74	0.14	~25*	2.3	-4.5
		End	2	11.8	7.32	42700	4.64	36.43	448.71	2.61	17.71	25.51	423.38	0.23	18.0	2.7	-6.4
Δ						3.68	35.26	417.30	2.31	3.16	19.67	411.63	0.09	-7.0			
CW/VM/FSM	FSM†	Beginning	2	15.0	7.40	156.6	0.94	0.49	0.48	0.06	1.72	0.12	0.18		~30*	-1.2	~-15*
		Middle	10	16.9	8.23	370.9	0.92	0.45	3.62	0.12	1.93	2.50	0.45	0.05	22.1	-3.1	-14.1
		End	3	15.0	8.12	4632	2.43	2.84	68.32	0.97	11.34	4.55	57.66	0.02	15.3	0.4	~-10*
		Δ					1.49	2.35	67.84	0.91	9.61	4.43	57.48		-14.7		
	VM	Beginning	3	14.7	7.32	166.6	0.91	0.47	0.64	0.06	1.72	0.12	0.18		~25*	1.7	~-15*
		Middle	9	19.8	8.16	222.2	0.38	0.20	2.54	0.17	2.39	0.32	0.44	0.01	34.2	-1.1	-11.9
		End	2	14.7	8.34	4614.5	2.17	3.15	65.69	0.96	6.99	6.79	57.42	0.05	12.7	-1.4	~-10*
		Δ					1.25	2.67	65.04	0.90	5.27	6.67	57.24		-12.3		
	CW	Beginning	4	15.0	7.49	177.3	1.10	0.65	0.59	0.13	2.19	0.13	0.14	0.01	21.7	-0.8	-19.0
		End	2	14.0	7.68	21628	4.09	33.93	353.60	1.34	10.25	4.05	343.79	0.02	18.0	4.6	~-10*
Δ						2.99	33.27	353.01	1.21	8.06	3.92	343.64	0.01	-3.7			
HLW	HWL†	4	41.3	8.43		0.40	0.09	2.17	0.03	1.73	0.67	0.26	0.10	45.4	-1.7	-12.8	
AML	AML†	4	82.8	8.64	820.8	0.90	0.02	10.23	0.16	0.60	6.03	4.13	0.18	85.7	1.0	-11.6	

Table 10. Honey Lake Basin sample data statistics, organized by location along each flow path. * indicates a sample location with more than one sampling event.

Flow Path	Name	Sample #	Water Source	Temp (°C)	pH	Cations (mg/L)					Anions (mg/L)				SO ₄ (mg/L)	Cl ⁻ (mg/L)	F ⁻ (mg/L)	S _T (mg/L)	TDS (mg/L)	TSS (mg/L)	Turbidity (NTU)	
						Ca ²⁺	Mg ²⁺	Na ⁺	K ⁺	HCO ₃ ⁻	SO ₄ ²⁻	Cl ⁻	F ⁻									
Small River Flow Path	MacDonald Dam	W30	well	BEGINNING	13.11	8.10	18.00	7.00	12.00	4.30	126.00	4.80	1.40									
	Plummer Spring	14097*	spring	MEAN	15.26	8.01	18.68	8.00	10.19	2.94	125.15	5.15	1.74	0.07	28.10	-15.28	74.72					
				MEDIAN	15.26	8.01	18.68	8.00	10.19	2.94	125.15	5.15	1.74	0.07	28.10	-15.28	74.72					
				Standard DEV	3.03	0.13	0.96	1.45	2.56	1.92	1.20	0.50	0.48									
	P.E. Nelson Dam	W17	well	BEGINNING	5.10	7.10	36.00	18.00	22.00	1.30	122.00	19.00	16.00									
	Ca Conery, Ca Dam	W18	well	BEGINNING	16.67	8.00	7.10	4.00	34.00	9.80	109.00	15.00	5.80									
	Johnson Ranch Dam	W19	well	BEGINNING	13.69	7.97	4.40	0.80	118.33	4.90	183.67	73.67	20.67	1.05	66.50							
	Fruit Growers Supply Ltd	W22	well	BEGINNING	23.61	8.05	13.00	2.50	126.00	4.00	90.00	158.50	58.50	1.65	36.50							
	Johnson Ranch Dam	W23	well	BEGINNING	16.67	7.20	22.00	10.00	38.00	3.70	95.00	91.00	38.00	0.30	52.00							
	Susawille Prison	V115	well	BEGINNING	33.20	8.80	1.90	0.10	71.30	1.71	85.80	38.40	17.50	4.53	72.90							
NW of Standish	14096*	well	BEGINNING	17.10	7.92	7.74	2.87	54.97	5.41	114.60	29.26	12.05	0.66	38.10	-7.7	46.7						
Trussell Well	14099*	well	BEGINNING	14.54	7.78	24.50	10.90	64.50	3.80	122.50	92.00	37.00	0.75	44.50	-20.7							
Johnsonville	14113*	well	BEGINNING	13.20	7.28	34.45	13.90	48.53	2.65	240.20	21.51	9.49	0.23	52.05								
Richardson School	14114*	well	BEGINNING	17.27	7.99	23.61	5.68	60.96	0.47	134.85	37.00	28.83	0.43	13.40	-14.4	54.5						
			MEAN	17.11	7.81	17.47	6.43	65.86	3.77	131.72	57.53	24.18	1.20	46.99	-14.25	50.60						
			MEDIAN	16.67	7.94	17.50	4.09	99.48	3.75	118.30	37.70	19.08	0.70	48.25	-14.40	50.60						
			Standard DEV	7.30	0.51	12.36	6.37	13.07	2.64	53.12	43.88	16.26	1.42	18.62	6.48	5.52						
McClure Ranch Irr	W10	well	BEGINNING	8.00	6.60	6.00	89.00	6.70	185.00	48.00	51.00	0.20	53.00									
E. Grant Dam	W12	well	BEGINNING	13.61	8.25	16.20	7.85	356.00	7.80	468.00	343.50	38.50	2.35	33.50								
T. Siskland Dam	W13	well	BEGINNING	13.75	8.30	16.90	7.87	239.67	8.20	432.67	210.67	28.33	1.00	42.50								
J. Ferns Dam	W14	well	BEGINNING	15.00	8.10	14.00	6.40	138.00	5.20	249.00	102.00	44.00	0.40	51.00								
Ca Fish & Game Irr	W42	well	BEGINNING	13.89	7.45	94.50	42.50	256.50	14.00	282.00	22.50	53.50	0.10	50.50								
Durkin Well	W43*	well	BEGINNING	14.10	6.90	45.10	24.00	224.00	11.00	351.50	79.36	294.38	0.02		-7.2	2.8						
Ca Fish & Game Irr	W44*	well	BEGINNING	11.00	8.35	99.50	17.50	245.00	6.75	326.00	98.50	237.50	0.45	46.00								
St. of Standish	V116*	well	BEGINNING	16.70	7.80	17.70	11.10	53.70	12.70	223.00	21.20	7.41	0.05	49.00								
Gene Well	14095*	well	BEGINNING	16.50	8.29	18.00	6.40	200.00	9.00	350.00	115.00	50.00	0.60	66.00								
			MEAN	14.57	7.90	30.88	14.40	200.21	9.04	319.69	117.86	142.76	0.57	47.79	-7.19	2.80						
			MEDIAN	13.99	8.10	17.70	7.85	224.00	8.20	336.00	98.50	50.00	0.40	50.15	-7.19	2.80						
			Standard DEV	1.27	0.51	20.23	12.17	103.28	2.95	101.23	103.23	177.00	0.74	30.89								
SR.AML Johnson I	V209*	geo well	BEGINNING	66.45	8.75	1.50	0.00	72.00	0.00	11.50	245.00	99.00	3.33	83.60	-11.9	10.6						
SR.HLW Morrison Church Heating	W17*	well	BEGINNING	52.20	7.70	9.50	0.00	56.00	0.90	143.00	20.00	5.90	0.00	62.00								
SR.HLW Roosevelt Swimming Pool	RE1	well	BEGINNING	35.80	8.01	19.00	3.40	20.00	3.80	120.00	11.00	2.00	-0.1	53.00								
			MEAN	51.65	8.15	14.00	2.00	82.67	2.52	91.50	92.00	32.30	1.33	67.87	-8.76	5.40						
			MEDIAN	52.20	8.01	13.50	2.00	56.00	2.87	120.00	20.00	5.90	1.33	62.00	-7.19	2.80						
			Standard DEV	15.86	0.54	4.77	1.98	79.43	1.48	70.23	125.54	90.14	18.51	27.2	4.50							
Shafter Mountain Flow Path																						
SHAF Earll Well	14100	well	BEGINNING	20.10	7.45	17.01	12.44	11.56	1.31	145.90	1.85	1.56	0.05	39.80								
SHAF Spring E. Horse Lake Mtn	14101*	spring	BEGINNING	16.60	7.77	19.52	13.39	12.01	1.46	160.00	1.20	1.57	0.02	23.70								
SHAF Crogina Well	14103	well	BEGINNING	26.70	8.13	2.51	1.18	28.07	3.18	77.70	3.70	5.43	0.11	52.90								
SHAF Spring S. of Snowstorm Mtn	14104*	spring	BEGINNING	20.80	8.29	0.94	0.51	41.17	1.87	88.10	11.08	9.47	0.12	34.20								
SHAF Railroad Spring	14105*	spring	BEGINNING	22.55	8.94	7.19	2.57	22.68	4.19	80.00	2.59	2.01	0.07	16.20								
SHAF Tule Patch Spring	14106*	spring	BEGINNING	17.10	7.82	13.96	8.33	11.44	3.39	109.60	4.03	2.95	0.08	15.70	-15.1	72.7						
			MEAN	20.64	8.07	10.19	6.40	21.16	2.57	111.72	4.07	3.83	0.07	30.42	-15.10	72.74						
			MEDIAN	20.45	7.98	10.57	5.45	17.35	2.53	99.30	3.14	2.48	0.07	28.95	-15.10	72.74						
			Standard DEV	3.71	0.52	2.76	3.76	12.01	1.18	33.87	3.60	3.12	0.04	14.64								
SHAF C.I. Curtis Dam	W16	well	BEGINNING	20.00	8.30	12.00	3.80	141.00	9.50	333.00	54.00	22.00										
SHAF/WSA Spring	W5	spring	BEGINNING	31.10	8.20	17.00	2.10	49.00	7.20	144.00	29.00	15.00	0.10	40.00								
SHAF BLM Horse Corral Well	14092*	well	BEGINNING	18.70	7.76	27.83	13.48	76.06	4.65	162.70	71.12	24.62	0.11	33.55	-1.9	79.9						
			MEAN	23.27	8.09	18.94	6.49	88.69	7.12	213.23	51.37	20.54	0.11	36.78	-1.90	79.90						
			MEDIAN	20.00	8.20	17.00	3.90	76.06	7.20	162.70	54.00	22.00	0.11	36.78	-1.90	79.90						
			Standard DEV	4.81	0.29	4.09	6.12	47.82	2.42	104.14	21.38	4.97	0.01	37.00								
SR.SHAIF Meigs Ranch Irr	W9	well	BEGINNING	23.30	8.10	51.00	7.50	574.00	22.00	227.00	295.00	651.00	0.30	79.00								
WSA/AML Hill Power Plant	14115*	spring/well	BEGINNING	62.71	8.30	25.30	0.12	276.70	11.71	492.25	342.20	188.91	2.87	53.00	-12.9							
			MEAN	43.25	8.20	38.15	3.71	425.35	16.86	338.13	318.60	419.96	1.59	66.00	-12.94							
			MEDIAN	43.25	8.20	38.15	3.71	425.35	16.86	338.13	318.60	419.96	1.59	66.00	-12.94							
			Standard DEV	27.51	0.14	18.18	5.08	210.22	7.28	125.69	13.38	326.75	1.82	18.18								
Small River Shafter Mtn																						
SR.SHAIF J. Deert Dam	W4	well	BEGINNING	15.50	8.50	12.00	3.20	129.00	4.50	365.00	11.00	7.00										
SR.SHAIF Ca Fish & Game Irr	W5	well	BEGINNING	15.50	8.80	18.00	6.80	244.00	7.20	456.00	83.00	66.00	0.50	51.00								
SR.SHAIF Turner Ranch Dam	W41	well	BEGINNING	13.61	8.30	50.50	27.50	194.50	4.50	472.00	175.50	71.00	0.55	34.50								
SR.SHAIF Fish & Game Well	14093*	well	BEGINNING	14.33	8.40	4.24	2.42	308.65	5.19	664.50	53.08	50.86	0.70	44.00	-11.9							
			MEAN	13.99	8.50	21.18	9.98	219.04	5.27	489.38	80.65	48.71	0.58	43.17	-11.87							
			MEDIAN	13.97	8.45	15.00	5.00	219.27	4.85	464.00	69.84	58.43	0.55	44.00	-11.87							
			Standard DEV	1.26	0.22	20.24	11.83	76.08	1.35	125.90	69.79	29.10	0.10	8.28								
Sierra Nevada Flow Path																						
SN Pluma National Forest	14082	well	BEGINNING	10.00	6.38	30.13	6.40	248.31	1.64	155	4.59	8.21</										

Flow Path	Name	Sample #	Water Source	Temp (°C)	pH	Cations (mg/L)				Anions (mg/L)				SO2 (mg/L)	d3°C (°C)	d4°C (°C)	
						Ca ²⁺	Mg ²⁺	Na ⁺	K ⁺	HCO ₃ ⁻	SO ₄ ²⁻	Cl ⁻	F ⁻				
First Steps Mountain Flow Path																	
FSM	ZFP Spring a	W152*	spring	BEGINNING	7.50	18.60	10.20	7.70	1.90	126.00	4.00	7.00					
FSM	Rat Spring a	W153*	spring	BEGINNING	15.00	7.30	19.20	1.80	14.50	3.10	84.10	8.00	6.00				
FSM	BEGINNING	n=2	MEDIAN	15.00	7.40	18.90	6.00	11.10	2.50	105.05	6.00	6.50					
				Standard DEV	0.14	0.42	5.94	4.81	0.85	29.63	2.83	0.31					
FSM	McCockle Dom. Well a	W104*	well	MIDDLE	13.00	7.36	18.70	22.40	31.00	8.10	181.00	49.00	5.00	0.30	12.00		
FSM	Austin Dom. Well a	W105*	well	MIDDLE	16.00	8.10	39.30	12.90	18.00	0.40	187.00	26.00	3.90	0.30	8.00		
FSM	Wilson #5 Well a	W107	well	MIDDLE	8.20	21.00	1.60	122.50	3.93	114.30	228.25	20.00	1.03				
FSM	Wilson Well e	W108*	well	MIDDLE	16.00	8.15	20.00	1.56	126.57	3.66	108.45	202.63	20.09	0.95	38.50		
FSM	Hull Dom. Well a	W117*	well	MIDDLE	2.00	8.60	12.00	-1.0	33.00	5.50	56.00	35.00	12.00	0.50	8.00		
FSM	W. Handl Dom. Well a	W118	well	MIDDLE	17.80	8.25	9.00	3.00	36.00	5.70	77.70	34.00	10.00	0.50			
FSM	26N1TE24F01 M.a	W119	well	MIDDLE		8.90	1.00	1.00	108.00	2.20	159.72	97.00	9.00	0.60			
FSM	26N1TE22G01 a	W120	well	MIDDLE	28.30	8.60	11.00	4.00	70.00	7.50	99.50	70.00	29.00	2.40			
FSM	Cal Neva Rd. - DWR West	V165*	well	MIDDLE							104.00			-14.1	59.0		
FSM	Not-Finucione Well	H412*	well	MIDDLE	23.25	7.88	34.45	2.65	206.00	4.40	88.30	339.50	36.00	1.40	44.00		
FSM	MIDDLE	MEAN	16.92	8.23	18.49	6.14	43.45	4.60	117.60	120.15	16.11	0.91	22.10	-14.10	59.00		
FSM	MIDDLE	MEDIAN	16.00	8.20	18.70	2.83	70.00	4.40	106.22	70.00	12.00	0.60	12.00	-14.10	59.00		
FSM	MIDDLE	Standard DEV	7.29	0.45	12.20	7.40	62.27	2.44	44.05	110.82	11.01	0.70	17.66				
FSM	Perkle Dom. Well a	W113*	well	MIDDLE	8.20	39.30	2.70	1130.00	30.00	1103.00	2.00	1122.00	0.70	10.50			
USA/FSM/VM	Stanley Well a	W115	well	END	8.30	25.00	60.00	2830.00	51.00	587.00	620.00	3960.00	0.20	20.00			
USA/FSM	B Viscay ln. Well a	W124	well	END	15.00	7.85	35.00	41.00	752.00	33.00	405.00	21.00	1050.00	0.50	17.00		
FSM	END	MEAN	15.00	8.12	48.77	34.57	1570.67	38.00	601.67	218.67	2044.00	0.47	15.25				
FSM	END	MEDIAN	15.00	8.20	52.00	41.00	1130.00	33.00	567.00	34.00	1122.00	0.50	15.25				
FSM	END	Standard DEV	0.24	12.47	29.19	1106.87	11.36	365.32	347.93	1659.70	0.25	6.72					
Virginia Mountains Flow Path																	
VM	Willow Spring a	W103*	spring	BEGINNING	16.60	7.47	16.10	5.95	10.65	2.65	97.32	8.00	5.10				
VM	Whiting Spring a	W114*	spring	BEGINNING	15.00	7.30	17.30	7.70	11.20	1.70	109.73	6.00	8.00				
VM	Sheep Spring a	W156*	spring	BEGINNING	12.50	7.20	17.50	3.60	22.30	2.20	107.00	6.10	5.85				
VM	BEGINNING	MEAN	14.70	7.32	18.30	5.75	14.72	2.18	104.68	5.70	6.32						
VM	BEGINNING	MEDIAN	15.00	7.30	17.50	5.95	11.20	2.20	107.00	6.00	5.85						
VM	BEGINNING	Standard DEV	2.07	0.13	2.69	2.06	6.57	0.48	6.52	0.61	1.51						
VM	First Fault a	W96*	well	MIDDLE	8.00	8.90	0.60	37.50	3.50	98.76	11.00	9.00	0.20				
VM	Dulles Well a	W91*	well	MIDDLE	21.00	8.14	12.55	4.32	27.46	6.54	120.16	10.17	7.12	0.16	44.00		
VM	Ferrel Playa Well a	W92	well	MIDDLE	8.30	7.10	1.10	77.00	5.80	154.85	22.00	27.00					
VM	Headquarters	W93*	well	MIDDLE	19.17	8.30	11.78	2.03	56.86	6.58	155.57	11.88	10.54	0.19	53.00	-13.4	43.5
VM	Fish Spring a	W97	spring	MIDDLE	22.80	8.00	3.00	3.00	78.00		179.00	17.00	18.00				
VM	Ferrel Test Well a	W109*	well	MIDDLE	20.33	8.27	5.96	1.58	66.50	6.08	136.09	17.67	18.22	0.31	43.50		
VM	Ferrel #1 Well a	W110*	well	MIDDLE	20.00	7.99	4.00	2.90	67.00	6.00	144.00	15.00	22.00				
VM	Fish Springs Ranch Dom. Well	H4136*	well	MIDDLE	15.85	8.67	5.59	2.05	75.49	7.87	185.11	21.40	18.10	0.15	17.40	-10.3	37.6
VM	Fish Springs Ranch Irrigation Well	H4137	well	MIDDLE	19.10	7.89	9.15	3.82	39.45	9.67	139.80	9.08	9.02	0.05	13.00		
VM	MIDDLE	MEAN	19.75	8.16	7.56	2.38	58.36	6.58	145.96	15.35	15.45	0.18	34.18	-11.86	40.54		
VM	MIDDLE	MEDIAN	20.00	8.14	7.10	2.05	66.50	6.54	144.00	17.00	18.00	0.17	43.50	-11.86	40.54		
VM	MIDDLE	Standard DEV	2.33	0.25	3.20	1.23	19.10	1.90	26.86	4.91	6.84	0.08	17.80	2.18	4.06		
VM	Ford #1 Well a	W112*	well	END	14.70	8.37	34.90	16.50	190.00	23.70	286.00	32.00	110.60	1.70	5.30		
USA/FSM/VM	Stanley Well a	W115	well	END	8.30	25.00	60.00	2830.00	51.00	567.00	620.00	3960.00	0.20	20.00			
VM	END	MEAN	14.70	8.34	43.45	38.25	1510.00	37.35	426.50	326.00	2035.30	0.95	12.65				
VM	END	MEDIAN	14.70	8.34	43.45	38.25	1510.00	37.35	426.50	326.00	2035.30	0.95	12.65				
VM	END	Standard DEV	0.05	12.09	30.76	1866.76	19.30	196.70	415.78	2721.94	1.06	10.39					
Cottonwood Flow Path																	
CW	Cottonwood Test Well a	W34*	well	BEGINNING	7.10	22.20	8.60	17.70	6.50	148.74	7.00	7.00	0.10				
CW	Upper Red Spring a	W146*	spring	BEGINNING	14.00	7.93	33.00	11.00	13.00	4.70	160.00	6.40	5.00				
CW	Black Canyon a	W147*	spring	BEGINNING	14.00	7.40	19.40	8.40	7.70	3.50	115.83	3.00	4.00				
CW	Newcombe Spring a	W148*	spring	BEGINNING	20	7.3	30	9	23	5.7	168.00	6.00	6.00				
CW	Cottonwood Springs	W96*	spring	BEGINNING	14.77	7.77	12.81	5.09	11.70	4.93	95.02	3.56	2.93	0.09	21.67	-19.0	
CW	Cottonwood Well #2 a	W99	well	BEGINNING	7.60	7.60	22.20	7.80	15.50	5.60	154.04	11.00	7.00	0.10			
CW	Cold Spring a	W150*	spring	BEGINNING	12.00	7.30	14.30	5.80	5.40	4.70	87.78	-3	4.00				
CW	BEGINNING	MEAN	14.95	7.49	21.99	7.96	13.43	5.09	132.89	6.16	5.13	0.10	21.67	-18.99			
CW	BEGINNING	MEDIAN	14.00	7.40	22.20	8.40	13.00	4.93	148.74	6.20	5.00	0.10	21.67	-18.99			
CW	BEGINNING	Standard DEV	3.00	0.29	7.48	1.99	5.98	0.96	32.81	2.86	1.59	0.01					
CW/ASP/NV	BD2-C a	W116*	well	END	15.67	8.27	13.87	4.60	157.33	10.47	300.33	39.33	73.33	0.40	18.00		
USA/CW/ASP	May Well a	W116*	well	END	12.40	7.09	150.00	820.00	16100.00	94.00	950.00	350.00	24300.00	0.40	18.00		
CW	END	MEAN	14.03	7.68	81.93	412.30	8128.67	52.23	625.17	194.67	12186.67	0.40	18.00				
CW	END	MEDIAN	14.03	7.68	81.93	412.30	8128.67	52.23	625.17	194.67	12186.67	0.40	18.00				
CW	END	Standard DEV	2.31	0.83	96.26	576.57	11273.17	59.07	459.39	219.67	17130.84	0.00					
Neversett Flow Path																	
NV	Hodge Well b	W100*	well	BEGINNING	18.75	7.88	9.77	3.95	37.48	8.08	127.33	6.33	5.07	0.11	51.00		
NV	BEGINNING	MEAN	18.75	7.88	9.77	3.95	37.48	8.08	127.33	6.33	5.07	0.11	51.00				
CW/ASP/NV	BD2-C a	W101*	well	BEGINNING	15.67	8.27	13.87	4.60	157.33	10.47	300.33	39.33	73.33	0.40	18.00		
NV	Never Sweet Ranch	W102*	well	MIDDLE	14.90	8.25	17.17	3.38	107.35	8.32	223.13	71.48	36.48	0.22	-11.2	76.7	
NV	MIDDLE	MEAN	15.28	8.26	15.52	3.99	132.34	9.39	261.73	55.41	54.91	0.31	-11.23	76.70			
NV	MIDDLE	MEDIAN	15.28	8.26	15.52	3.99	132.34	9.39	261.73	55.41	54.91	0.31	-11.23	76.70			
NV	MIDDLE	Standard DEV	0.54	0.02	2.34	0.86	35.9	1.52	54.59	22.73	26.06	0.13					
USA/CW/ASP	May Well a	W116*	well	END	12.40	7.09	150.00	820.00	16100.00	94.00	950.00	350.00	24300.00	0.40	18.00		
NV	END	MEAN	12.4	7.09	150	820	16100	94	950	350	24300	0.4	18				
NV	END	MEDIAN	12.4	7.09	150	820	16100	94	950	350	24300	0.4	18				
NV	END	Standard DEV	0.85	0.32	40.67	533.56	8181.23	11.38	184.55	1238.07	13140.87	5.69					
Astor Sand Pass Flow Path																	
ASP	Astor Pass 1 a	W69	well	BEGINNING		8.30	13.00	12.00	828.00	12.20	940.00	367.00	447.00	3.10			